

## The Continuous-Spin Ising Model, $g_0:\phi^4_d$ Field Theory, and the Renormalization Group

George A. Baker, Jr.<sup>1</sup> and John M. Kincaid<sup>2</sup>

*Received March 28, 1980*

---

We have used the method of high-temperature series expansions to investigate the critical point properties of a continuous-spin Ising model and  $g_0:\phi^4_d$  Euclidean field theory. We have computed through tenth order the high-temperature series expansions for the magnetization, susceptibility, second derivative of the susceptibility, and the second moment of the spin-spin correlation function on eight different lattices. Our analysis of these series is made using integral and Padé approximants. In three dimensions we find that hyperscaling fails for sufficiently Ising-like systems; the strong coupling limit of  $g_0:\phi^4_3$  depends on how the ultraviolet cutoff is removed. The level contours of the renormalized coupling constant for this model in the  $g_0$ , correlation-length plane exhibit a saddle point. If the ultraviolet cutoff is removed before  $g_0 \rightarrow \infty$ , the usual field theory results and the renormalization-group fixed point with hyperscaling is obtained. If the order of these limits is reversed, the Ising model limit where hyperscaling fails and the field theory is trivial is obtained. In four dimensions, we find that hyperscaling fails completely;  $g_0:\phi^4_4$  is trivial for all  $g_0$  when the ultraviolet cutoff is removed.

---

**KEY WORDS:** Ising ferromagnet; Boson field theory; renormalization group; hyperscaling relations; high-temperature series expansions; Padé and integral approximants.

### 1. INTRODUCTION AND SUMMARY

In the early 1960s, greatly improved perturbation series combined with the powerful Padé method of analysis to yield accurate estimates of the critical indices for the spin-1/2 Ising model and other prototypical models. These

---

Work supported in part by the U.S. Department of Energy.

<sup>1</sup> Theoretical Division, Los Alamos Scientific Laboratory, University of California, Los Alamos, New Mexico.

<sup>2</sup> Thermophysics Division, National Bureau of Standards, Washington, D.C.

results and the emergence of scaling theories led to the recognition that there were several different classes of relations between the critical indices.<sup>(1,2)</sup> Most of these relations comprise what are now called scaling laws; these relations follow from the assumption (or its equivalent) that free energies and correlation functions are homogeneous functions in the neighborhood of a critical point. Results from experiments, exactly soluble models, and numerous numerical studies provide strong support for the scaling laws.<sup>(2)</sup> The other class of relations, for which the evidence was then the weakest, have become known as hyperscaling laws; they are relations between critical indices in which the spatial dimensionality explicitly appears. The idea of hyperscaling arose out of the assumption that the two-point correlation length of a single homogeneous phase was the *only* important length scale on which critical phenomena should be gauged.<sup>(2)</sup> Alternatives to this “strong” scaling assumption have been developed by Stell<sup>(3)</sup> and Fisher.<sup>(4)</sup> (These “weak” scaling theories allow for the possibility that one or more additional lengths, such as the width of the interfacial boundary between two coexisting phases, become important in the critical region.) The assumption of critical point dominance of the correlation length supported various arguments that the details of interaction potentials do not play an essential role in determining the critical behavior. Thus it was expected that physical systems with the same basic “symmetries”<sup>3</sup> would have the same set of critical indices—i.e., they would show the same universal behavior at the critical point.<sup>(5)</sup> The validity of the hyperscaling relations in two dimensions has been established for a variety of systems. Most notably, it holds for the spin-1/2 Ising model.<sup>4</sup> In three and higher dimensions, however, the evidence in support of hyperscaling has not been convincing—as evidenced by the many analyses of Ising-model high-temperature series expansions that have been reported.<sup>(11–14)</sup> Similarly, the idea of universality in its original form has not been confirmed by experimental or theoretical investigations, although there is strong experimental evidence in the case of simple fluids that is consistent with hyperscaling.<sup>(15,16)</sup> The basic set of “symmetries” (i.e., qualifiers used to define a universality class), has been repeatedly enlarged, thereby decreasing the size of the associated universality class.<sup>5</sup>

<sup>3</sup> We use the word “symmetries” loosely to denote the set of properties that defines a universality class. See Ref. 5.

<sup>4</sup> The critical exponents of the two-dimensional Ising model that appear in the hyperscaling relations have been calculated in numerous ways by many authors; for a survey see Refs. 2 and 6. The proof by Kadanoff<sup>(7)</sup> depends on a hypothesis shown by Stephensen along diagonals,<sup>(8)</sup> as explained by McCoy and Wu.<sup>(9)</sup> For a discussion of the two-dimensional Ising model field theory see Ref. 10.

<sup>5</sup> See, for instance, model calculations on systems having tricritical and higher order critical points.<sup>(17)</sup>

In the early 1970s, powerful calculational techniques developed for field theory were applied to the statistical mechanics of the critical point,<sup>(18,19)</sup> and attention shifted away from the questions of hyperscaling and correlation length dominance. The field theory techniques, known as renormalization group methods, grew out of the connection between field theory and statistical mechanics pointed out by Symanzik<sup>(20)</sup> and elaborated by Wilson<sup>(18)</sup> and others.<sup>(21,22)</sup> The renormalization group approach has intrinsic to its structure both scaling and hyperscaling relations, so that the values of all the critical indices are determined from just two indices plus the spatial dimension. The structure of the renormalization group methods appears to support the idea of universality.<sup>6</sup> Unfortunately, the language of field theory and its precise connection with statistical mechanics was not immediately clear; there has been some uncertainty concerning the rigorous status of the renormalization group theory of critical phenomena. In particular, it has not been made clear whether hyperscaling and the critical point dominance of the correlation length are consequences of the renormalization group theory or are assumptions that have been appended to the theory.

The field-theoretic approach, in its most basic form, is tied to the properties of  $g_0:\phi^4:d$  Euclidean field theory. The connection between this model field theory and a continuous-spin Ising model provides the basis for the renormalization group theory of critical phenomena. It is the point of view of this paper that the direct calculation of the properties of the continuous-spin Ising model, by the method of (convergent, not asymptotic) series expansions, should greatly clarify the status of the renormalization group theory of critical phenomena. Section 2 of this paper illustrates clearly the connection between  $g_0:\phi^4:d$  Euclidean field theory and a continuous-spin Ising model with a spin density distribution given by  $\exp(-\tilde{g}_0 s^4 - \tilde{A} s^2)$ . We show that if hyperscaling fails, then the conventional renormalized coupling constant of the field theory vanishes. We find that the number of universality classes for the continuous-spin systems we consider is given by the number of values that the renormalized coupling constant attains in the strong coupling limit of  $g_0:\phi^4:d$ , i.e.,  $g_0 \rightarrow \infty$ . (See Section 3.) In the course of our numerical investigations we believe we have developed good numerical evidence on the following points.

(1) The renormalization group theory of critical phenomena is seen to depend on the *key assumption* that, within the context of a  $g_0:\phi^4:d$  field theory, *the limits  $g_0 \rightarrow \infty$  and  $a \rightarrow 0$  commute*. Here  $g_0$  is the bare coupling constant and  $a$  is the ultraviolet cutoff (lattice spacing). Our calculations show that the numerical evidence is consistent with this assumption for models in one and two dimensions. In three dimensions this assumption

<sup>6</sup> Reference 18, Sections 10 and 12, and Hohenberg (Ref. 15).

fails. There appears to be at least two values for the renormalized coupling constant  $g$  in the strong coupling limit, depending on how the limits  $g_0 \rightarrow \infty, a \rightarrow 0$  are taken. For sufficiently Ising-like spin distributions, the renormalized coupling constant goes, numerically, to zero.

(2) A contour plot of  $g$  as a function of the sharpness of the spin density distribution  $\tilde{g}_0$  and the correlation length  $\xi$  ( $\sim 1/a$ ) exhibits a saddle point. It is evident that the simple structure assumed in the renormalization group theory of critical phenomena is inadequate to describe the full richness of the subject.

(3) In four dimensions, the renormalized coupling constant as a function of the bare coupling constant for fixed (and sufficiently large) correlation length is a singly peaked curve. The numerical evidence is consistent with the idea that the peak height shrinks to zero inversely proportional to the logarithm of the correlation length. The strong coupling tail shrinks more rapidly to zero, roughly like  $\xi^{-0.54 \pm 0.08}$ . Thus, although the field theory of this model is trivial, it is not unreasonable to suppose that interesting statistical mechanics can result (i.e., these models display critical point properties that are distinct from those of the Gaussian model).

(4) Our numerical studies are in agreement with the rigorous results of constructive field theory for one and two dimensions, and those results appear to continue to hold up to and including the strong coupling limit. For the case of three dimensions, we find that the rigorous results for small  $g_0$  extend to all finite  $g_0$  when the ultraviolet cutoff is removed and there is a well-defined strong coupling limit ( $\lim_{g_0 \rightarrow \infty} \lim_{a \rightarrow 0}$ ). In four dimensions, the numerical results are consistent with the idea that the removal of the ultraviolet cutoff leads to a trivial (i.e., no scattering) field theory.

We conclude that the renormalization group theory of critical phenomena, as currently formulated, is in fact the theory of the first maximum of the renormalized coupling constant as a function of the bare coupling constant. This maximum may ( $d = 1, 2$ ) or may not ( $d = 3, 4$ ) coincide with the spin-1/2 Ising model.

In Section 2 we set out in detail the mathematical formulation of our model and relate it to both the usual statistical mechanical and field theory languages. We discuss the strong coupling limit in Section 3. There we trace how the key assumption (described above) of the renormalization group leads, in the context of our formulation, to some of the usual results of that theory. The generation of the high-temperature series expansions for the magnetization, susceptibility, second derivative of the susceptibility with respect to magnetic field, and correlation length is described in Section 4. Subsequently, in Section 5, we obtain the limiting large- and small- $\tilde{g}_0$  behavior of the series in addition to other related quantities. [Here  $\tilde{g}_0$  is a parameter characterizing the spin-distribution density, defined in Eq.

(2.17).] In Section 6, we describe the series in the correlation length, and finally, in Section 7, we discuss our numerical results.

## 2. DEFINITION OF THE MODEL

The continuous-spin model which we treat can be thought of in two ways. One may consider the model to be a one-component, ferromagnetic Ising model in which the spin variables are continuously distributed from  $-\infty$  to  $+\infty$ . Alternatively, it can be viewed as a lattice cutoff  $g_0:\phi^4:_d$  Euclidean, Boson field theory. To make clear the relationship between these two interpretations, we will begin by defining the model within the context of field theory and then translate the model to the statistical mechanical form which, from a computational point of view, will be the one most convenient for our purposes.

It is usual to think of the Euclidean field theory as defined by the generating functional of the Schwinger functions (complete Euclidean Green's functions)  $S_N$ ,<sup>(23)</sup>

$$Z(H) = \sum_{N=0}^{\infty} \frac{1}{N!} \int dx_1 \cdots dx_N H(x_1) \cdots H(x_N) S_N(x_1, \dots, x_N) \quad (2.1)$$

We give the usual formal expression for this generating functional as the functional integral

$$Z(H) = M^{-1} \int [d\phi] \exp \left\{ - \int d\mathbf{x} [\mathcal{L}(\phi) - \phi H] \right\} \quad (2.2)$$

where the Lagrangian density  $\mathcal{L}$  is a function of the field variable  $\phi$  and the integral in the exponent is over  $d$ -dimensional Euclidean space. The formal constant  $M$  is supposed to impose the condition

$$Z(0) = 1 \quad (2.3)$$

The usual expression for the action in a  $g_0:\phi^4:_d$  field theory is

$$\int d\mathbf{x} \mathcal{L}(\phi(\mathbf{x})) = \frac{1}{2} \int_{-\infty}^{\infty} \cdots \int d\mathbf{x} \left\{ [\nabla\phi(\mathbf{x})]^2 + m_0^2:\phi^2(\mathbf{x}): + \frac{g_0}{4!} g_0:\phi^4(\mathbf{x}): \right\} \quad (2.4)$$

where  $m_0$  is the bare mass,  $g_0$  the bare coupling constant, and  $: :$  denotes the Wick ordered product.

The first step in moving toward the statistical mechanics of an Ising system is to replace (2.4) by a finite difference approximation on a finite portion (i.e.,  $N$  points) of a regular space lattice. We therefore replace Eq.

(2.2) by

$$Z(H) = M^{-1} \int_{-\infty}^{\infty} \cdots \int \prod_{j=1}^N d\phi_j \exp \left\{ -\frac{\nu}{2} \sum_{i=1}^N \left[ \frac{2d}{q} \sum_{\{\delta\}} \frac{(\phi_i - \phi_{i+\delta})^2}{a^2} + m_0^2 \phi_i^2 + \frac{2}{4!} g_0 \phi_i^4 + H_i \phi_i \right] \right\} \quad (2.5)$$

where  $M$  is a new normalization constant,  $a$  is the lattice spacing,  $d$  the spatial dimension,  $\nu$  ( $\propto a^d$ ) the volume per lattice site,  $q$  the lattice coordination number, the sum over  $\{\delta\}$  is the sum over half the nearest neighbor sites, and  $H_i$  is the source, or magnetic field, term at site  $i$ .

If we attempt to calculate the scattering amplitude for this field theory as a perturbation expansion about  $q_0 = 0$  we find, as is well known,<sup>(24)</sup> that the coefficients in the expansion are dependent upon the lattice spacing  $a$  and diverge as  $a \rightarrow 0$ . These divergences can be removed by following the renormalization procedure of Bogolubov.<sup>(25)</sup> In the case of the  $g_0 \phi^4$  field theory this procedure leads to amplitude, mass, and coupling constant renormalization. The first two of the renormalizations can be accomplished by replacing  $H_i$  by  $H_i Z_3^{-1/2}$  and making the substitutions

$$\phi_i = Z_3^{1/2} \psi_i \quad (2.6)$$

and

$$m_0^2 = m^2 + \delta m^2 \quad (2.7)$$

Thus, redefining  $M$ , we have, using Eqs. (2.5)–(2.7),

$$Z(H) = M^{-1} \int_{-\infty}^{\infty} \cdots \int \prod_{j=1}^N d\psi_j \exp \left\{ -\frac{\nu}{2} \sum_{i=1}^N \left[ \frac{2dZ_3}{q} \sum_{\{\delta\}} \frac{(\psi_i - \psi_{i+\delta})^2}{a^2} + m^2 Z_3 \left( \psi_i^2 - \frac{C}{Z_3} \right) + \frac{2}{4!} g_0 Z_3^2 \left( \psi_i^4 - \frac{6C\psi_i^2}{Z_3} + \frac{3C}{Z_3^2} \right) + \delta m^2 Z_3 \left( \psi_i^2 - \frac{C}{Z_3} \right) + H_i \psi_i \right] \right\} \quad (2.8)$$

In Eq. (2.8) we have expressed the normal ordered products  $:(\phi_j)^p$ : in terms of the Boson commutator  $C = [\phi^-, \phi^+]$  and ordinary products of  $\phi_j$  using the relation<sup>(21)</sup>

$$:(\phi_j)^p := \sum_{n=0}^{\lfloor p/2 \rfloor} (-1)^n \frac{p!}{(p-2n)! n!} 2^{-n} C^n (\phi_j)^{p-2n} \quad (2.9)$$

The commutator  $C$  is just the sum over the lattice Green's function and is given by

$$C = \frac{1}{V} \sum_{\mathbf{k}} \left[ m^2 + \frac{8d}{qa^2} \sum_{\{\delta\}} \sin^2(\pi \mathbf{k} \cdot \delta a) \right]^{-1} \tag{2.10}$$

where  $V$  is the total volume, the summation on  $\mathbf{k}$  is over the reciprocal lattice, and  $\{\delta\}$  is again one-half the nearest-neighbor sites. It is easily seen that in the limit  $a \rightarrow 0$

$$\lim_{V \rightarrow \infty} C \propto \begin{cases} a^{2-d}, & d > 2 \\ -\ln(am), & d = 2 \\ \text{finite}, & d < 2 \end{cases} \tag{2.11}$$

The renormalization constants  $Z_3$  and  $\delta m^2$  are determined by the requirements that

$$\Gamma_R^{(2)}(\mathbf{p}, -\mathbf{p}) = m^2 + 4\pi^2 p^2 \tag{2.12}$$

for  $p$  near zero. Here  $\Gamma_R^{(2)}(\mathbf{p}, -\mathbf{p})$  is the propagator defined by

$$\Gamma_R^{(2)}(\mathbf{p}, -\mathbf{p}) = \left\{ v \sum_{j=0}^{N-1} \frac{\partial^2 \ln Z(H)}{\partial H_0 \partial H_j} \Bigg|_{H=0} \exp[-2\pi i \mathbf{p} \cdot \mathbf{j} a] \right\}^{-1} \tag{2.13}$$

Before using Eqs. (2.12) and (2.13) to obtain explicit equations for  $Z_3$  and  $\delta m^2$ , it is convenient to introduce yet another change of variable. Let

$$\psi_i = \sigma_i (2dZ_3 v / qKa^2)^{-1/2} \tag{2.14}$$

In terms of these new variables  $\sigma_i$  and  $K$ ,  $Z(H)$  assumes the form of the partition function of a continuous-spin ferromagnetic Ising model

$$Z(\tilde{H}) = M^{-1} \int_{-\infty}^{\infty} \cdots \int \prod_{j=1}^N [d\sigma_j F(\sigma_j)] \exp \left[ K \sum_{i, \{\delta\}} \sigma_i \sigma_{i+\delta} \right] \tag{2.15}$$

with a spin distribution density  $F(\sigma)$  given by

$$F(\sigma) = \exp(-\tilde{g}_0 \sigma^4 - \tilde{A} \sigma^2 + \tilde{H} \sigma) \tag{2.16}$$

where

$$\begin{aligned} \tilde{A} &= (qK/4a)(2d + m^2 a^2 + \delta m^2 a^2 - \frac{1}{2} Ca^2 g_0) \\ \tilde{g}_0 &= g_0 K^2 q^2 a^4 / 96 d^2 v \\ \tilde{H}_i &= H_i (2dZ_3 v / qKa^2)^{-1/2} \end{aligned} \tag{2.17}$$

(Note that we have again redefined  $M$ .) The variable  $K$  adds an additional degree of freedom to the model. We eliminate the additional degree of

freedom by imposing the condition  $I_2(0) = 1$ , where

$$I_n(\tilde{H}) = \frac{\int_{-\infty}^{\infty} d\sigma \sigma^n F(\sigma)}{\int_{-\infty}^{\infty} d\sigma F(\sigma)} \tag{2.18}$$

Thus,  $Z(\tilde{H})$  depends on the parameters  $K$ ,  $\tilde{g}_0$ , and  $H_i$ ; the other parameter,  $\tilde{A}$ , is a function of  $\tilde{g}_0$  as determined by the condition  $I_2(0) = 1$ . Figure 1 shows the function  $\tilde{A}(\tilde{g}_0)$ . We remark that for  $\tilde{g}_0 = 0$ ,  $\tilde{A} = \frac{1}{2}$  and  $Z(\tilde{H})$  defines the Gaussian model<sup>(26)</sup>; in the limit  $\tilde{g}_0 \rightarrow \infty$ ,  $\tilde{A} \rightarrow -2\tilde{g}_0$  and  $Z(\tilde{H})$  represents the usual spin- $\frac{1}{2}$  Ising model.<sup>(27)</sup> We may now reexpress Eq. (2.13) in terms of the expectation values of the  $\sigma$ 's:

$$\Gamma_R^{(2)}(\mathbf{p}, -\mathbf{p}) = \left[ \frac{qKa^2}{2dZ_3} \sum_{j=0}^{N-1} \langle \sigma_0 \sigma_j \rangle \exp(-2\pi i \mathbf{p} \cdot \mathbf{j}a) \right]^{-1}$$

$$= \frac{2dZ_3}{qKa^2} \chi^{-1} [1 + (2\pi)^2 \xi^2 a^2 p^2 + \dots] \tag{2.19}$$

where the magnetic susceptibility  $\chi$  is defined by

$$\chi = \sum_{j=0}^{N-1} \langle \sigma_0 \sigma_j \rangle - \langle \sigma_0 \rangle^2 \tag{2.20}$$

and the correlation length  $\xi$  is defined in terms of the second moment of

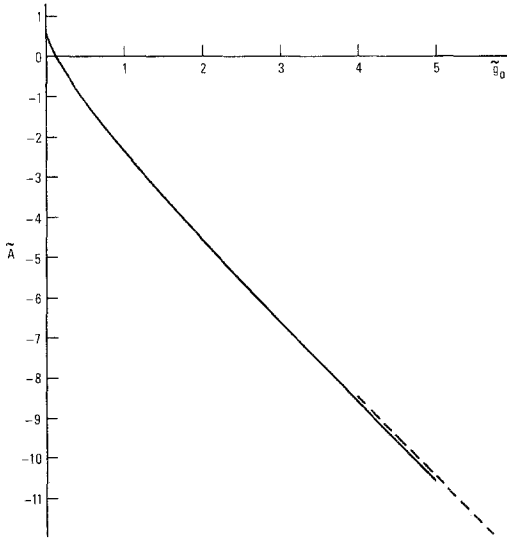


Fig. 1.  $\tilde{A}$  versus  $\tilde{g}_0$ .  $\tilde{A}(\tilde{g}_0)$  is obtained from the constraint  $I_2(0) = 1$ . When  $\tilde{g}_0 = [\Gamma(3/4) / \Gamma(1/4)]^2$ ,  $\tilde{A} = 0$ . As  $\tilde{g}_0 \rightarrow \infty$ ,  $\tilde{A} \rightarrow -2\tilde{g}_0 - 1/2$ .



the spin-spin correlation function:

$$\begin{aligned} \mu_2 &= \sum_{j=0}^N \left(\frac{j}{a}\right)^2 [\langle \sigma_0 \sigma_j \rangle - \langle \sigma_0 \rangle^2] \\ \xi^2 &= \mu_2 / 2d\chi \end{aligned} \tag{2.21}$$

Here the angular brackets denote the usual ensemble average and  $\xi$  is measured relative to the lattice spacing  $a$ . Comparing Eqs. (2.12) and (2.19), we find that

$$m^2 = (2dZ_3 / qKa^2)\chi^{-1} \tag{2.22}$$

$$m^2 \xi^2 a^2 = 1 \tag{2.23}$$

The selection of a mass in field theory is equivalent to the selection of a length scale for the statistical mechanical model. For example,  $m = \xi^{-1}$  would select a lattice of unit spacing as is common in statistical mechanical applications. A fixed mass,  $m = 1$ , on the other hand, would scale the lattice spacing  $a$  to zero as  $\xi \rightarrow \infty$  when the temperature approaches the critical temperature (i.e.,  $K \rightarrow K_c$ ).

Now let us consider the third and final renormalization. A renormalized coupling constant  $g_R$  is obtained by rescaling the zero-momentum scattering amplitude:

$$\begin{aligned} g_R &= \Gamma_R^{(4)}(0, 0, 0, 0) \\ &= -v^3 \sum_{j,k,l=0}^{N-1} \frac{\partial^4 \ln Z(H)}{\partial H_0 \partial H_j \partial H_k \partial H_l} \Big|_{H=0} \left[ v \sum_{j=0}^{N-1} \frac{\partial^2 \ln Z(H)}{\partial H_0 \partial H_j} \right]^{-4} \end{aligned} \tag{2.24}$$

This quantity is important from the field theory point of view because if it vanishes there is no scattering described by the model—i.e., the model represents a generalized free field.<sup>(28)</sup> If we reexpress (2.24) in terms of the  $\sigma$  variable, we get, using Eq. (2.22),

$$g_R = -vm^4 \frac{\partial^2 \chi / \partial \tilde{H}^2}{\chi^2} \tag{2.25}$$

where we define

$$\frac{\partial^2 \chi}{\partial \tilde{H}^2} = \sum_{j,k,l=0}^{N-1} u_4(\sigma_0, \sigma_j, \sigma_k, \sigma_l) \tag{2.26}$$

Here  $u_4$  is the fourth Ursell function.<sup>(29)</sup> Equations (2.25) and (2.23) can be used to define the dimensionless, renormalized coupling constant  $g$ ,

$$g \equiv g_R m^{d-4} = -\frac{v}{a^d} \frac{\partial^2 \chi / \partial \tilde{H}^2}{\chi^{2\xi^d}} \tag{2.27}$$

which is a convenient form because  $v/a^d$  is a pure number and the other factors in Eq. (2.27) are directly expressible in terms of the expectation values of the  $\sigma$ 's.

It is clear from the form of Eq. (2.27) why  $g$  is important to the theory of ferromagnetic Ising models. As we approach the critical point from temperatures above the critical temperature ( $K < K_c$ , with  $H = 0$ ) we know that<sup>(2)</sup>

$$\chi \sim A_+ (1 - K/K_c)^{-\gamma}, \quad \xi \sim D_+ (1 - K/K_c)^{-\nu}$$

$$\partial^2 \chi / \partial \tilde{H}^2 \sim -B_+ (1 - K/K_c)^{-\gamma - 2\Delta} \quad (2.28)$$

thus as  $K \rightarrow K_c$ ,

$$g \sim \frac{v}{a^d} \frac{B_+}{A_+ D_+^d} \left( \frac{1 - K}{K_c} \right)^{\gamma + d\nu - 2\Delta} \quad (2.29)$$

It has been proven rigorously that as  $K \rightarrow K_c$ ,  $g$  remains finite,<sup>(30)</sup> which implies that

$$\gamma + d\nu \geq 2\Delta \quad (2.30)$$

Equation (2.30), taken as an equality, is a "hyperscaling relation" between the critical exponents  $\gamma$ ,  $\Delta$ , and  $\nu$  and the spatial dimension  $d$ . Thus the behavior of  $g$  as  $K \rightarrow K_c$  is a diagnostic of whether this hyperscaling relation fails ( $g \rightarrow 0$ ) or holds ( $g$  remains finite).

We may solve Eqs. (2.22), (2.23), and (2.28) to determine how the various parameters behave as  $K \rightarrow K_c$  with  $\tilde{g}_0$  fixed. We obtain

$$a \sim \frac{1}{mD_+} \left( \frac{1 - K}{K_c} \right)^\nu$$

$$Z_3 \sim \frac{qKA_+}{2dD_+^2} \left( \frac{1 - K}{K_c} \right)^{\eta\nu} \sim \frac{qKA_+}{2dD_+^{2-\eta}} (ma)^\eta \quad (2.31)$$

$$g \sim \frac{v}{a^d} \frac{B_+}{a_+ D_+^d} (mD_+ + a)^{\omega^*}$$

where  $\eta = 2 - \gamma/\nu$  and we have defined the "anomalous dimension of the vacuum"  $\omega^*$  by the relation

$$\gamma + (d - \omega^*)\nu = 2\Delta \quad (2.32)$$

The actual computations reported in this paper depend on the properties of  $g$  as a direct function of  $K$  (the inverse temperature) and parametrically as a function of  $\tilde{g}_0$ . The further dependence on  $\tilde{H}$  is not studied.

### 3. THE STRONG COUPLING REGION

In the previous section we saw that the plan of the renormalization scheme in field theory is to arrange the parameters of the model and the quantities computed from the model so that they are all finite and nonzero in the limit where  $a$ , the ultraviolet cutoff, goes to zero—that is,  $K \rightarrow K_c$ . In statistical mechanical applications  $\tilde{g}_0$  is fixed. This condition means, by Eq. (2.17), that  $g_0$  tends to infinity ( $d < 4$ ) as  $a \rightarrow 0$  (as long as  $d > 1$  so that  $K_c$  is not infinite). Thus it is the strong coupling region,  $a \rightarrow 0$ ,  $g_0 \rightarrow \infty$ , that characterizes the critical point of statistical mechanics. The application of renormalization group methods as developed by Wilson to the study of critical phenomena is strongly dependent upon the properties of the field theory in the strong coupling region. The key assumption of the renormalization group approach is that *all renormalized quantities are continuously differentiable in the neighborhood of  $a = 0$ ,  $0 \leq g_0 \leq \infty$* . In particular, for example,  $g(g_0, a)$  is assumed to be continuous in the quadrant  $0 \leq g_0 \leq \infty$ ,  $a \geq 0$  including the point  $(\infty, 0)$ . To illustrate this point we present a brief review of those aspects of the Callan–Symanzik equation approach to Wilson’s renormalization group theory that focus upon the nature of the strong coupling region.

We begin by considering the consequences of the key assumption mentioned above. For any fixed, nonzero value of  $\tilde{g}_0$ , Eq. (2.17) implies that the limit  $a \rightarrow 0$  corresponds to  $g_0 = \infty$ ,  $a = 0$ . Thus, all continuous-spin Ising models defined by Eq. (2.15) (of the same dimension) have the same value of  $g$ , i.e., it is universal. After we have taken the limit  $a \rightarrow 0$ , (fixing  $K$  at  $K_c$ ), there remains only one parameter left to describe the model; the renormalization group choice is to make this parameter  $g$ . Since  $g$  can be expanded in a power series in  $g_0$ , and this series can be formally reverted to  $g_0$  as a formal series in  $g$ , we can reexpress the various quantities of interest as formal series in  $g$  instead of  $g_0$ . (Proper rules have been given to perform this expansion directly in terms of Feynman diagrams.) This procedure now points to the desirability of finding the universal value of  $g$ , denoted  $g^*$ , that corresponds to all the statistical mechanical models. We mention that the reversion of  $g(g_0, 0)$  to  $g_0(g, 0)$  depends on Schrader’s monotonicity hypothesis,<sup>(31)</sup>  $g(g_0, a)$  is a monotonic increasing function of  $g_0$ ,  $0 \leq g_0 \leq \infty$  for fixed  $a$ . If there should be a maximum, then there would necessarily be a branch point in the reverted function  $g_0(g, a)$ . While in principle one can analytically continue around such a branch point to the proper Riemann sheet, no practical calculation that we know of has contemplated this added complication.

To find the value of  $g^*$ , the renormalization group procedure is to construct a discriminant function, which can be used directly in the limit

$a \rightarrow 0$ , to find  $g^*$ . The one proposed is

$$\beta(g) = (d - 4) g_0 \left( \frac{\partial g}{\partial g_0} \right)_{m,a,d} \tag{3.1}$$

If  $g \rightarrow g^* < \infty$  as  $g_0 \rightarrow \infty$  as assumed (i.e., monotonically), then it follows that  $\beta(g^*) = 0$ . From the formal expansion  $g(g_0, 0)$  one can directly compute  $\beta(g)$  by formal manipulations; the series can then be summed<sup>(32,33)</sup> and  $g^*$  sought as the zero of the  $\beta$  function.

The critical indices can be computed using the following approach, which, by way of example, we apply to the calculation of the index  $\eta$ . Using Eqs. (2.23) and (2.31), we find

$$\eta = \lim_{a \rightarrow 0} a \left( \frac{\partial \ln Z_3}{\partial a} \right)_{\tilde{g}_0} \tag{3.2}$$

In order to use the field theory methods, we need to “turn” the direction of the derivative to the  $g_0$  direction. To do this we write

$$Z_3(g_0, a) = Z_3(ca^{d-4}\tilde{g}_0, a) \tag{3.3}$$

with  $c = 96d(v/a^d)/K^2q^2$ , so that

$$\begin{aligned} a \left( \frac{\partial Z_3}{\partial a} \right)_{\tilde{g}_0} &= (d - 4)ca^{d-4}\tilde{g}_0 \left( \frac{\partial Z_3}{\partial g_0} \right)_a + a \left( \frac{\partial Z_3}{\partial a} \right)_{g_0} \\ &= (d - 4)g_0 \left( \frac{\partial Z_3}{\partial g_0} \right)_a + a \left( \frac{\partial Z_3}{\partial a} \right)_{g_0} \end{aligned} \tag{3.4}$$

Thus by the continuous differentiability assumed, we have, from Eqs. (3.4) and (3.2)

$$\lim_{g_0 \rightarrow \infty} (d - 4)g_0 \frac{\partial \ln Z_3(g_0, 0)}{\partial g_0} = \eta \tag{3.5}$$

Rewriting this equation in terms of  $g$ , using Eq. (3.1),

$$\eta = \lim_{g \rightarrow g^*} \beta(g) \frac{\partial \ln Z_3}{\partial g} \tag{3.6}$$

Similar expressions can be developed for other critical exponents.<sup>(19)</sup> We point out that for  $d = 2, 3$ , these differentiability conditions have been rigorously proved for sufficiently small  $g_0$ . That is, the field theory is well defined by the (asymptotic) perturbation theory. With a lattice cutoff,  $g = g(g_0, 0) + 0(a^2)$  for  $d = 1, 2$  and  $g = g(g_0, 0) + 0(a)$  for  $d = 3$ , as can be shown by term-by-term calculations in small- $g_0$  perturbation theory.

In summary, we see that the cornerstone of the renormalization group scheme is the assumption that the perturbation theory (in  $g_0$ ) is both correct

and complete. We will discuss in a later section how the point ( $g_0 = \infty, a = 0$ ) is not always a point of joint continuity in  $g_0$  and  $a$ , and how the turning of the direction of the derivative [see Eqs. (3.2) and (3.6)] is affected by this result.

#### 4. GENERATION OF THE HIGH-TEMPERATURE SERIES

In this section we describe how we obtained the high-temperature series expansions (i.e., expansions in powers of  $K$ ) of the various quantities needed to calculate  $g$ . The series were generated using the method of Wortis.<sup>(34)</sup> Our starting point is the partition function given by Eq. (2.15) and the series coefficients are found to depend upon the moments  $I_n(\tilde{H})$  of the spin distribution density  $F$  given by Eqs. (2.18) and (2.16), respectively. Some previous results of this type have been given by Camp and van Dyke.<sup>(35)</sup>

We will describe briefly the Wortis method in order to put our calculations in context. Fundamentally, this method is based on Taylor's theorem:

$$w(x) = \exp\left(x \frac{\partial}{\partial y}\right) w(y)|_{y=0} = \sum_{n=0}^{\infty} \frac{x^n}{n!} \left. \frac{\partial^n \omega}{\partial y^n} \right|_{y=0} \quad (4.1)$$

for  $|x|$  less than the radius of convergence of the series. The idea then is to expand the function  $W(K, \tilde{H})$  defined by

$$Z(\tilde{H}) = \exp[ W(K, \tilde{H}) ] \quad (4.2)$$

in a Taylor series. Using Eq. (4.1), we have

$$W(K, \tilde{H}) = \exp\left( \sum_{i < j} K_{ij} \frac{\partial}{\partial \tilde{K}_{ij}} \right) W(\tilde{K}, \tilde{H})|_{\tilde{K}=0} \quad (4.3)$$

Here we have rewritten the nearest-neighbor interaction term  $K \sum_{i, \{ \delta \}} s_i s_{i+\delta}$  by the more general two-spin interaction energy given by  $\sum_{i < j} K_{ij} s_i s_j$ , where  $K_{ij} = K$  if  $i$  and  $j$  label nearest-neighbor sites and  $K_{ij} = 0$  otherwise. The next step is to convert the derivatives  $\partial/\partial K_{ij}$  to equivalent derivatives with respect to  $\tilde{H}$ . This process will leave us with a derivative operator on  $W(0, \tilde{H})$  that factors into individual site terms and can be explicitly evaluated. The simplest such conversion formula is

$$\frac{\partial W}{\partial K_{ij}} = \frac{\partial^2 W}{\partial \tilde{H}_i \partial \tilde{H}_j} + \frac{\partial W}{\partial \tilde{H}_i} \frac{\partial W}{\partial \tilde{H}_j} \quad (4.4)$$

The complete rule is given by Wortis in terms of the cumulants

$$M_n^0(h) = \frac{d^n}{dh^n} \ln I_0(h) \quad (4.5)$$

where  $I_0$  is given by (2.18). The rule is

$$W(K, \tilde{H}) = N \sum_{\tau} \left\{ \frac{M_f(\tau)}{s(\tau)} \left[ \prod_{v_i \in \tau} M_{m(i)}^0(\tilde{H}_i) \right] K^{l(\tau)} \right\} \tag{4.6}$$

Here the sum over  $\tau$  is the sum over all topologically distinct, unrooted, possibly multilined, connected graphs. The product over  $v_i$  is a product over the vertex set of  $\tau$  with  $m(i)$  the multiplicity of the  $i$ th vertex and  $\tilde{H}_i$  the magnetic field at that vertex. The function  $l(\tau)$  is the number of lines of  $\tau$ , and  $M_f(\tau)$  is the free multiplicity per site of  $\tau$  on the edge set defined by the partition function  $Z(\tilde{H})$ .

We mention that the free multiplicity<sup>(34)</sup> used here differs from the more usual weak multiplicity in its lack of the self-avoiding requirement on the embeddings of  $\tau$  on the lattice under consideration. For example, the free multiplicity of an  $n$ -edge, linear chain, or any  $n$ -edge tree for that matter, is just  $q^n$ , where  $q$  is the lattice coordination number. The free multiplicity has the important property that if a graph has an articulation point, then the free multiplicity for that graph is the product of the free multiplicities of the subgraphs formed by cutting the graph at its articulation point. Capitalizing on this property, Wortis has further reduced the combinatorial problem, at the cost of increased algebraic complexity, by means of a vertex renormalization procedure. Any graph with one or more articulation points can be separated into its component star (multiply connected) graphs by cutting it at every articulation point. Conversely, the class of all topologically distinct, unrooted, connected graphs can be constructed by joining star graphs together; however, care must be taken not to generate the same graph more than once. To accomplish this construction it is convenient to consider the decoration of a single vertex. We need for this task the sum of all one-rooted graphs  $G_l(i)$ , where there are  $l$  edges incident on the root at site  $i$ . If we self-consistently assume that every vertex in  $G_l(i)$  is already replaced by the sum of all the required decorations, then we only need the single-rooted stars to construct the  $G_l(i)$ . For example,

$$\begin{aligned} G_1(i) &= \text{---} \\ G_2(i) &= \text{---} + \text{---} + \text{---} + \text{---} + \mathcal{O}(K^5) \\ G_3(i) &= \text{---} + \text{---} + \mathcal{O}(K^5) \end{aligned} \tag{4.7}$$

Now we can write the equations for a single decorated vertex with  $n$  edges attached as

$$M_n(i) = M_n^0(i) + \sum_{l=i}^{\infty} G_l(i) M_{n+l}^0(i) + \frac{1}{2!} \sum_{l,m=1}^{\infty} G_l(i) G_m(i) M_{n+l+m}^0(i) + \dots \tag{4.8}$$

and the equation for the  $G_l$  is

$$G_l(i) = \sum_{\tau} \left\{ \frac{M_f(\tau)}{s(\tau)} \left[ \prod_{v_j \in \tau \setminus i} M_{m(j)}(\tilde{H}_j) \right] K^{l(\tau)} \right\} \quad (4.9)$$

where the sum over  $\tau$  is over all  $l$ -valent, singly rooted star graphs. The product over  $v_j$  is over the vertex set of  $\tau$  except for the root point. The  $G_l$  depend on the  $M_n$  and vice versa, so that we must solve Eqs. (4.8) and (4.9) self-consistently. Since  $G_l$  begins as  $O(K^l)$ , we can begin by replacing the  $M_n$  by  $M_n^0$  in Eq. (4.9) and then use those  $G_l$  to compute the  $M_n$ . These  $M_n$  will be good through at least order  $K$ . If they are now substituted into Eq. (4.9), new  $G_l$  good to one higher order in  $K$  are produced. Hence, in  $j$  iterations we can produce  $M_n$  which are good to the  $j$ th order in  $K$ . Given a list of one-rooted star graphs, with up to  $L$  lines, ordered by root valence, together with their symmetry numbers  $s(\tau)$  and free multiplicities (the multiplicities are the same as those of their skeleton, single-line star graphs), we can compute from Eqs. (4.8) and (4.9) the expansion of the  $M_n(i)$  to order  $K^L$ . These algebraic manipulations were performed using the ALTRAN<sup>(36)</sup> system on a CDC 7600 computer. The  $M_n$  were first expressed in terms of the  $M_n^0$  and then, using the usual moment-cumulant relations, reexpressed in terms of the  $I_n(\tilde{H})$ . Here all  $\tilde{H}_i$  are taken as equal to a single  $\tilde{H}$ . Since  $M_1(i)$  is the magnetization per site in a uniform field  $\tilde{H}$ , we can use it to find the series expansions for the susceptibility  $\chi$  and  $\partial^2\chi/\partial\tilde{H}^2$  by direct differentiation. The resulting series are listed in the Appendix for the linear chain (LC), plane square (PSQ), triangular (TRI), simple cubic (SC), body-centered-cubic (BCC), face-centered-cubic (FCC), hyper-simple-cubic (HCS), and hyper-body-centered-cubic (HBCC) lattices.

In order to assemble the necessary combinatorial data we must start with a list of the basic single-line, unrooted star graphs. This list has been taken from Baker *et al.*<sup>(37)</sup> except for the ten-line, nine- and eight-vertex graphs (cyclotomic numbers  $c = 2$  and  $c = 3$ ), where the list was not complete. We are grateful to M. F. Sykes<sup>(38)</sup> for the lists of these stars. Here there are seven theta graphs ( $c = 2$ ) and eleven alpha, nine beta, fifteen gamma, and five delta graphs ( $c = 3$ ). In Table I, we list the number of stars<sup>(39)</sup> by number of lines and cyclotomic number ( $c = 1 + l - v$ , where  $v$  is the number of vertices). We have adapted the method of Baker *et al.*<sup>(37)</sup> to count the free multiplicities of these stars on the eight lattices mentioned above. These data are reported elsewhere.<sup>(40)</sup>

The next step is to produce the list of multiline stars. We have done this by systematically adding extra lines to the single-line stars, and then checking to eliminate duplicates by the use of our weak-embedding-graph-on-graph-counting program. The number of such multiline stars is given in Table II. By adding a root point to the unrooted multiline stars we obtain the singly rooted multiline stars. We have added a root in all possible ways

**Table I. The Number of Single-Line Stars Having  $l$  Lines and Cyclotomic Index  $c$**

		$l$										
$c$	1	2	3	4	5	6	7	8	9	10	Total	
0	1	0	0	0	0	0	0	0	0	0	1	
1			1	1	1	1	1	1	1	1	8	
2					1	2	3	4	6	7	23	
3						1	3	9	20	40	73	
4								2	14	50	66	
5									1	12	13	
6										1	1	
Total	1	0	1	1	2	4	7	16	42	111	185	

**Table II. The Number of Multiline Stars Having  $l$  Lines and Cyclotomic Index  $c$**

		$l$										
$c$	1	2	3	4	5	6	7	8	9	10	Total	
0	1	0	0	0	0	0	0	0	0	0	1	
1		1	1	1	1	1	1	1	1	1	9	
2			1	1	2	3	4	5	7	8	31	
3				1	2	6	11	23	40	70	153	
4					1	3	11	33	96	234	378	
5						1	4	22	89	345	461	
6							1	5	38	212	256	
7								1	7	63	71	
8									1	8	9	
9										1	1	
Total	1	1	2	3	6	14	32	90	279	942	1370	

and again used a version of our graph-on-graph-counting program to weed out duplicates. The number of such graphs, classified by root valence and number of lines, is given in Table III. These graphs and those of Table II are described in detail by Kincaid *et al.*<sup>(40)</sup> This completes our brief description of the combinatorial data needed to derive the magnetization,  $\chi$ , and  $(\partial^2\chi/\partial\tilde{H}^2)$  by the method of Eqs. (4.8) and (4.9) as described above. We remark, as is generally true in computations of this sort, that to extend this method by one more order would be substantially more work than was required to derive the first ten orders.

The ALTRAN system was also used to calculate the derivatives of  $\chi$ ,  $\partial^2\chi/\partial\tilde{H}^2$ , and  $\mu_2$  with respect to  $\tilde{g}_0$ . Using these derived series and the



**Table III. The Number of One-Rooted Multiline Stars with  $l$  Lines in the Set of Graphs  $G_i$  Such that  $i$  Lines are Incident Upon the Root Point**

	$l$										
	1	2	3	4	5	6	7	8	9	10	Total
$G_1$	1	0	0	0	0	0	0	0	0	0	1
$G_2$		1	1	2	4	11	31	104	369	1439	1962
$G_3$			1	1	3	9	28	97	371	1468	1978
$G_4$				1	2	6	19	68	252	1020	1368
$G_5$					1	2	8	30	123	514	678
$G_6$						1	3	12	50	217	283
$G_7$							1	3	15	70	89
$G_8$								1	4	20	25
$G_9$									1	4	5
$G_{10}$										1	1
Total	1	1	2	4	10	29	90	315	1185	4753	6390

relation

$$\begin{aligned}
 [\partial I_n(0)/\partial \tilde{g}_0]_{I_2(0)} &= I_{n+4}(0) - I_n(0)I_4(0) \\
 &+ [I_{n+2}(0) - I_n(0)][I_4(0) - I_6(0)]/[I_4(0) - 1] \quad (4.10)
 \end{aligned}$$

we were able to produce the series required to calculate  $\beta(g)$ , which can be expressed as

$$\beta(g) = (4 - d) \tilde{g}_0 \left( \frac{\partial g}{\partial \tilde{g}_0} \right)_K \left[ 1 + 2 \frac{\tilde{g}_0(\partial \xi^2 / \partial \tilde{g}_0)_K}{K(\partial \xi^2 / \partial K)_{\tilde{g}_0}} \right]^{-1} \quad (4.11)$$

The series for  $(\partial \chi / \partial \tilde{g}_0)_K$ ,  $(\partial^3 \chi / \partial \tilde{g}_0 \partial \tilde{H}^2)_K$ , and  $(\partial \mu_2 / \partial \tilde{g}_0)_K$  are considerably longer than the other series; they are listed in the report by Kincaid *et al.*<sup>(40)</sup>

We have computed the correlation length  $\xi^2$  from the second moment definition [see Eq. (2.21)] in zero magnetic field. Since every  $G_{\text{odd}}$  has at least one odd vertex (as each line has two ends), it must vanish by spin symmetry as  $\tilde{H} \rightarrow 0$ . The same is also true of  $M_{\text{odd}}$ . By the definition of  $\xi^2$ , we must sum over the lattice, the spin-spin correlation function times the distance squared between the two spins. According to the rules of Wortis for graphs with renormalized vertex functions, the required graphs are therefore those with less than eleven edges and with exactly two odd vertices (the two root points). Following Wortis, it is convenient to classify all such graphs into those with articulation points (nodes) and those without. We will just consider the multiline star graphs with exactly two odd vertices. These comprise a subgroup of the multiline stars reported in

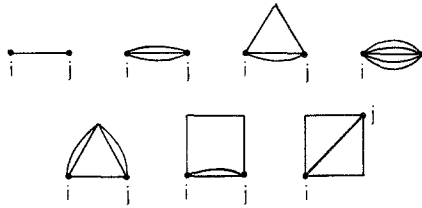


Fig. 2. Doubly rooted, multiline stars with exactly two odd vertices (the root points). These stars belong to class A, since the root points are nearest neighbors.

Table II. The first few are shown in Fig. 2. It is convenient to further classify the graphs as class A, in which the root points are nearest neighbors, and class B, in which they are not. It is to be noted that all the graphs in Fig. 2 are in class A. In Table IV we list the breakdown of such graphs.

Graphs with articulation points consist only of strings of star graphs joined at the odd root points by the conservation of evenness and oddness. For terms through tenth order, the only graphs which may be repeated are those with five edges or less, i.e, just those shown in Fig. 2. We may formally write the sum of all graphs linking points  $i$  and  $j$  as<sup>(34)</sup>

$$C(ij) = \sum_{\epsilon, \lambda} M_{\epsilon+1}(i) I_{\epsilon\lambda}(ij) M_{\lambda+1}(j) + \sum_{\epsilon, \lambda, \mu, \nu, k} M_{\epsilon+1}(i) I_{\epsilon\lambda}(ik) M_{\lambda+\mu}(k) I_{\mu\nu}(kj) M_{\nu+1}(j) + \dots \quad (4.12)$$

where  $I_{\epsilon\lambda}(ik)$  is the sum of all star graphs (divided by their symmetry numbers) with a root of valence  $\epsilon$  at  $i$  and valence  $\lambda$  at  $k$ . More formally we may rewrite Eq. (4.12) as

$$C(ij) = [(1 - MI)^{-1} - 1]M \quad (4.13)$$

We emphasize at this point that the star graphs summed to form  $I_{\epsilon\lambda}(ik)$  have *labeled* roots and so are more numerous than the unlabeled stars of Table IV. We list the number of such stars in Table V. If we separate

**Table IV. The Number of Multiline Stars of Class A and Class B with  $l$  Lines and Exactly Two Odd, Unlabeled Root Points**

	$l$										Total
	1	2	3	4	5	6	7	8	9	10	
A	1	0	1	1	4	5	17	36	117	311	493
B	0	0	0	0	0	2	4	16	53	199	274
Total	1	0	1	1	4	7	21	52	170	510	767

**Table V. The Number of Class A and Class B Multiline Stars with  $l$  Lines and Exactly Two Odd, Labeled Root Points**

	$l$										
	1	2	3	4	5	6	7	8	9	10	Total
A	1	0	1	1	4	6	19	45	142	411	630
B	0	0	0	0	0	2	5	24	88	350	469
Total	1	0	1	1	4	8	24	69	230	761	1099

explicitly the star graphs into class A and B, we notice that the smallest class B graph has six edges and so is not repeated through tenth order. Thus, exact through tenth order we may rewrite Eq. (4.13) as

$$\begin{aligned}
 C(ij) &= \left[ (1 - MI^A - MI^B)^{-1} - 1 \right] M \\
 &= \left[ (1 - MI^A)^{-1} - 1 \right] M + (1 - MI^A)^{-1} MI^B (1 - MI^A)^{-1} M \quad (4.14)
 \end{aligned}$$

We are now in a position to reduce the contribution of class A alone,

$$\mu_2^A = \sum_{j \neq 0}^{N-1} \left( \frac{r_{0j}}{a} \right)^2 C^A(0j) \quad (4.15)$$

to a simple calculation. Through tenth order the matrix  $I^A$  may be taken as a five by five parametric matrix labeled by (1, 3, 5, 7, 9). Its entries are constructed from the sums of powers of  $K$  and of products of renormalized vertex functions [Eq. (4.8)], as computed in the first part of this section, which are appropriate to the star graphs involved. Now, insofar as summation over lattice sites is concerned, since we are using the free multiplicities, the free multiplicity divided by the symmetry number of a string of star graphs is just the product of the respective free multiplicities divided by the symmetry number; we may simply attach this factor to each star graph used in the construction of the  $I^A$  matrix. To obtain the correct contribution to  $\mu_2$  we define the matrix

$$V_{\epsilon\mu} = \sum_{\lambda=1, \text{odd}}^9 I_{\epsilon\lambda} M_{\lambda+\mu} \quad (4.16)$$

for class A and the vectors

$$\mathbf{m} = \begin{bmatrix} M_2 \\ M_4 \\ M_6 \\ M_8 \\ M_{10} \end{bmatrix}, \quad \mathbf{V}_1 = \begin{bmatrix} V_{1,1} \\ V_{3,1} \\ V_{5,1} \\ V_{7,1} \\ V_{9,1} \end{bmatrix}, \quad \mathbf{v}_{i+1} = V\mathbf{v}_i \quad (4.17)$$

in terms of the renormalized functions  $M_n$ . Then

$$\mu_2^A = \sum_{i=1}^n c_i \mathbf{m} \cdot \mathbf{v}_i \tag{4.18}$$

follows by a short calculation, where  $c_i$  is the mean square length of an  $n$ -step random walk on the lattice of interest. Following Domb,<sup>(41)</sup> we can compute that

$$c_j = jq^j \tag{4.19}$$

where  $q$  is the lattice coordination number. Again the necessary algebra for the contributions of class A to  $\mu_2$  has been done using the ALTRAN system.<sup>(36)</sup>

To obtain the contributions from a graph of class B, we must first compute directly the  $\sum_j r_{ij}^2$  for  $\mathbf{i}$  and  $\mathbf{j}$  the two, odd-valence roots for those graphs of class B. To include the class A pre- and postfactors determined from Eq. (4.14), we make use of the following observation. If we add a single line  $\overline{jk}$  to site  $j$  (a root) of any fixed configuration of a graph  $G$  on a lattice, then

$$\begin{aligned} \sum_{\mathbf{k}} (\mathbf{r}_{ij} + \mathbf{r}_{jk})^2 &= \sum_{\mathbf{k}} (\mathbf{r}_{ij})^2 + 2 \sum_{\mathbf{k}} \mathbf{r}_{ij} \cdot \mathbf{r}_{jk} + \sum_{\mathbf{k}} (\mathbf{r}_{jk})^2 \\ &= q(\mathbf{r}_{ij})^2 + 0 + qa^2 \\ &= q[(\mathbf{r}_{ij})^2 + 1] \end{aligned} \tag{4.20}$$

where the zero follows by lattice symmetry,  $q$  is again the lattice coordination number, and  $a$  is the lattice spacing, which for present purposes can be taken as unity. Now, if we sum (4.20) over all configurations of  $G$  we obtain

$$\sum_G \sum_{\mathbf{k}} (\mathbf{r}_{ij} + \mathbf{r}_{jk})^2 = q [c_G + M_f(G)] \tag{4.21}$$

where

$$c_G = \sum_G (\mathbf{r}_{ij})^2 \tag{4.22}$$

and  $\sum_G$  is the sum over the free embeddings of  $G$  on the lattice. This calculation is easily extended to add an arbitrary number of class A decorations (in a string) to one or both roots of the class B graph. The result, for the addition of  $n$  class A graphs  $\tau_i$ , is

$$\sum \mathbf{r}_{12}^2 = \left[ \prod_{i=1}^n \frac{M_f(\tau_i)}{s_l(\tau_i)} \right] [c_G + nM_f(G)] \tag{4.23}$$

where **1** and **2** are the two odd vertices of the resultant string and  $s_l(\tau_i)$  is the symmetry number of  $\tau_i$  with its two roots labeled.

Since, through tenth order, only 13 decorations are possible on B graphs with six edges (for graphs with seven edges only six, for graphs with eight edges only three, for graphs with nine edges only two, and, of course, none for graphs with ten edges), there are a total of 654 separate contributions from the class B graphs to be obtained (see Table V), and the only additional combinatorial information needed is the  $c_G$  for the class B graphs.

All the methods and data discussed in this section are fully reported elsewhere.<sup>(40)</sup> The zero-field series for  $\chi$ ,  $\partial^2\chi/\partial\tilde{H}^2$ , and  $\mu_2$  are given in the Appendix.

Finally, we report here the new terms which we have added to the known spin-1/2 Ising model series. We have added for  $\mu_2 (= 2d\chi\xi^2)$  on the triangular lattice<sup>7</sup>

$$+ 5765546236416K^9/9! + 271060330512384K^{10}/10! \quad (4.24)$$

We have added for the  $\partial^2\chi/\partial\tilde{H}^2$  series the terms

$$- 29883457877071616K^9/9! - 39510128291537117184K^{10}/10! \quad (4.25)$$

on the FCC lattice,<sup>(43)</sup> and

$$- 601493660302278656K^{10}/10! \quad (4.26)$$

on the HSC lattice (this term agrees with the new results of Gaunt *et al.*<sup>(12)</sup>) Finally, we have added the entire series for the HBCC lattice:

$$\begin{aligned} & -2 - 128K - 9792K^2/2! - 886784K^3/3! \\ & - 92722944K^4/4! - 11014965248K^5/5! \\ & - 1465369976832K^6/6! \\ & - 215937597784064K^7/7! \\ & - 34916329300783104K^8/8! \\ & - 6147843514432913408K^9/9! \\ & - 1170908043876450435072K^{10}/10! \dots \end{aligned} \quad (4.27)$$

### 5. LARGE- AND SMALL- $\tilde{g}_0$ BEHAVIOR

Some aspects of the large- and small- $\tilde{g}_0$  behavior of various quantities can be obtained without extensive numerical calculations. We begin this section by first considering how the moments  $I_n(0)$  and  $\tilde{A}(\tilde{g}_0)$  depend upon  $\tilde{g}_0$ ; we then go on to discuss the behavior of  $\chi$ ,  $\partial^2\chi/\partial\tilde{H}^2$ ,  $\xi^2$ ,  $g$ , and  $\beta(g)$ .

In order to use the series derived in the previous section and tabulated

<sup>7</sup> The coefficient of  $K^{10}$  in Eq. (4.24) is not identical to that given by Moore.<sup>(42)</sup>

in the Appendix, it is necessary to evaluate with high precision the moment integrals  $I_n(0)$  defined by Eq. (2.18). The direct numerical evaluation of these integrals presents no problem as long as  $\tilde{g}_0$  is not too large. In this latter region, however, it is desirable to use an expansion in powers of  $\tilde{g}_0^{-1}$  to obtain the results. Before we discuss this expansion we will point out a few simple properties of these moment integrals. First let

$$J_n = \int_0^\infty dx x^{2n} \exp(-\tilde{g}_0 x^4 - \tilde{A} x^2) \tag{5.1}$$

so that

$$I_{2n}(0) = J_n/J_0 \tag{5.2}$$

If we integrate by parts we find, using Eq. (5.1), that

$$J_n = 4\tilde{g}_0 J_{n+2}/(2n+1) + 2\tilde{A} J_{n+1}/(2n+1), \quad n > -1/2 \tag{5.3}$$

Thus we obtain the recursion relation

$$R_{n+1} = -\tilde{A}/(2\tilde{g}_0) + (2n+1)/(4\tilde{g}_0 R_n) \tag{5.4}$$

where  $R_n = J_{n+1}/J_n$ . If  $\tilde{A} \leq 0$ , then (5.4) can be used to recur upward in  $n$ , starting from  $\tilde{A}(\tilde{g}_0)$  and  $R_0 = 1$ . If, on the other hand,  $\tilde{A} > 0$ , then cancellation can occur between the terms on the right-hand side of Eq. (5.4). This cancellation can be quite significant as  $\tilde{g}_0 \rightarrow 0$ . Alternatively, we can rewrite Eq. (5.4) as

$$R_n = (2n+1)/(2\tilde{A} + 4\tilde{g}_0 R_{n+1}) \tag{5.5}$$

which is quite stable for downward recursion in  $n$  when  $\tilde{A} > 0$ . If one starts with the asymptotic guess

$$R_n \sim \text{Max}[(n/(2\tilde{g}_0))^{1/2}, (2n+1)/(2\tilde{A})] \tag{5.6}$$

for large  $n$  and the result that  $R_0(R_n)$  is monotonic increasing or decreasing as  $n$  is even or odd, one can rapidly obtain from  $R_0 = 1$  and  $\tilde{A}(\tilde{g}_0)$  the set of  $R_n$  from Eq. (5.6) to the desired accuracy by a set of successive approximations to  $R_{n_{\text{max}}}$ , where  $n_{\text{max}}$  is the largest value of  $n$  required. Since

$$I_{2n}(0) = \prod_{j=0}^n R_j \tag{5.7}$$

this analysis reduces the numerical problem to the evaluation of  $\tilde{A}(\tilde{g}_0)$ , plus some other well-defined calculations.

To obtain  $\tilde{A}(\tilde{g}_0)$  we first discuss the problem of expansions near  $\tilde{g}_0 = 0$  and  $\infty$ . We follow the analysis of Wehner and Baeriswyl<sup>(44)</sup> of the function

$$Z(p) = \int_{-\infty}^\infty dy \exp(-2py^2 - y^4) \tag{5.8}$$

First, however, we remark that one can easily solve for the crossover value

of  $\tilde{g}_0$  from  $R_0 = 1$  and Eq. (5.1) as

$$\tilde{g}_0(\tilde{A} = 0) = [\Gamma(3/4)/\Gamma(1/4)]^2 \simeq 0.1142366452 \quad (5.9)$$

Now in the range  $\tilde{A} > 0$ , we can use the change of variable  $\tilde{g}_0 x^4 = y^4$ , which implies that  $p \rightarrow +\infty$  as  $\tilde{g}_0 \rightarrow 0$ . Wehner and Baeriswyl give in this case the result

$$Z(p) = (\pi/2p)^{1/2} {}_2F_0(1/4, 3/4; -1/p^2) \quad (5.10)$$

where  ${}_2F_0$  is a confluent hypergeometric function whose expansion is only asymptotic. This result leads directly to the equation

$$\tilde{A} = {}_2F_0(5/4, 7/4; -4\tilde{g}_0/\tilde{A}^2) / [2 {}_2F_0(1/4, 3/4; -4\tilde{g}_0/\tilde{A}^2)] \quad (5.11)$$

which can be used to solve for the series expansion of  $\tilde{A}(\tilde{g}_0)$

$$\tilde{A} = 1/2 - 6\tilde{g}_0 + 48\tilde{g}_0^2 + O(\tilde{g}_0^3) \quad (5.12)$$

In the case  $\tilde{A} < 0$  we see that the corresponding limit is  $p \rightarrow -\infty$ . Here Wehner and Baeriswyl give

$$Z(p) = (\pi/-p)^{1/2} \exp(p^2) {}_2F_0(1/4, 3/4; 1/p^2) \quad (5.13)$$

Again, this result leads to an equation

$$\begin{aligned} \tilde{A} &= -2\tilde{g}_0 + \tilde{g}_0/\tilde{A} \\ &+ 3(\tilde{g}_0^2/\tilde{A}^3) {}_2F_0(5/4, 7/4; 4\tilde{g}_0/\tilde{A}^2) / {}_2F_0(1/4, 3/4; 4\tilde{g}_0/\tilde{A}^2) \end{aligned} \quad (5.14)$$

which can be used to solve for the series expansion of  $\tilde{A}(\tilde{g}_0)$  in powers of  $\tilde{g}_0^{-1}$ . We find

$$\begin{aligned} \tilde{A} &= -2\tilde{g}_0 - 1/2 - (1/4)\tilde{g}_0^{-1} - (7/16)\tilde{g}_0^{-2} \\ &- (83/64)\tilde{g}_0^{-3} - (1357/256)\tilde{g}_0^{-4} \\ &- (27933/1024)\tilde{g}_0^{-5} - (688971/4096)\tilde{g}_0^{-6} \\ &- (19746759/16384)\tilde{g}_0^{-7} + O(\tilde{g}_0^{-8}) \end{aligned} \quad (5.15)$$

As a practical matter we have in fact used the expansions (5.15) for  $\tilde{A}$  when  $\tilde{g}_0$  is near  $\infty$  and used an accelerated binary search procedure on the integral definition otherwise. Once a reliable value of  $\tilde{A}$  is obtained the computation of the moments is not hard using Eqs. (5.4), (5.5), and (5.7); we have, however, verified all values of the moments by direct integration except for  $\tilde{g}_0$  very near  $\infty$ .

It is interesting to consider as well the expansions of the moments  $I_{2n}(0)$  in powers of  $\tilde{g}_0$  and  $\tilde{g}_0^{-1}$ . First, for small  $\tilde{g}$  we can compute using Eq. (5.12) that

$$I_{2n}(0) = 1 \cdot 3 \cdot 5 \cdots (2n-1) [1 - 4n(n-1)\tilde{g}_0] + O(\tilde{g}_0^2) \quad (5.16)$$

From Eqs. (5.16) and (3.5) we compute that

$$\begin{aligned}
 M_2^0(0) &= 1.0, & M_4^0(0) &= -4! \tilde{g}_0 + O(\tilde{g}_0^2) \\
 M_{2n}^0(0) &= O(\tilde{g}_0^2), & n &\geq 3
 \end{aligned}
 \tag{5.17}$$

Hence in the high-temperature expansions, to compute a thermodynamic quantity to order  $\tilde{g}_0$  we can ignore all vertices at which more than four lines meet, including in our count the field derivatives as lines. For example, we show in Fig. 3 the topologically distinct graphs which contribute to  $\partial^2\chi/\partial\tilde{H}^2$  through order  $K^4$  and  $\tilde{g}_0$ . It is not difficult from considerations of this type and Eq. (3.20) to deduce

$$\begin{aligned}
 \chi &= 1/(1 - qK) + O(\tilde{g}_0), & \xi^2 &= qK/[2d(1 - qK)] + O(\tilde{g}_0) \\
 (\partial^2\chi/\partial\tilde{H}^2) &= -4! \tilde{g}_0/(1 - qK)^4 + O(\tilde{g}_0^2)
 \end{aligned}
 \tag{5.18}$$

By combining Eqs. (2.17), (2.22), and (5.18) we may rewrite Eq. (2.25) as

$$g_R = g_0 + O(g_0^2) \tag{5.19}$$

independent of  $K$  or lattice. This formula is in line with the idea that  $g_R$  is a renormalized version of  $g_0$ .

To consider the expansion in powers of  $\tilde{g}_0^{-1}$  we return to the recursion formulas for the moments and their ratios. (See Caginalp, Constantinescu, and Bender *et al.*<sup>(27)</sup> for different approaches.) Using Eqs. (5.4), (5.15), and  $R_0 = 1$ , we deduce that

$$R_{n+1} = 1 + (n + 1)/2\tilde{g}_0 + O(\tilde{g}_0^{-2}) \tag{5.20}$$

so that

$$I_{2n}(0) = 1 + n(n - 1)/4\tilde{g}_0 + O(\tilde{g}_0^{-2}) \tag{5.21}$$

It is not difficult to extend these series to higher orders in  $\tilde{g}_0^{-1}$ . Plainly, by virtue of the fact that the coefficients of every power of  $K$  in the high-temperature series listed in the Appendix is a polynomial in the  $I_{2n}(0)$ , it follows that algebraic substitution of Eq. (5.21) into these series leads to the spin-1/2 Ising model term plus correction terms containing powers of  $\tilde{g}_0^{-1}$ .

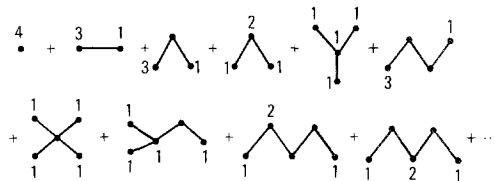


Fig. 3. The topologically distinct graphs that contribute to  $\partial^2\chi/\partial\tilde{H}^2$  through order  $K^4$  and  $\tilde{g}_0$ .



Since the high-temperature series are convergent for all temperatures above some temperature [ $\geq T_c(\tilde{g}_0)$ ], we can use analytic continuation to extend the following result to all  $T > T_c$  for the spin-1/2 Ising model. A direct analysis of Eq. (3.11) shows that term by term

$$\lim_{\tilde{g}_0 \rightarrow \infty} \beta(g, T > T_c) \propto \lim_{\tilde{g}_0 \rightarrow \infty} \tilde{g}_0^{-1} = 0 \tag{5.22}$$

Thus the  $\beta$  function necessarily goes smoothly to zero for any fixed correlation length as the bare coupling constant  $g_0$  goes to infinity. Thus

$$\beta(g_0 = \infty, \xi^2) \equiv 0 \tag{5.23}$$

This result is consistent with the idea that  $g_0 = \infty$  corresponds to the renormalization-group fixed point [ $\beta(g^*) = 0$ ] and the idea that the approach as  $\xi^2 \rightarrow \infty$  is a smooth one. However, this result certainly does not preclude the possibility that Schrader monotonicity fails and that this zero of the  $\beta$  function is not the renormalization group zero. Clearly, if  $\partial g / \partial(\tilde{g}_0^{-1}) < 0$  near  $\xi^2 = \infty$ , then Schrader monotonicity will have had to have failed. Thus a study of the possibility of a change of sign of the first expansion coefficient of  $g$  in powers of  $\tilde{g}_0^{-1}$  can reveal the failure of Schrader monotonicity in a way that is likely to be numerically more satisfactory than analyzing the asymptotic behavior at the critical point.

We remark that Eq. (5.23) shows that the heuristic underpinnings of efforts to “turn” the direction of the derivatives, such as that of Nickel and Sharp,<sup>(13)</sup> need more careful discussion since their analogous function is manifestly not identically zero for the spin-1/2 Ising model as is the usual  $\beta$  function.

## 6. THE CORRELATION-LENGTH SERIES

In order to analyze effectively the series data that we have derived it is desirable to utilize any exact information that is available. In particular, exact knowledge of the critical point location is of great benefit in the study of critical indices. In general we do not have such exact knowledge of the critical temperature for the models we are studying, but we do, of course, for the correlation length: at the critical point the correlation length  $\xi$  is infinite. Since the correlation length series begins

$$\xi^2(K) = (q/2d)K + O(K^2) \tag{6.1}$$

and  $\xi^2(K)$  appears to be a monotonic function between  $K = 0$  and  $K = K_c$ , it is possible, for a fixed value of  $\tilde{g}_0$ , to revert the series  $\xi^2(K)$  to give

$$K = \sum_{i=1}^{\infty} t_i \xi^{2i} \tag{6.2}$$

This series can then be substituted into  $\chi(K)$  and  $(\partial^2\chi/\partial\tilde{H}^2)(K)$  to re-express these series as power series in  $\xi^2$ .

A further technical device is to transform the variable  $\xi^2$  so that the critical point  $\xi^2 = \infty$  is mapped into a finite point. This mapping is conveniently accomplished by the Euler transformation

$$x = A\xi^2/(1 + A\xi^2) \tag{6.3}$$

Clearly, when  $\xi^2 \rightarrow \infty$ ,  $x \rightarrow 1$ . This transformation has a parameter  $A$  at our disposal that determines the point ( $\xi^2 = -A^{-1}$ ) in the  $\xi^2$  plane that is mapped into  $\infty$  in the  $x$  plane. In order to choose  $A$  in the most helpful manner, we have analyzed the singularity structure of  $g$  [Eq. (2.25)] in the  $\xi^2$  plane by means of  $d \log$  Padé approximants.<sup>(45)</sup> The  $[L/M]$  Padé approximant to a function  $f(x)$  is

$$[L/M] = P_L(x)/Q_M(x) \tag{6.4}$$

where  $P_L$  and  $Q_M$  are polynomials of degrees  $L$  and  $M$ , respectively. The coefficients are determined by the equations

$$Q_M(x)f(x) - P_L(x) = O(x^{L+M+1}), \quad Q_M(0) = 1.0 \tag{6.5}$$

By their nature they approximate well a polar singularity and by clustering poles and zeros they can approximate the behavior near more complex types of singularities. If  $f(x)$  has a singularity of the form  $(x - x_0)^{-\psi}$ , then the logarithmic derivative of  $f$  has a simple pole at  $x = x_0$  with residue  $-\psi$ . Consequently, the  $d \log$  Padé approximants form a useful tool to survey the complex plane for singularities. In particular, we note that the  $[M - 2/M]$  approximants to  $d(\ln f)/dx$  are invariant under the transformation on  $f$  defined by Eq. (6.3). As a result of this survey we find that for  $A = 2(d + 1)$  the transformation moves  $\xi^2 = \infty$  to  $x = 1$  and generally moves all the other singularities outside the unit circle, which is a desirable manipulation for methods of analysis for series data that are not completely invariant under such transformations.

Once the series for

$$g = \frac{-v \frac{\partial^2\chi}{\partial\tilde{H}^2}(\xi^2(x))}{a^d \chi^2(\xi^2(x)) [\xi^2(x)]^{d/2}} \tag{6.6}$$

has been produced, the next step is to analyze its behavior in the neighborhood of  $x = 1$ . We begin by investigating the possibility of a confluence of singularities. Our method of analysis is due to Baker and Hunter.<sup>(46)</sup> Suppose that

$$f(x) \simeq \sum_{n=1}^{\infty} A_n(1 - x)^{\alpha_n}, \quad \alpha_n < \alpha_{n+1} \tag{6.7}$$

If  $x = 1 - e^{-y}$ , then from

$$w(y) = f(1 - e^{-y}) = \sum_{m=0}^{\infty} w_m y^m \tag{6.8}$$

we can form the auxiliary function

$$W(y) = \sum_{m=0}^{\infty} w_m (m!) y^m = \sum_{n=1}^{\infty} \frac{A_n}{1 - \alpha_n y} \tag{6.9}$$

Clearly, Padé approximants to  $W(y)$  reveal the amplitudes and index of such confluent singularities.

We have performed this type of analysis on the function  $Q(x)$  defined by

$$Q(x) = (\partial^2 \chi / \partial \tilde{H}^2) / \chi^2 \tag{6.10}$$

with  $\chi$  given by Eq. (6.3). For small  $\tilde{g}_0 (\lesssim 10^{-3})$ , Gaussian model behavior dominates on all lattices; we find that

$$Q(x) \sim \frac{Q_0}{(1-x)^p} [1 + Q_1(1-x) + \dots] \tag{6.11}$$

with  $p = 2$  (i.e., only “analytic” corrections are present). On the one- and four-dimensional lattices,  $Q(x)$  maintains the structure shown in Eq. (6.11) except that the index  $p = 2$ , for  $\tilde{g}_0$  near zero, decreases to approximately 0.5 and 1.7, respectively, in the Ising limit  $\tilde{g}_0 = \infty$ . The large- $\tilde{g}_0$  behavior of  $Q(x)$  on the two- and three-dimensional lattices also takes the form of Eq. (6.11); however, when  $\tilde{g}_0 \sim 0.1$  the possibility of a significant confluence cannot be ruled out. The Padé analysis did not appear to be stable in the neighborhood of  $\tilde{g}_0 = 0.1$ , so that we do not have a clear picture of the confluent structure there. We conclude from our analysis that there is no troublesome confluence near the Ising limit and we will proceed with our series evaluation by assuming that there is only one dominant singularity at  $x = 1$ .

Having checked for possible confluent singularities, we finally come to the numerical aspects of this work, i.e., the calculation of  $g(\tilde{g}_0, \xi^2)$ . The main technique we shall use is the integral approximant method.<sup>(47,48)</sup> In this method a set of three polynomials is determined from

$$Q_M(x)(df/dx) + P_L(x)f(x) + R_N(x) = O(x^{L+M+N+2}) \tag{6.12}$$

and the  $[N/L; M]$  integral approximant is determined by integrating Eq. (6.12) with the right-hand side set equal to zero. With some exceptions<sup>(47)</sup> this solution has the structure

$$[N/L; M] \approx A(x)(x - x_i)^{-\gamma_i} + B(x) \tag{6.13}$$

near the roots  $x_i$  of  $Q_M(x)$ . The functions  $A$  and  $B$  are regular near the  $x_i$ . Solutions of this nature allow us to compute an accurate approximation to  $\xi^d g$  near  $x = 1$  which reproduces the expected range of behavior near  $x = 1$ . The imposition of the condition that there be a singularity at  $x = 1$  is easily accomplished by the addition of a linear equation between the polynomial coefficients

$$Q_M(1) = 0 \quad (6.14)$$

The description of the results of the analysis of our data by this method is given in the next section.

The bare coupling constant  $g_0$  defined by Eq. (2.17) is calculated using values of  $K(\xi^2)$  obtained from the [5/5] Padé to the series given in Eq. (6.2). This procedure is straightforward and fast from a computational point of view, but we do not expect that this is the most accurate method for obtaining estimates of  $K$  in the limit  $\xi^2 \rightarrow \infty$ , i.e.,  $K_c$ . (Experience on other models suggests that  $K_c$  is most accurately obtained from an analysis of the susceptibility series.) We emphasize, however, that the possible errors in our estimates of  $g_0$  will not have any significant effect on the analysis of  $g(g_0, \xi^2)$  that follows.

## 7. THE RENORMALIZED COUPLING CONSTANT

In this section we present our numerical analysis of the dependence of  $g$  on  $g_0$ ,  $\tilde{g}_0$ , and  $\xi^2$ . In previous sections we have described the methods by which series for  $g$  and  $g_0$  in terms of  $\xi^2$  are generated. The coefficients of these series are determined by a choice of the parameter  $\tilde{g}_0$ . For any given lattice a table of  $g$  and  $g_0$  for various choices of  $\tilde{g}_0$  and  $\xi^2$  can be constructed. The study of this table, for the eight lattices we consider, is given below. The strong coupling region  $g_0 \rightarrow \infty$ ,  $\xi^2 \rightarrow \infty$  is of special interest (see Section 3) and we note that in this limit it is more illuminating to study the dependence of  $g$  on  $\tilde{g}_0$  instead of  $g_0$ . We choose  $\tilde{g}_0$  as our important variable in the strong coupling limit rather than the customary<sup>(49)</sup> choice of  $g_0 \xi^{d-4}$  because we have direct calculational control over  $\tilde{g}_0$  and we bypass the problem of having to obtain precise values for  $K(\tilde{g}_0, \xi^2)$ .

We note that lattices of the same dimensionality lead to quite similar estimates of  $g$  and  $g_0$ . The apparent errors (defined below) in the calculated values of  $g$ , however, seem to vary considerably from lattice to lattice (with  $\tilde{g}_0$  and  $\xi^2$  fixed). The body-centered cubic family of lattices (LC, PSQ, BCC, and HBCC) was found to give the best results. The approximants for  $g$  on the triangular lattice exhibit so many interfering singularities that we were unable to obtain any meaningful estimates for  $g$ .

The values of  $g(\tilde{g}_0, \xi^2)$  cited here represent the simple average value of  $g$  obtained from those integral approximants  $[N/L; M]$ , where  $N + L + M + 1 = 10$  ( $N, L, M \geq 1$ ), that have no singularities in the closed interval  $-0.5 \leq x \leq 1.1$  except the expected singularity at  $x = 1$ . [Recall  $x = A\xi^2/(1 + A\xi^2)$ ,  $A = 2(d + 1)$ .] The apparent error assigned to this average value of  $g$  was obtained using the method of Hunter and Baker.<sup>(45)</sup> In our case this method is a simple one: let  $g'_p$  and  $g''_p$  be the smallest and largest values of  $g$  obtained from the integral approximants for which  $N + L + M + 1 = p$ ; the apparent error is  $\max\{|g'_9 \text{ or } g''_9\} - \{g'_{10} \text{ or } g''_{10}\}$ .

Many of the approximants used to calculate  $g$  for two- and three-dimensional lattices were often flawed in the sense that they had additional singularities within the interval  $[0.5, 1.1]$ . The presence of these singularities was a problem for values of  $\tilde{g}_0 \lesssim 0.5$ . The region around  $\tilde{g}_0 = 0.1$ , where the spin density  $F$  changes from Gaussian-like to Ising-like, was especially troublesome. We cannot explain conclusively why the approximants are so unstable in this region. However, one obvious possibility is that our series do not extend to high enough order in  $\xi^2$  to adequately represent  $g$  for large  $\xi^2$  when  $\tilde{g}_0 \lesssim 0.5$ ; another possibility is that there is a confluence of singularities in the region around  $\tilde{g}_0 = 0.1$ . The problems described above were not evident on the four-dimensional lattices.

In these troublesome regions of large apparent error, we find that  $g \rightarrow \infty$  as  $\xi^2 \rightarrow \infty$  for fixed  $\tilde{g}_0$ . This behavior implies a violation of Eq. (2.30). Therefore, in those cases where this type of spurious behavior is obtained, we have substituted an unproven, but compelling, procedure for estimating  $g$ ; it is based on our observation that for the small values of  $g_0$  in all cases where very stable approximants to  $g$  are obtained,  $g(\xi^2)$  is a monotonic decreasing function for fixed  $g_0$ :

For  $\tilde{g}_0 \lesssim 0.7$ ,  $g(\xi^2)$  is a monotonic decreasing function for fixed  $g_0$ . When we observe that  $g(\xi^2)$  begins to increase for  $\xi^2 > \xi_m^2$  then we set  $g(\xi^2) = g(\xi_m^2)$ . In this way we can obtain upper bounds for (7.1) the curves  $g(g_0)$  or  $g(\tilde{g}_0)$  in the limit  $\xi^2 \rightarrow \infty$ . *Curves obtained in this manner are drawn with a dashed line.*

### 7.1. $d=1$ (LC)

In Figs. 4 and 5 we have drawn  $g$  as a function of  $g_0$  and  $\tilde{g}_0$  for several values of  $\xi^2$ . The curves show that  $g$  is a monotonic increasing function of  $g_0$  and  $\tilde{g}_0$ , as expected from the work of Isaacson<sup>(50)</sup> and Marchesin.<sup>(51)</sup> The thick curve represents our estimate of the  $\xi^2 \rightarrow \infty$  limit. This limiting curve is in agreement with the numerical calculations of Marchesin.<sup>(51)</sup> It is clear from Fig. 4 that  $g(\xi^2)$  for fixed  $g_0$  is monotonic decreasing. We also note that the  $[2/2]$  Padé approximant to  $d(\ln Q)/dx$  appears to be exact

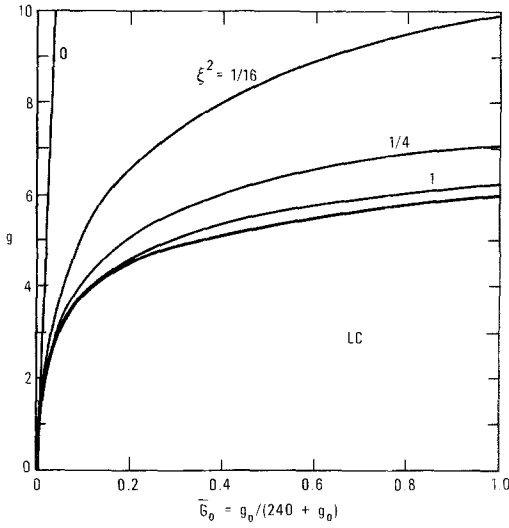


Fig. 4. The renormalized coupling constant  $g$  as a function of the bare coupling constant  $g_0$  for several values of the correlation length  $\xi$  on the linear chain lattice. The thick curve represents our estimate of  $g(g_0)$  in the limit  $\xi^2 \rightarrow \infty$ .

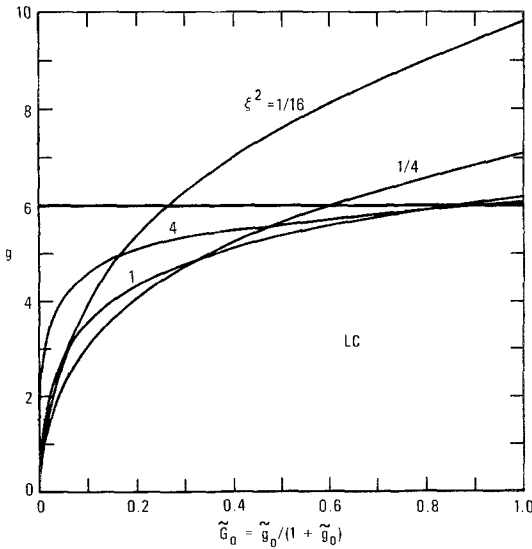


Fig. 5. The renormalized coupling constant  $g$  as a function of  $\tilde{g}_0$  for several values of the correlation length  $\xi$  on the linear chain lattice. The thick curve represents our estimate of  $g(\tilde{g}_0)$  in the limit  $\xi^2 \rightarrow \infty$ .

when  $\tilde{g}_0 = \infty$ . [ $Q$  is defined in Eq. (6.10).] We find that  $g(\tilde{g}_0 = \infty, \xi^2 = \infty) = 6.0$ .<sup>8</sup>

**7.2.  $d = 2$  (PSQ)**

Here, as for the case  $d = 1$ ,  $g(g_0)$  and  $g(\tilde{g}_0)$  with  $\xi^2$  fixed are smooth, monotonic increasing functions of  $g_0$  and  $\tilde{g}_0$ , respectively. (See Figs. 6 and 7.) For large  $g_0$  and  $\xi$ , the curve becomes flat [i.e.,  $(\partial g / \partial g_0)_{\xi^2} \rightarrow 0$  as  $g_0, \xi^2 \rightarrow \infty$ ]. This behavior is more easily indentified when  $g$  is plotted against  $\tilde{g}_0$  as in Fig. 7. In the parlance of the renormalization group and field theory methods, the strong coupling limit  $g_0 \rightarrow \infty$  commutes with the limit  $\xi^2 \rightarrow \infty$ ; this double limit represents a fixed point of the field theory.<sup>(53)</sup> Our estimate for the fixed point coupling constant  $g^*$  is  $14.5 \pm 0.2$  (PSQ); it is consistent with the calculations of Baker<sup>(11)</sup> and Baker *et al.*<sup>(32)</sup>

A unique value of  $g^*$  indicates that all continuous-spin models, of the type defined by Eqs. (2.15) and (2.16), have critical point properties that are described by a single field theory with renormalized coupling constant  $g^*$ .

<sup>8</sup> Bender *et al.*<sup>(52)</sup> have shown that 6.0 is in fact the exact result.

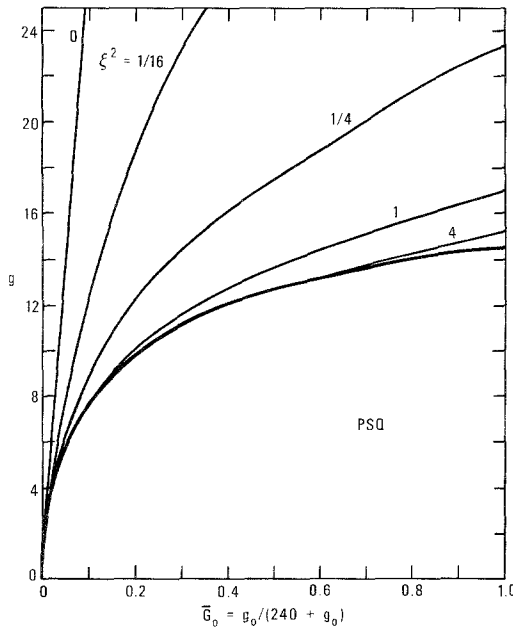


Fig. 6. The renormalized coupling constant  $g$  as a function of the bare coupling constant  $g_0$  for several values of the correlation length  $\xi$  on the plane square lattice. The thick curve represents our estimate of  $g(g_0)$  in the limit  $\xi^2 \rightarrow \infty$ .

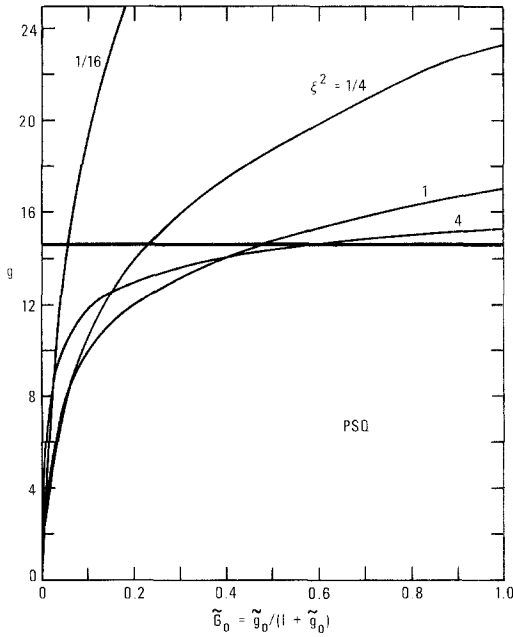


Fig. 7. The renormalized coupling constant  $g$  as a function of  $\tilde{g}_0$  for several values of the correlation length  $\xi$  on the plane square lattice. The thick curve represents our estimate of  $g(\tilde{g}_0)$  in the limit  $\xi^2 \rightarrow \infty$ .

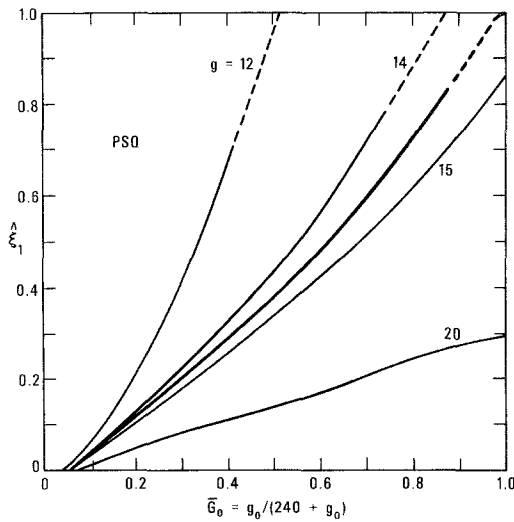


Fig. 8. Contours of the renormalized coupling constant  $g$  in the  $\hat{\xi}_1, \tilde{G}_0$  plane for the plane square lattice. Here  $\hat{\xi}_1 = \xi^2 / (1 + \xi^2)$  and  $\tilde{G}_0 = g_0 / (240 + g_0)$ . The thick curve represents  $g^* = 14.5$ .



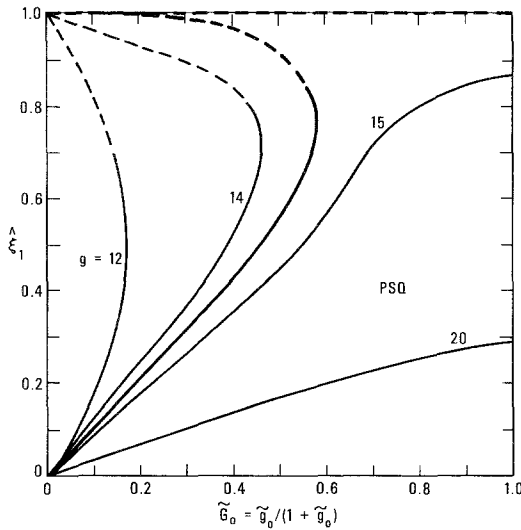


Fig. 9. Contours of the renormalized coupling constant  $g$  in the  $\hat{\xi}_1, \tilde{G}_0$  plane for the plane square lattice. Here  $\hat{\xi}_1 = \xi^2/(1 + \xi^2)$  and  $\tilde{G}_0 = \tilde{g}_0/(1 + \tilde{g}_0)$ . The thick curve represents  $g^* = 14.5$ .

That is, the set of continuous-spin models that we have considered all belong to the same “universality class”<sup>9</sup> (except the  $\tilde{g}_0 = 0$  case).

Note that here, as for  $d = 1$ ,  $g(\xi^2)$  with  $g_0$  fixed appears to be a monotonic decreasing function. This monotonicity is apparent in Fig. 6 and also in Fig. 8, where we have drawn contours of constant  $g$  in the  $g_0$ - $\xi^2$  plane. The constant- $g$  contours, when drawn in the  $\tilde{g}_0$ - $\xi^2$  plane (see Fig. 9), clearly show that  $g(\xi^2)$  for fixed  $\tilde{g}_0$  is not monotonic. [We remark that our numerical analysis does not yield enough reliable information for us to predict the large- $\xi^2$  region in Figs. 8 and 9. The topology of Fig. 9 is quite sensitive to the behavior of  $(d\hat{\xi}_1/d\tilde{G}_0)_g$  when  $\hat{\xi}_1 = 1$ . We have assumed that  $(d\hat{\xi}_1/d\tilde{G}_0)_g$  is greater than zero for  $g < g^*$  and equal to zero for  $g = g^*$  when  $\hat{\xi}_1 = \infty$ . Here  $\hat{\xi}_1 = \xi^2/(1 + \xi^2)$  and  $\tilde{G}_0 = g_0/(240 + g_0)$ .]

### 7.3. $d = 3$ (SC, BCC, FCC)

In three dimensions a qualitative change in  $g(g_0, \xi^2)$  is evident. The small- $g_0$  behavior of  $g$  at fixed  $\xi^2$  is consistent with the rigorous results of constructive field theory.<sup>(55)</sup> For small  $\xi^2$ , the curves (see Figs. 10 and 11) are similar to those shown for  $d = 1$  and  $d = 2$ . For large values of  $\xi^2$ , however,  $g$  no longer increases monotonically with  $g_0$  (see Fig. 12). This behavior is more easily discernible when one examines  $g(\tilde{g}_0)$  for fixed  $\xi^2$ .

<sup>9</sup> See Refs. 13, 15, 16, and 54.

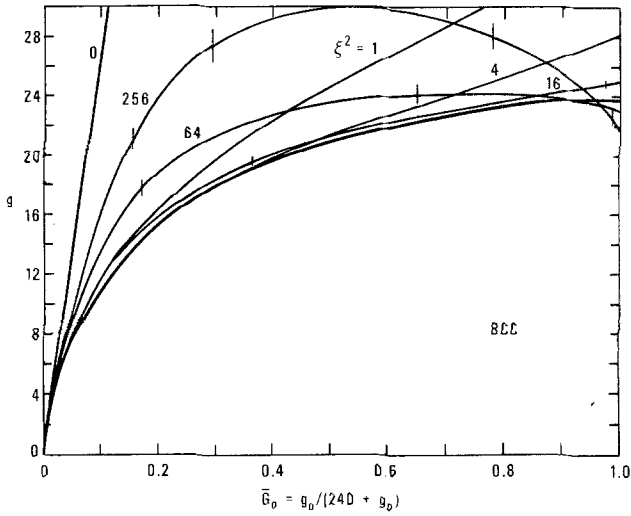


Fig. 10. The renormalized coupling constant  $g$  as a function of the bare coupling constant  $g_0$  for several values of the correlation length  $\xi$  on the body-centered-cubic lattice. The thick curve represents our estimate of  $g(g_0)$  in the limit  $\xi^2 \rightarrow \infty$ . The apparent error is indicated by the vertical bars.

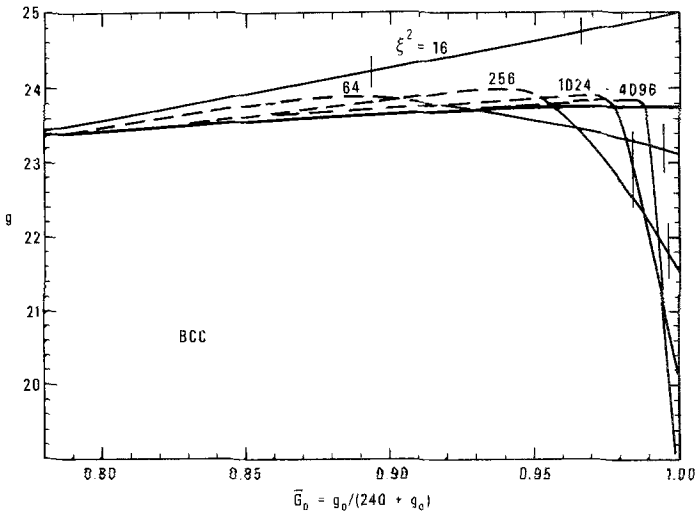


Fig. 11. An enlargement of upper right-hand corner of Fig. 10. The dashed curves are drawn in keeping with the procedure described in (7.1). The apparent error is indicated by the vertical bars.

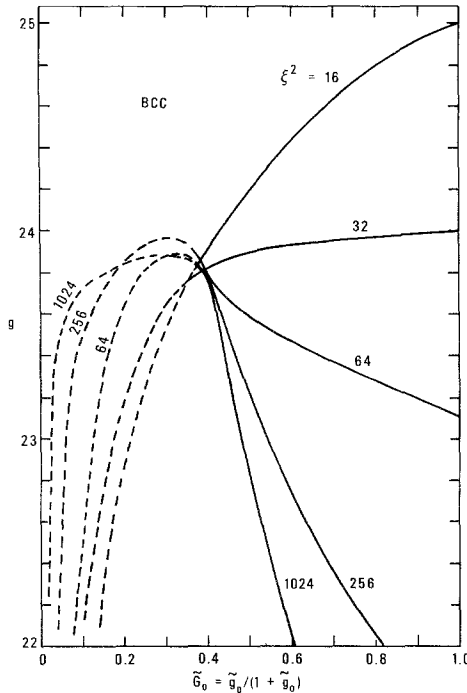


Fig. 12. The renormalized coupling constant  $g$  as a function of  $\tilde{g}_0$  for several values of the correlation length  $\xi$  on the body-centered-cubic lattice.

There are clear indications that  $g$  rises to a maximum value and then for  $\tilde{g}_0 \gtrsim 0.7$  decreases; thus the hypothesis of Schrader<sup>(31)</sup> that  $g$  is a monotonic function of  $g_0$  for fixed  $\xi^2$  does not appear to be valid. In Table VI we list values of  $g$  and  $\tilde{g}_0$  near the maximum and in the Ising limit ( $\tilde{g}_0 = \infty$ ) for several values of  $\xi^2$ .

Using the diagonal  $d$ log Padé approximants to the function  $Q(\xi^2) = (\partial^2 \chi / \partial \tilde{H}^2) / \chi^2$ , we have estimated the value of  $\omega^*$  [defined in Eq. (2.32)]. These estimates are shown in Table VII near the Ising limit; they are consistent with estimates of  $\omega^*$  obtained from the integral approximants. As  $\tilde{g}_0$  moves away from the Ising limit,  $\omega^*$  approaches zero. We conclude that for Ising-like systems, hyperscaling fails. Our values for  $\omega^*$  at  $\tilde{g}_0 = \infty$  are consistent with the analysis of Baker,<sup>(11)</sup> but the method we have used does not seem to be as accurate.

The existence of two universality classes (Ising-like and non-Ising-like) for this model, i.e., the fact that the limits  $g_0 \rightarrow \infty$  and  $\xi^2 \rightarrow \infty$  do not commute, is strikingly apparent when one constructs a picture of the entire  $g(\tilde{g}_0, \xi^2)$  surface. We exhibit this surface by drawing lines of constant  $g$  on

**Table VI. The Decay of the Renormalized Coupling Constant  $g(\tilde{g}_0, \xi^2)$  from its Fixed-Point Value as the Ising Limit ( $\tilde{g}_0 = \infty$ ) is Approached**

	$\xi^2$	$\tilde{g}_0 = 0.35$	$\tilde{g}_0 = 1.0$	$\tilde{g}_0 = \infty$
SC	4	25.1 ± 0.1	24.7 ± 0.2	29.7 ± 0.3
	16	24.1 ± 0.4	24.9 ± 0.6	25.5 ± 0.8
	64	23.7 ± 0.8	23.3 ± 1.0	22.8 ± 1.2
	256	23.5 ± 1.2	22.0 ± 1.4	20.6 ± 1.8
	1024	23.4 ± 1.6	20.9 ± 1.8	18.8 ± 2.0
	4096	23.3 ± 2.0	19.8 ± 2.2	17.0 ± 2.3
	10 <sup>6</sup>	22.9 ± 3.7	16.1 ± 3.3	11.6 ± 2.6
	$\xi^2$	$\tilde{g}_0 = 0.7$	$\tilde{g}_0 = 1.0$	$\tilde{g}_0 = \infty$
BCC	4	23.85 ± 0.01	25.55 ± 0.05	28.0 ± 0.1
	16	23.97 ± 0.02	24.2 ± 0.2	25.0 ± 0.1
	64	23.76 ± 0.04	23.6 ± 0.3	23.1 ± 0.3
	256	23.72 ± 0.07	23.2 ± 0.4	21.6 ± 0.4
	1024	23.7 ± 0.1	22.8 ± 0.5	20.2 ± 0.5
	4096	23.7 ± 0.1	22.5 ± 0.2	18.8 ± 0.5
	10 <sup>6</sup>	23.8 ± 0.2	21.2 ± 1.0	14.4 ± 0.7
	$\xi^2$	$\tilde{g}_0 = 0.8$	$\tilde{g}_0 = 1.0$	$\tilde{g}_0 = \infty$
FCC	4	24.77 ± 0.05	25.22 ± 0.01	27.78 ± 0.08
	16	23.9 ± 0.2	24.10 ± 0.01	25.1 ± 0.2
	64	23.7 ± 0.3	23.65 ± 0.03	23.3 ± 0.4
	256	23.6 ± 0.4	23.36 ± 0.03	21.8 ± 0.6
	1024	23.5 ± 0.6	23.11 ± 0.03	20.6 ± 0.7
	4096	23.5 ± 0.8	22.87 ± 0.05	19.3 ± 0.7
	10 <sup>6</sup>	23.3 ± 1.3	22.0 ± 0.1	15.2 ± 1.3

**Table VII. The Anomalous Dimension  $\omega^*$ , Defined by Eq. (2.32), as a Function of  $\tilde{g}_0$**

	$\tilde{g}_0$				
Lattice	1	10	$\infty$		
SC	0.12 ± 0.06	0.20 ± 0.10	0.22 ± 0.10		
BCC	0.02 ± 0.02	0.10 ± 0.06	0.10 ± 0.08		
FCC	0.02 ± 0.04	0.08 ± 0.08	0.10 ± 0.06		
	$\tilde{g}_0$				
Lattice	0.01	0.1	1	10	$\infty$
HSC	0.16 ± 0.02	0.40 ± 0.04	0.50 ± 0.08	0.58 ± 0.08	0.58 ± 0.08
HBCC	0.10 ± 0.02	0.26 ± 0.06	0.38 ± 0.12	0.44 ± 0.14	0.44 ± 0.16

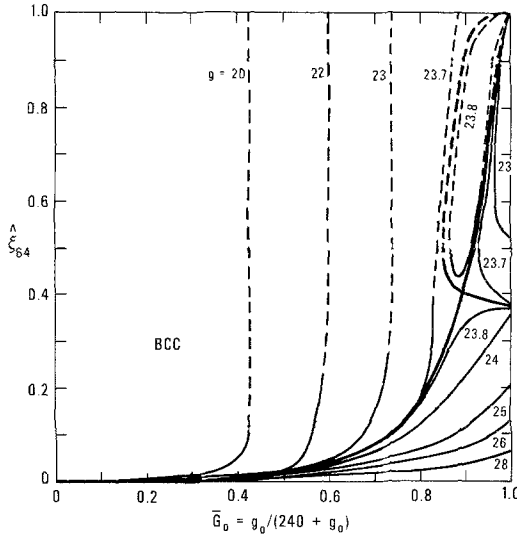


Fig. 13. Contours of the renormalized coupling constant  $g$  in the  $\hat{\xi}_{64}$ ,  $\bar{G}_0$  plane for the body-centered-cubic lattice. Here  $\hat{\xi}_{64} = \xi^2 / (64 + \xi^2)$  and  $\bar{G}_0 = g_0 / (240 + g_0)$ . The thick curve represents  $g^* = 23.78$ .

the  $\bar{G}_0 = \tilde{g}_0 / (1 + \tilde{g}_0)$  and  $\hat{\xi}_{64} = \xi^2 / (64 + \xi^2)$  plane. This surface (Fig. 13) was obtained graphically from plots of  $g$  versus  $\xi^2$  for fixed values of  $\tilde{g}_0$  (see Fig. 14). The analysis of the  $g$  surface indicates that a saddle point of elevation  $g = 23.78 \pm 0.08$  is located at  $\tilde{g}_0 = 0.64 \pm 0.02$  and  $\xi = 6.5 \pm 1.0$ . The saddle point is also apparent in the  $g_0$ - $\hat{\xi}_{64}$  plane, as shown in Fig. 15. The failure of the Schrader monotonicity hypothesis,<sup>(31)</sup> the noncommutativity of the  $g_0 \rightarrow \infty$  and  $\xi^2 \rightarrow \infty$  limits, and the failure of hyperscaling for Ising-like systems are bound up with the presence of the saddle point. We wish to emphasize the fact that our numerical methods are very accurate at small correlation lengths ( $\xi < 8$ ). Since the saddle point is located at  $\xi = 6.5 \pm 1.0$ , we are quite confident of its existence.

We remark that Schrader<sup>(31)</sup> has shown that if the correlation length (second moment definition) is monotonic in the Ising model limit, and the transformation from the set of variables  $\tilde{g}_0$ ,  $K$ , and  $\tilde{A}$  to the variables  $\chi$ ,  $\mu_2$ , and  $\partial^2 \chi / \partial \tilde{H}^2$  has a nonvanishing Jacobian everywhere in the relevant region, then  $g$  takes on its maximum value at the Ising limit for fixed two-point renormalization. That is, we impose Eqs. (2.22) and (2.23). Since  $\chi$  and  $\mu_2$  are proportional to the scale of the spins squared, and  $\partial^2 \chi / \partial \tilde{H}^2$  to the scale to the fourth power, we can look for zeros of the Jacobian in the reduced two-by-two, scale-free transformation  $(\tilde{g}_0, K) \rightarrow (g, \xi^2)$ . Numeri-

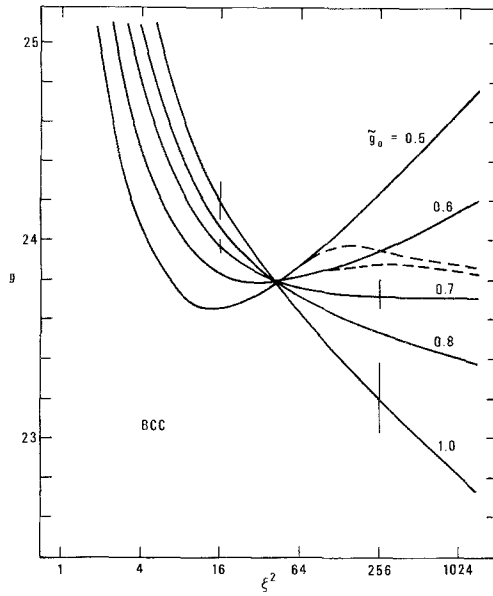


Fig. 14. The renormalized coupling constant  $g$  as a function of the correlation length squared  $\xi^2$  for several values of  $\tilde{g}_0$  on the body-centered-cubic lattice. The vertical bars represent the apparent error.

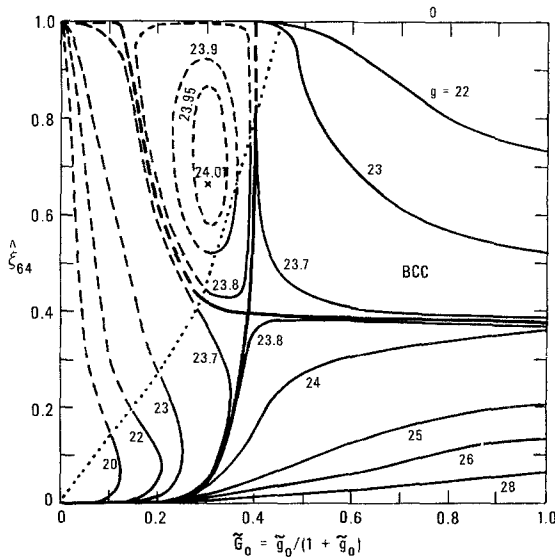


Fig. 15. Contours of the renormalized coupling constant  $g$  in the  $\hat{\xi}_{64}$ ,  $\hat{G}_0$  plane for the body-centered-cubic lattice. Here  $\hat{\xi}_{64} = \xi^2 / (64 + \xi^2)$  and  $\hat{G}_0 = \tilde{g}_0 / (1 + \tilde{g}_0)$ . The thick curve represents  $g^* \approx 23.78$ .

cally we see no breakdown for any  $\tilde{g}_0$  in the monotonicity of  $\xi^2(K)$ ,<sup>10</sup> as all the series terms are positive and look very regular at the highest orders computed, and we find that the Jacobian vanishes at the above-mentioned saddle point, thus destroying the basis of Schrader’s proof and reconciling our numerical results with his important and deep rigorous result.

A study of  $g(\xi^2)$  at the maximum yields the following estimates for  $g$  at the saddle point:  $23.8 \pm 0.8$  (SC),  $23.78 \pm 0.08$  (BCC), and  $23.7 \pm 0.3$  (FCC), all of which agree with the estimate<sup>11</sup> of  $g^* = 23.81 \pm 0.07$  found using an approach based on the Callen–Symanzik equation.<sup>(32,33)</sup>

The controversy over the validity of the hyperscaling laws has existed for as long as the idea of hyperscaling; and it may be that there are some practitioners of hyperscaling who will not be totally convinced by our “numerical conclusion” that hyperscaling fails for sufficiently Ising-like continuous-spin models in three dimensions. Only a rigorous mathematical proof that hyperscaling is or is not valid will put an end to this controversy. While we await such a proof, it is important to keep in mind that, irrespective of the hyperscaling question in three dimensions, our work clearly indicates the existence of more than one “fixed point” for the continuous-spin Ising model: non-Ising-like systems have  $g^* = 23.78 \pm 0.08$ , while for Ising-like systems  $g^*$  is certainly much less than 23.8. In other words, it is likely that the structure of  $g_0:\phi^4_3$  is more complicated than previously anticipated.

### 7.4. $d = 4$ (HSC and HBCC)

In four dimensions the behavior of  $g(g_0, \xi^2)$  is similar to that observed in lower dimensions if  $\xi^2$  is kept small. For larger values of  $\xi^2$ ,  $g(g_0)$  rises to a maximum at the point  $(g_0^{\max}, g^{\max})$  and then falls as  $g_0$  approaches infinite (see Fig. 16). The location of the maximum of this curve approaches the origin as  $\xi^2$  approaches infinity. In Table VIII we list  $g^{\max}$  for several values of  $\xi^2$ . Figure 17 shows that the dependence of  $g^{\max}$  on  $\xi^2$  is roughly consistent with the  $1/\ln \xi^2$  decline predicted from the perturbation theory result that  $g = g_0 - c(\ln \xi^2)g_0^2 + O(g_0^3)$ . (Here  $c$  is a constant, independent of  $\xi^2$  or  $g_0$ .)

The entire  $g(\tilde{g}_0, \xi^2)$  surface is shown in Fig. 18 for the HBCC lattice. The figure was obtained graphically from plots of  $g$  versus  $\xi^2$  for fixed  $\tilde{g}_0$ . The structure of the surface is much simpler than its three-dimensional counterpart; it clearly indicates that for each  $g_0 > 0$ ,  $\lim_{\xi^2 \rightarrow \infty} g(g_0, \xi^2) = 0$ . That is, the field theory is trivial.

<sup>10</sup> Related monotonicity properties have been rigorously established. See, for example, Ref. 56.

<sup>11</sup> Baker *et al.* (1978), Ref. 32, report a value of  $1.416 \pm 0.0015$  for  $v^*$ , where  $v^* = 9g^*/48\pi$ .

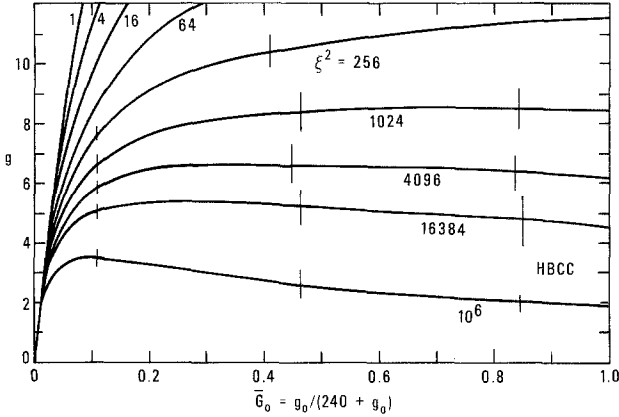


Fig. 16. The renormalized coupling constant  $g$  as a function of the bare coupling constant  $g_0$  for several values of the correlation length  $\xi$  on the hyper-body-centered-cubic lattice. The apparent error is indicated by the vertical bars.

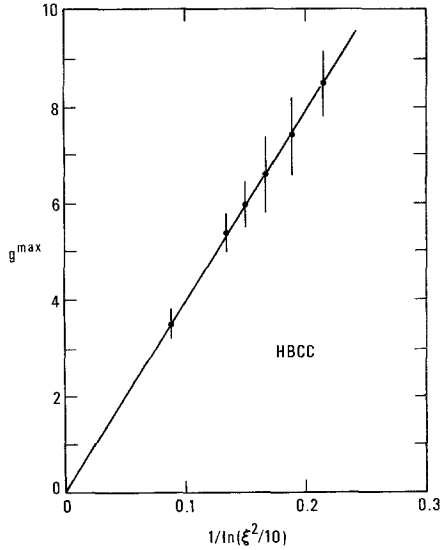


Fig. 17. The maximum value of the renormalized coupling constant  $g^{\max}$  as a function of the correlation length  $\xi$ . The dots represent the data in Table VIII. The apparent error is indicated by the vertical bars.

**APPENDIX: HIGH-TEMPERATURE SERIES FOR  $\chi$ ,  $\partial^2\chi/\partial\tilde{H}^2$ , AND  $\mu^2$**

The high-temperature series for  $\chi$ ,  $\partial^2\chi/\partial\tilde{H}^2$ , and  $\mu^2$  are given, through tenth order, in Tables AI, AII, and AIII, respectively. The series are for the case  $\tilde{H} = 0$ ; the expansion variable is  $K$ . [See Eq. (2.15).] The format of the tables is most easily explained by example: the susceptibility on the plane



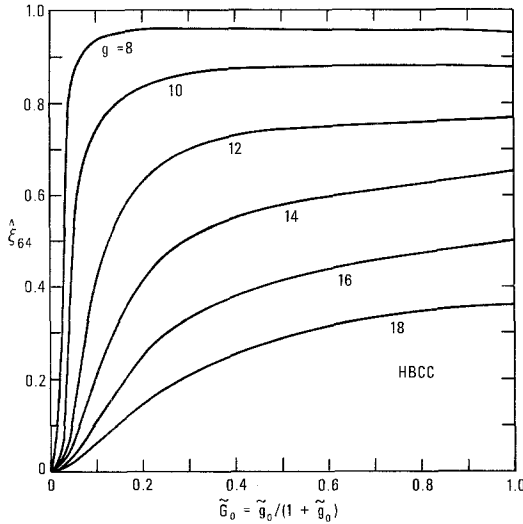


Fig. 18. Contours of the renormalized coupling constant  $g$  in the  $\hat{\xi}_{64}, \tilde{G}_0$  plane for the hyper-body-centered-cubic lattice. Here  $\hat{\xi}_{64} = \xi^2 / (64 + \xi^2)$  and  $\tilde{G}_0 = \tilde{g}_0 / (1 + \tilde{g}_0)$ .

**Table VIII. The Maximum Value of the Renormalized Coupling Constant  $g^{\max}$  on the HSC and HBCC Lattices as a Function of the Correlation Length Squares  $\xi^2$**

$\xi^2$	$g_{\text{HSC}}^{\max}$	$g_{\text{HBCC}}^{\max}$
1024	$8.3 \pm 1.0$	$8.5 \pm 0.7$
2048	$7.3 \pm 0.7$	$7.4 \pm 0.8$
4096	$6.4 \pm 0.6$	$6.6 \pm 0.8$
8192	$5.8 \pm 0.4$	$6.0 \pm 0.5$
16384	$5.3 \pm 0.3$	$5.4 \pm 0.4$
$10^6$	$3.4 \pm 0.2$	$3.5 \pm 0.3$

square lattice (PSQ) through order  $K^4$  is given by

$$\begin{aligned} \chi = & I_2(0) + 4I_2(0)^2K + [20I_2(0)^3 + 4I_2(0)I_4(0)]K^2/2! \\ & + [132I_2(0)^4 + 72I_2(0)^2I_4(0) + 4I_4(0)^2]K^3/3! \\ & + [1032I_2(0)^5 + 972I_2(0)^3I_4(0) + 36I_2(0)^2I_6(0) \\ & + 164I_2(0)I_4(0)^2 + 4I_4(0)I_6(0)]K^4/4! \end{aligned}$$

The factors  $I_n(0)$  are the moments of the spin-density distribution. [See Eqs. (2.16) and (2.18).]

Table AI. The Susceptibility  $\chi$

P	LC	PSQ	P	LC	PSQ
-0-			-9-		
( 1.0,0,0,0,0 )	1	1	( 10,0,0,0,0 )	2086560	489706560
( 2.0,0,0,0,0 )	2	4	( 8,1,0,0,0 )	-6168960	979594560
( 3,0,0,0,0 )	2	20	( 7,0,1,0,0 )	0	28486080
( 1,1,0,0,0 )	2	4	( 6,2,0,0,0 )	5995080	919734480
( 4,0,0,0,0 )	-6	132	( 6,0,0,1,0 )	0	-1088640
( 2,1,0,0,0 )	12	72	( 5,1,1,0,0 )	589680	154738080
( 0,2,0,0,0 )	2	4	( 5,0,0,0,1 )	0	0
( 5,0,0,0,0 )	-12	1032	( 4,3,0,0,0 )	-2192400	511025760
( 3,1,0,0,0 )	-6	972	( 4,1,0,1,0 )	0	8074080
( 2,0,1,0,0 )	6	36	( 4,0,2,0,0 )	-153720	20215440
( 1,2,0,0,0 )	26	164	( 3,2,1,0,0 )	-594720	152449920
( 0,1,1,0,0 )	2	4	( 3,1,0,0,1 )	0	151200
( 6,0,0,0,0 )	240	10560	( 3,0,1,1,0 )	-12096	2356704
( 4,1,0,0,0 )	-480	11760	( 2,4,0,0,0 )	246960	103602240
( 3,0,1,0,0 )	0	720	( 2,2,0,1,0 )	-15120	5508720
( 2,2,0,0,0 )	210	5460	( 2,1,2,0,0 )	97776	9658656
( 1,1,1,0,0 )	60	360	( 2,0,1,0,1 )	0	30240
( 0,3,0,0,0 )	0	0	( 2,0,0,2,0 )	2682	55908
( 0,0,2,0,0 )	2	4	( 1,3,1,0,0 )	85680	12902400
( 7,0,0,0,0 )	720	132480	( 1,2,0,0,1 )	0	75600
( 5,1,0,0,0 )	-360	154440	( 1,1,1,1,0 )	21672	454608
( 4,0,1,0,0 )	-360	11160	( 1,0,3,0,0 )	0	0
( 3,2,0,0,0 )	-780	116760	( 1,0,0,1,1 )	180	1080
( 3,0,0,1,0 )	0	360	( 0,5,0,0,0 )	0	0
( 2,1,1,0,0 )	360	14400	( 0,3,0,1,0 )	0	0
( 1,3,0,0,0 )	330	9540	( 0,2,2,0,0 )	10416	508704
( 1,1,0,1,0 )	30	180	( 0,1,1,0,1 )	840	5040
( 1,0,2,0,0 )	52	320	( 0,1,0,2,0 )	0	0
( 0,2,1,0,0 )	70	420	( 0,0,2,1,0 )	0	0
( 0,0,1,1,0 )	2	4	( 0,0,0,2,0 )	2	4
( 8,0,0,0,0 )	-16380	1917720	-10-		
( 6,1,0,0,0 )	40320	2439360	( 11,0,0,0,0 )	10432800	9662587200
( 5,0,1,0,0 )	0	100800	( 9,1,0,0,0 )	-1587600	19951596000
( 4,2,0,0,0 )	-28140	2221800	( 8,0,1,0,0 )	-6350400	885880800
( 4,0,0,1,0 )	0	5040	( 7,2,0,0,0 )	-3780000	23791622400
( 3,1,1,0,0 )	-4200	438480	( 7,0,0,1,0 )	0	-17690400
( 2,3,0,0,0 )	5040	537600	( 6,1,1,0,0 )	13456800	2963822400
( 2,1,0,1,0 )	0	10080	( 6,0,0,0,1 )	0	-1814400
( 2,0,2,0,0 )	924	20552	( 5,3,0,0,0 )	13381200	13248295200
( 1,2,1,0,0 )	2240	47040	( 5,1,0,1,0 )	567000	102135600
( 1,0,1,1,0 )	112	672	( 5,0,2,0,0 )	181440	415265760
( 0,4,0,0,0 )	70	12460	( 5,0,0,0,1 )	0	0
( 0,2,0,1,0 )	140	840	( 4,2,1,0,0 )	-6400800	4588567200
( 0,1,2,0,0 )	0	0	( 4,1,0,0,1 )	0	4384800
( 0,0,0,2,0 )	2	4	( 4,0,1,1,0 )	-284760	70716240
( 9,0,0,0,0 )	-65520	29161440	( 3,4,0,0,0 )	-4901400	4863978000
( 7,1,0,0,0 )	63000	47612880	( 3,2,0,1,0 )	-529200	240798600
( 6,0,1,0,0 )	37800	1154160	( 3,1,2,0,0 )	-1267560	533589840
( 5,2,0,0,0 )	63000	41277600	( 3,1,0,0,1 )	0	75600
( 5,0,0,1,0 )	0	17640	( 3,0,1,0,1 )	-10080	1975680
( 4,1,1,0,0 )	-59640	9176160	( 3,0,0,2,0 )	-5220	2837880
( 4,0,0,1,0 )	0	2520	( 2,3,1,0,0 )	88200	1132588800
( 3,3,0,0,0 )	-66360	19078080	( 2,2,0,0,1 )	-12600	5304600
( 3,1,0,1,0 )	-3360	398840	( 2,1,1,1,0 )	151200	43626240
( 3,0,2,0,0 )	-1792	684992	( 2,0,3,0,0 )	83160	7817040
( 2,2,1,0,0 )	11480	3456320	( 2,0,1,0,1 )	0	15120
( 2,1,0,0,1 )	0	5040	( 2,0,0,1,1 )	3780	115200
( 2,0,1,1,0 )	1400	46592	( 1,5,0,0,0 )	352800	208303200
( 1,4,0,0,0 )	11060	1246280	( 1,3,0,1,0 )	37800	21798000
( 1,2,0,1,0 )	1750	75460	( 1,2,2,0,0 )	482160	65730000
( 1,1,2,0,0 )	5264	122080	( 1,2,0,0,1 )	0	37800
( 1,0,1,0,1 )	56	336	( 1,1,1,0,1 )	15960	670320
( 1,0,0,2,0 )	86	524	( 1,1,0,2,0 )	22590	496620
( 0,3,1,0,0 )	1540	83720	( 1,0,2,1,0 )	18900	430920
( 0,2,0,0,1 )	70	420	( 1,0,0,1,0,1 )	90	540
( 0,1,1,1,0 )	420	2520	( 1,0,0,0,2,0 )	128	776
( 0,0,3,0,0 )	0	0	( 0,4,1,0,0 )	96600	14044800
( 0,0,0,1,1 )	2	4	( 0,3,0,0,1 )	0	138600
			( 0,2,1,1,0 )	34020	1317960
			( 0,1,3,0,0 )	10080	927360
			( 0,1,1,0,0,1 )	420	2520
			( 0,1,0,1,1,0 )	990	5940
			( 0,0,2,0,1,0 )	924	5544
			( 0,0,1,2,0,0 )	0	0
			( 0,0,0,0,1,1 )	2	4

Continuous-Spin Ising Model

P	T	SC	P	T	SC
-0-			-9-		
( 1,0,0,0,0,0 )	1	1	( 10,0,0,0,0,0 )	46238895360	216250443360
( -1-			( 8,1,0,0,0,0 )	75124596960	216899000640
( 2,0,0,0,0,0 )	6	6	( 7,0,1,0,0,0 )	2954387520	7401119040
-2-			( 6,2,0,0,0,0 )	59126555880	101944354680
( 3,0,0,0,0,0 )	54	54	( 6,0,0,1,0,0 )	80740800	115123680
( 1,1,0,0,0,0 )	6	6	( 5,1,1,0,0,0 )	9768412080	9534445200
-3-			( 5,0,0,0,1,0 )	2449440	136800
( 4,0,0,0,0,0 )	594	702	( 4,3,0,0,0,0 )	27312571440	20411591760
( 2,1,0,0,0,0 )	216	180	( 4,1,0,1,0,0 )	350360640	230519520
( 0,2,0,0,0,0 )	6	6	( 4,0,2,0,0,0 )	547835400	352651320
-4-			( 3,2,1,0,0,0 )	4838369760	2388022560
( 5,0,0,0,0,0 )	7884	11772	( 3,1,0,0,1,0 )	3900960	2268000
( 3,1,0,0,0,0 )	5526	4662	( 3,0,1,1,0,0 )	32768064	19613664
( 2,0,1,0,0,0 )	90	90	( 2,4,0,0,0,0 )	2739040920	1354041360
( 1,2,0,0,0,0 )	558	414	( 2,2,0,1,0,0 )	109113480	44180640
( 0,1,1,0,0,0 )	6	6	( 2,1,2,0,0,0 )	229851216	70425936
-5-			( 2,0,1,0,1,0 )	235872	151200
( 6,0,0,0,0,0 )	129600	248400	( 2,0,0,2,0,0 )	362718	230526
( 4,1,0,0,0,0 )	126000	127440	( 1,3,1,0,0,0 )	279054720	90039600
( 3,0,1,0,0,0 )	5040	3600	( 1,2,0,0,1,0 )	619920	378000
( 2,2,0,0,0,0 )	31590	22950	( 1,1,1,1,0,0 )	6896232	1818936
( 1,1,1,0,0,0 )	1140	900	( 1,0,3,0,0,0 )	2324448	0
( 0,3,0,0,0,0 )	480	6	( 1,0,0,1,1,0 )	3564	2700
( 0,0,2,0,0,0 )	6	6	( 0,5,0,0,0,0 )	20442240	0
-6-			( 0,3,0,1,0,0 )	2358720	0
( 7,0,0,0,0,0 )	2627640	6162480	( 0,2,2,0,0,0 )	5264280	1775088
( 5,1,0,0,0,0 )	2866860	3931200	( 0,1,1,0,1,0 )	18648	12600
( 4,0,1,0,0,0 )	168300	128880	( 0,1,0,2,0,0 )	21600	0
( 3,2,0,0,0,0 )	1371060	1013580	( 0,0,2,1,0,0 )	53928	0
( 3,0,0,1,0,0 )	1800	1800	( 0,0,0,2,0,0 )	6	6
( 2,1,1,0,0,0 )	97920	64440	-10-		
( 1,3,0,0,0,0 )	77130	37710	( 11,0,0,0,0,0 )	1451248293600	882507512880
( 1,1,0,1,0,0 )	450	450	( 9,1,0,0,0,0 )	2751717225600	9932152608000
( 1,0,2,0,0,0 )	1164	804	( 8,0,1,0,0,0 )	117430236000	343399240800
( 0,2,1,0,0,0 )	3030	1050	( 7,2,0,0,0,0 )	2327516402400	5316170680800
( 0,0,1,1,0,0 )	6	6	( 7,0,0,1,0,0 )	1033527600	5407138800
-7-			( 6,1,1,0,0,0 )	337073788800	503085945600
( 8,0,0,0,0,0 )	62109180	178230780	( 6,0,0,0,1,0 )	52390800	48308400
( 6,1,0,0,0,0 )	72666720	135898560	( 5,3,0,0,0,0 )	1303714440000	1345723016400
( 5,0,1,0,0,0 )	4369680	4415040	( 5,1,0,1,0,0 )	14396470200	12670295400
( 4,2,0,0,0,0 )	50334480	44963100	( 5,0,2,0,0,0 )	24859003680	19520948160
( 4,0,0,1,0,0 )	120960	75600	( 5,0,0,0,1,0 )	680400	680400
( 3,1,1,0,0,0 )	5705280	3767400	( 4,2,1,0,0,0 )	303627970800	180779256000
( 2,3,0,0,0,0 )	7273980	3996720	( 4,1,0,0,1,0 )	285087600	185749200
( 2,1,0,1,0,0 )	75600	50400	( 4,0,1,1,0,0 )	2297597400	1356558840
( 2,0,2,0,0,0 )	128184	85092	( 3,4,0,0,0,0 )	267822298800	143381107800
( 1,2,1,0,0,0 )	567840	188160	( 3,2,0,1,0,0 )	9619740900	4338646200
( 1,0,1,1,0,0 )	2184	1680	( 3,1,2,0,0,0 )	21619611720	8032658760
( 0,4,0,0,0,0 )	74970	43890	( 3,1,0,0,1,0 )	1134000	1134000
( 0,2,0,1,0,0 )	2940	2100	( 3,0,1,0,1,0 )	31615920	18779040
( 0,1,2,0,0,0 )	6972	0	( 3,0,0,2,0,0 )	4306860	23264820
( 0,0,0,2,0,0 )	6	6	( 2,3,1,0,0,0 )	42821200800	15636537000
-8-			( 2,2,0,0,1,0 )	117047700	51710400
( 9,0,0,0,0,0 )	1623751920	5853118320	( 2,1,1,1,0,0 )	1099307160	332942400
( 7,1,0,0,0,0 )	2184182280	5174948520	( 2,0,3,0,0,0 )	338231880	55467720
( 6,0,1,0,0,0 )	103957560	174628440	( 2,0,1,0,0,1 )	75600	75600
( 5,2,0,0,0,0 )	1704273480	2069648280	( 2,0,0,1,1,0 )	856980	507060
( 5,0,0,1,0,0 )	4074840	3107160	( 1,5,0,0,0,0 )	7654500000	2506442400
( 4,1,1,0,0,0 )	258408360	189108360	( 1,3,0,1,0,0 )	703117800	156907800
( 4,0,0,0,1,0 )	37800	37800	( 1,2,2,0,0,0 )	1775025000	452571840
( 3,3,0,0,0,0 )	497039760	303516360	( 1,2,0,0,1,0 )	189000	189000
( 3,1,0,1,0,0 )	6284880	3931200	( 1,1,1,0,1,0 )	8552880	3031560
( 3,0,2,0,0,0 )	9656304	5668992	( 1,1,0,2,0,0 )	8316810	1970730
( 2,2,1,0,0,0 )	61197360	26412120	( 1,0,2,1,0,0 )	18383400	1689660
( 2,1,0,0,1,0 )	25200	25200	( 1,0,0,1,1,0 )	1350	1350
( 2,0,1,1,0,0 )	334824	206136	( 1,0,0,0,2,0 )	3024	1944
( 1,4,0,0,0,0 )	19694220	8927100	( 0,4,1,0,0,0 )	459660600	95823000
( 1,2,0,1,0,0 )	834330	342090	( 0,3,0,0,1,0 )	3465000	693000
( 1,1,2,0,0,0 )	17236112	480816	( 0,2,1,1,0,0 )	29943900	4698540
( 1,0,1,0,1,0 )	840	840	( 0,1,3,0,0,0 )	14311080	3024000
( 1,0,0,2,0,0 )	1986	1314	( 0,1,1,0,1,0 )	6300	6300
( 0,3,1,0,0,0 )	980700	293580	( 0,1,0,1,1,0 )	58770	14850
( 0,2,0,0,1,0 )	1050	1050	( 0,0,2,0,1,0 )	63000	13860
( 0,1,1,1,0,0 )	22092	6300	( 0,0,1,2,0,0 )	156240	0
( 0,0,3,0,0,0 )	9240	0	( 0,0,0,0,1,1 )	6	6
( 0,0,0,1,1,0 )	6	6			

P	BCC	FCC	P	BCC	FCC
0			-9		
( 1.0,0.0,0.0 )	1	1	( 10.0,0.0,0.0 )	5527262240640	303601312849960
( 2.0,0.0,0.0 )	8	12	( 8.1,0.0,0.0 )	4309745408640	197749196527680
( 3.0,0.0,0.0 )	104	252	( 7.0,1.0,0.0 )	121195219840	4826433003840
( 4.0,0.0,0.0 )	8	12	( 6.2,0.0,0.0 )	1477552497120	54913237893360
( 5.0,0.0,0.0 )	104	252	( 6.0,0.1,0.0 )	17762971600	59390392320
( 6.0,0.0,0.0 )	8	12	( 5.1,1.0,0.0 )	102238718400	2943054505440
( 7.0,0.0,0.0 )	1992	7452	( 5.0,0.0,1.0 )	12700800	310262400
( 8.0,0.0,0.0 )	336	936	( 4.3,0.0,0.0 )	206833193280	6235971507360
( 9.0,0.0,0.0 )	8	12	( 4.1,0.1,0.0 )	1692290880	34358476320
( 10.0,0.0,0.0 )	8	12	( 4.0,2.0,0.0 )	2341715040	44471715120
( 11.0,0.0,0.0 )	48336	285336	( 3.2,1.0,0.0 )	15969542400	379611308160
( 12.0,0.0,0.0 )	13368	61368	( 3.1,0.0,1.0 )	10584000	123832800
( 13.0,0.0,0.0 )	168	396	( 3.0,1.1,0.0 )	8255200	921697056
( 14.0,0.0,0.0 )	776	2412	( 2.4,0.0,0.0 )	8918159040	199989246240
( 15.0,0.0,0.0 )	8	12	( 2.2,0.1,0.0 )	189332640	3119724720
( 16.0,0.0,0.0 )	1464000	13461120	( 2.1,2.0,0.0 )	299113920	6396866784
( 17.0,0.0,0.0 )	558240	4113360	( 2.0,1.0,1.0 )	423360	2509920
( 18.0,0.0,0.0 )	10080	54000	( 2.0,0.2,0.0 )	621576	3736044
( 19.0,0.0,0.0 )	62760	330300	( 1.3,1.0,0.0 )	446019840	8154699940
( 20.0,0.0,0.0 )	1680	4920	( 1.2,0.0,1.0 )	1058400	6577200
( 21.0,0.0,0.0 )	0	1920	( 1.1,1.1,0.0 )	5021856	71605296
( 22.0,0.0,0.0 )	8	12	( 1.0,3.0,0.0 )	0	24635520
( 23.0,0.0,0.0 )	1464000	13461120	( 1.0,0,1.1,0.0 )	5040	15336
( 24.0,0.0,0.0 )	558240	4113360	( 0.5,0.0,0.0 )	0	652821120
( 25.0,0.0,0.0 )	10080	54000	( 0.3,0.1,0.0 )	0	25280640
( 26.0,0.0,0.0 )	62760	330300	( 0.2,2.0,0.0 )	5916288	66265920
( 27.0,0.0,0.0 )	1680	4920	( 0.1,1.0,1.0 )	23520	79632
( 28.0,0.0,0.0 )	0	1920	( 0.1,0.2,0.0 )	0	86400
( 29.0,0.0,0.0 )	8	12	( 0.0,2.1,0.0 )	0	215712
( 30.0,0.0,0.0 )	1464000	13461120	( 0.0,0.0,2.0 )	8	12
( 31.0,0.0,0.0 )	558240	4113360	( 11.0,0.0,0.0 )	325382704214400	27960309337867200
( 32.0,0.0,0.0 )	10080	54000	( 9.1,0.0,0.0 )	286074500241600	20614373055309600
( 33.0,0.0,0.0 )	62760	330300	( 8.0,1.0,0.0 )	8419005604800	520997701946400
( 34.0,0.0,0.0 )	1680	4920	( 7.2,0.0,0.0 )	113290264483200	6680663080963200
( 35.0,0.0,0.0 )	0	1920	( 7.0,0.1,0.0 )	127421683200	6864442653600
( 36.0,0.0,0.0 )	8	12	( 6.1,1.0,0.0 )	8182030752000	384686341905600
( 37.0,0.0,0.0 )	1464000	13461120	( 6.0,0.0,1.0 )	1191153600	49353494400
( 38.0,0.0,0.0 )	558240	4113360	( 5.3,0.0,0.0 )	20593050811200	998371268042400
( 39.0,0.0,0.0 )	10080	54000	( 5.1,0.1,0.0 )	155281341600	5444321635600
( 40.0,0.0,0.0 )	62760	330300	( 5.0,2.0,0.0 )	206630827200	6827110647840
( 41.0,0.0,0.0 )	1680	4920	( 5.0,0.0,1.0 )	6350400	898112800
( 42.0,0.0,0.0 )	0	1920	( 4.2,1.0,0.0 )	1923859828800	73917161690400
( 43.0,0.0,0.0 )	8	12	( 4.1,0.0,1.0 )	1499299200	32407452000
( 44.0,0.0,0.0 )	1464000	13461120	( 4.0,1.1,0.0 )	9211839840	195028994160
( 45.0,0.0,0.0 )	558240	4113360	( 3.4,0.0,0.0 )	1455184836000	54389454512400
( 46.0,0.0,0.0 )	10080	54000	( 3.2,0.1,0.0 )	30390519600	832911244200
( 47.0,0.0,0.0 )	62760	330300	( 3.1,2.0,0.0 )	54959879520	1695991515120
( 48.0,0.0,0.0 )	1680	4920	( 3.1,0.0,0.1 )	5292000	37422000
( 49.0,0.0,0.0 )	0	1920	( 3.0,1.0,1.0 )	81849600	945967680
( 50.0,0.0,0.0 )	8	12	( 3.0,0.2,0.0 )	96989040	1176654600
( 51.0,0.0,0.0 )	1464000	13461120	( 2.3,1.0,0.0 )	111954124800	3328520580000
( 52.0,0.0,0.0 )	558240	4113360	( 2.2,0.0,1.0 )	228186000	3516420600
( 53.0,0.0,0.0 )	10080	54000	( 2.1,1.1,0.0 )	1438819200	30999235680
( 54.0,0.0,0.0 )	62760	330300	( 2.0,3.0,0.0 )	249994080	9847661040
( 55.0,0.0,0.0 )	1680	4920	( 2.0,1.0,0.1 )	211680	831600
( 56.0,0.0,0.0 )	0	1920	( 2.0,0.1,1.0 )	1386720	8912160
( 57.0,0.0,0.0 )	8	12	( 1.5,0.0,0.0 )	18295401600	597611498400
( 58.0,0.0,0.0 )	1464000	13461120	( 1.3,0.1,0.0 )	771271200	20733829200
( 59.0,0.0,0.0 )	558240	4113360	( 1.2,2.0,0.0 )	2294916960	54706856400
( 60.0,0.0,0.0 )	10080	54000	( 1.2,0.0,0.1 )	529200	2079000
( 61.0,0.0,0.0 )	62760	330300	( 1.1,1.0,1.0 )	8410080	88567920
( 62.0,0.0,0.0 )	1680	4920	( 1.1,0.2,0.0 )	5511960	87483780
( 63.0,0.0,0.0 )	0	1920	( 1.0,2.1,0.0 )	4793040	194108040
( 64.0,0.0,0.0 )	8	12	( 1.0,0.1,0.1 )	2520	5940
( 65.0,0.0,0.0 )	1464000	13461120	( 1.0,0.0,2.0 )	3632	12888
( 66.0,0.0,0.0 )	558240	4113360	( 0.4,1.0,0.0 )	552316800	15161025600
( 67.0,0.0,0.0 )	10080	54000	( 0.3,0.0,1.0 )	1940400	35947800
( 68.0,0.0,0.0 )	62760	330300	( 0.2,1.1,0.0 )	15155280	354475800
( 69.0,0.0,0.0 )	1680	4920	( 0.1,3.0,0.0 )	10946880	205541280
( 70.0,0.0,0.0 )	0	1920	( 0.1,1.0,0.1 )	1760	27720
( 71.0,0.0,0.0 )	8	12	( 0.1,0.1,1.0 )	27720	241020
( 72.0,0.0,0.0 )	1464000	13461120	( 0.0,2.0,1.0 )	25872	257544
( 73.0,0.0,0.0 )	558240	4113360	( 0.0,1.2,0.0 )	0	624960
( 74.0,0.0,0.0 )	10080	54000	( 0.0,0.0,1.1 )	0	12

P	HSC	H8CC	P	HSC	H8CC
( 0.0,0.0,0.0 )	1	1	( 10.0,0.0,0.0 )	7181444188800	9354327812686080
( 1.0,0.0,0.0 )	8	16	( 8.1,0.0,0.0 )	4782295728000	3169676093310720
( 2.0,0.0,0.0 )	8	16	( 7.0,1,0,0,0 )	121529600640	43689694567680
( 3.0,0.0,0.0 )	104	464	( 6.2,0,0,0,0 )	1402898464800	438261588636480
( 1,1,0,0,0,0 )	8	16	( 6.0,0,1,0,0 )	1580342400	308756448000
( 4.0,0,0,0,0 )	1992	20112	( 5.1,1,0,0,0 )	88493912640	12963630234240
( 2,1,0,0,0,0 )	336	1440	( 5.0,0,0,1,0 )	12700800	990662400
( 0,2,0,0,0,0 )	8	16	( 4,3,0,0,0,0 )	172113197760	23993177443200
( 5.0,0,0,0,0 )	50064	1137696	( 4,1,0,1,0,0 )	1491981120	94811472000
( 3,1,0,0,0,0 )	12792	131184	( 4,0,2,0,0,0 )	2008167840	115943123520
( 2,0,1,0,0,0 )	168	720	( 3,2,1,0,0,0 )	13146819840	775523105280
( 1,2,0,0,0,0 )	776	3344	( 3,1,0,0,1,0 )	10584000	275184000
( 0,1,1,0,0,0 )	8	16	( 3,0,1,1,0,0 )	75781440	1765814400
( 6.0,0,0,0,0 )	1576320	80417280	( 2,4,0,0,0,0 )	6930241920	407767288320
( 4,1,0,0,0,0 )	529440	12782400	( 2,2,0,1,0,0 )	167801760	4001256000
( 3,0,1,0,0,0 )	10080	100800	( 2,1,2,0,0,0 )	257140800	6095053440
( 2,2,0,0,0,0 )	59880	580560	( 2,0,1,0,1,0 )	4233600	4233600
( 1,1,1,0,0,0 )	1680	7200	( 2,0,0,2,0,0 )	597384	5694480
( 0,3,0,0,0,0 )	0	0	( 1,3,1,0,0,0 )	315020160	9039179520
( 0,0,2,0,0,0 )	8	16	( 1,2,0,0,1,0 )	1058400	10584000
( 7.0,0,0,0,0 )	59040000	6769762560	( 1,1,1,1,0,0 )	4634784	45460800
( 5,1,0,0,0,0 )	24715440	1380261600	( 1,0,0,1,1,0 )	5040	21600
( 4,0,1,0,0,0 )	550800	14320800	( 0,5,0,0,0,0 )	0	0
( 3,2,0,0,0,0 )	3949680	93531360	( 0,3,0,1,0,0 )	0	0
( 3,0,0,1,0,0 )	5040	50400	( 0,2,2,0,0,0 )	4089792	51354240
( 2,1,1,0,0,0 )	172800	1704960	( 0,1,1,0,1,0 )	23520	100800
( 1,3,0,0,0,0 )	94920	988560	( 0,1,0,2,0,0 )	0	0
( 1,0,1,0,0,0 )	840	3600	( 0,0,2,1,0,0 )	8	16
( 1,0,2,0,0,0 )	1504	6464	( 0,0,0,2,0,0 )	8	16
( 0,2,1,0,0,0 )	1960	8400	( 11,0,0,0,0,0 )	445470745910400	1304692960823481600
( 0,0,1,1,0,0 )	8	16	( 9,1,0,0,0,0 )	333348468070400	501283746915638400
( 8.0,0,0,0,0 )	2580102000	664905437280	( 8,0,1,0,0,0 )	8701393377600	7259693503708800
( 6,1,0,0,0,0 )	1292618880	165275953920	( 7,2,0,0,0,0 )	112236629702400	81144716812185600
( 5,0,1,0,0,0 )	30280320	1944633600	( 7,0,0,1,0,0 )	117476956800	56922126105600
( 4,2,0,0,0,0 )	265193040	15047239200	( 6,1,1,0,0,0 )	7259328518400	2567057478451200
( 4,0,0,1,0,0 )	352800	9172800	( 6,0,0,0,1,0 )	973425600	250472476800
( 3,1,1,0,0,0 )	14679840	347054400	( 5,3,0,0,0,0 )	17466995857600	5819256740707200
( 2,3,0,0,0,0 )	14716800	344628480	( 5,1,0,1,0,0 )	130847724000	21807166852800
( 2,1,0,1,0,0 )	141120	1411200	( 5,0,0,2,0,0 )	173124907200	252712680859520
( 2,0,2,0,0,0 )	220752	2119712	( 5,0,0,0,0,1 )	6350400	495331200
( 1,2,1,0,0,0 )	479360	4704000	( 4,2,1,0,0,0 )	1527450321600	227821140489600
( 1,0,1,1,0,0 )	3136	13440	( 4,1,0,0,1,0 )	1336003200	93139200000
( 0,4,0,0,0,0 )	101080	1326640	( 4,0,1,1,0,0 )	8008590240	474479691840
( 0,2,0,1,0,0 )	3920	16800	( 3,4,0,0,0,0 )	1113735319200	160115777236800
( 0,1,2,0,0,0 )	0	0	( 3,2,0,1,0,0 )	25011126000	1549371247200
( 0,0,0,2,0,0 )	8	16	( 3,1,2,0,0,0 )	43446241440	2648029124160
( 9.0,0,0,0,0 )	128333096640	7435398382720	( 3,1,0,0,0,1 )	5292000	137592000
( 7,1,0,0,0,0 )	74905881120	21842745664320	( 3,0,1,0,1,0 )	76769280	1864396800
( 6,0,1,0,0,0 )	1848601440	283789840320	( 3,0,0,2,0,0 )	89454960	2064111840
( 5,2,0,0,0,0 )	18671546880	2504136680480	( 2,3,1,0,0,0 )	81274737600	5297420016000
( 5,0,0,1,0,0 )	24055920	1798927200	( 2,2,0,0,1,0 )	213670800	5267556000
( 4,1,1,0,0,0 )	1129416960	67312680960	( 2,1,1,1,0,0 )	1236332160	29871394560
( 4,0,0,0,1,0 )	176400	4586400	( 2,0,3,0,0,0 )	198767520	5064897600
( 3,3,0,0,0,0 )	1672520640	96647026560	( 2,0,1,0,0,1 )	211680	2116800
( 3,1,0,1,0,0 )	16215360	400848000	( 2,0,0,1,1,0 )	1352160	13135680
( 3,0,2,0,0,0 )	21816704	508234496	( 1,5,0,0,0,0 )	11990059200	82322210800
( 2,2,1,0,0,0 )	97858880	2402529920	( 1,3,0,1,0,0 )	557474400	15799896000
( 2,1,0,0,1,0 )	70560	705600	( 1,2,2,0,0,0 )	1566697440	46388233920
( 2,0,1,1,0,0 )	550592	5382272	( 1,2,0,0,0,1 )	529200	5292000
( 1,4,0,0,0,0 )	31823120	848103200	( 1,1,1,0,1,0 )	8168160	80740800
( 1,2,0,1,0,0 )	922600	9125200	( 1,1,0,2,0,0 )	4993560	49765680
( 1,1,2,0,0,0 )	1211840	12272512	( 1,0,2,1,0,0 )	4248720	43092000
( 1,0,1,0,1,0 )	1568	6720	( 1,0,0,1,0,1 )	2520	10800
( 1,0,0,2,0,0 )	2456	10544	( 1,0,0,0,2,0 )	3632	15584
( 0,3,1,0,0,0 )	678160	8533280	( 0,4,1,0,0,0 )	329246400	11283081600
( 0,2,0,0,1,0 )	1960	8400	( 0,3,0,0,1,0 )	1940400	19404000
( 0,1,1,0,0,0 )	11760	50400	( 0,2,1,1,0,0 )	11022480	132279840
( 0,0,1,0,0,0 )	0	0	( 0,1,3,0,0,0 )	6572160	93219840
( 0,0,0,1,1,0 )	8	16	( 0,1,1,0,0,1 )	11760	50400
			( 0,1,0,1,1,0 )	27720	118800
			( 0,0,2,0,1,0 )	25872	110880
			( 0,0,1,2,0,0 )	0	0
			( 0,0,0,0,1,1 )	8	16

Table AII. The Second Derivative of the Susceptibility  $\partial^2 \chi / \partial \tilde{H}^2$ 

P	LC	PSQ	T
( 2.0.0.0.0.0.0.0 )	-3	-3	-3
( 0.1.0.0.0.0.0.0 )	1	1	1
( 3.0.0.0.0.0.0.0 )	-24	-48	-72
( 1.1.0.0.0.0.0.0 )	8	16	24
( 4.0.0.0.0.0.0.0 )	-126	-732	-1818
( 2.1.0.0.0.0.0.0 )	14	188	522
( 1.0.1.0.0.0.0.0 )	2	4	6
( 0.2.0.0.0.0.0.0 )	6	12	18
( 5.0.0.0.0.0.0.0 )	-432	-11808	-48384
( 3.1.0.0.0.0.0.0 )	-312	1392	9036
( 2.0.1.0.0.0.0.0 )	24	144	396
( 1.2.0.0.0.0.0.0 )	72	528	1584
( 0.1.1.0.0.0.0.0 )	8	16	24
( 6.0.0.0.0.0.0.0 )	-540	-200376	-1372788
( 4.1.0.0.0.0.0.0 )	-3396	-16680	54324
( 3.0.1.0.0.0.0.0 )	-48	2736	15840
( 2.2.0.0.0.0.0.0 )	-156	15072	82260
( 2.0.0.1.0.0.0.0 )	6	36	90
( 1.1.1.0.0.0.0.0 )	188	1224	3684
( 0.3.0.0.0.0.0.0 )	66	404	1878
( 0.1.0.1.0.0.0.0 )	2	4	6
( 0.0.2.0.0.0.0.0 )	6	12	18
( 7.0.0.0.0.0.0.0 )	0	-3657600	-41867280
( 5.1.0.0.0.0.0.0 )	-7680	-1145760	-5861160
( 4.0.1.0.0.0.0.0 )	-1920	32160	454680
( 3.2.0.0.0.0.0.0 )	-16560	245280	3098160
( 3.0.0.1.0.0.0.0 )	0	1440	8640
( 2.0.1.0.0.0.0.0 )	640	50240	297120
( 1.3.0.0.0.0.0.0 )	1640	46480	285360
( 1.1.0.1.0.0.0.0 )	120	720	2040
( 1.0.2.0.0.0.0.0 )	176	1152	3648
( 0.2.1.0.0.0.0.0 )	280	1680	9360
( 0.0.1.1.0.0.0.0 )	8	16	24
( 8.0.0.0.0.0.0.0 )	-52920	-72232560	-1379002320
( 6.1.0.0.0.0.0.0 )	142200	-39684960	-461880360
( 5.0.1.0.0.0.0.0 )	-2520	-180000	7967160
( 4.2.0.0.0.0.0.0 )	-200340	-384480	75153960
( 4.0.0.1.0.0.0.0 )	-360	27720	436860
( 3.1.1.0.0.0.0.0 )	-30840	1380720	16684200
( 3.0.0.0.1.0.0.0 )	0	360	1800
( 2.3.0.0.0.0.0.0 )	-7380	2210040	25042500
( 2.1.0.1.0.0.0.0 )	270	41580	267570
( 2.0.2.0.0.0.0.0 )	1764	66528	393372
( 1.2.1.0.0.0.0.0 )	7980	234720	1894140
( 1.1.0.0.1.0.0.0 )	30	180	450
( 1.0.1.1.0.0.0.0 )	378	2364	7398
( 0.4.0.0.0.0.0.0 )	990	51180	341910
( 0.2.0.1.0.0.0.0 )	420	2520	9720
( 0.1.2.0.0.0.0.0 )	416	2504	23184
( 0.0.1.0.1.0.0.0 )	2	4	6
( 0.0.0.2.0.0.0.0 )	6	12	18
( 9.0.0.0.0.0.0.0 )	-423360	-1550223360	-49084056000
( 7.1.0.0.0.0.0.0 )	614880	-1195306560	-26135071200
( 6.0.1.0.0.0.0.0 )	171360	-23284800	-112432320
( 5.2.0.0.0.0.0.0 )	126000	-241547040	-6139400040
( 5.0.0.0.1.0.0.0 )	0	151200	14182560
( 4.1.1.0.0.0.0.0 )	-416640	20435520	693403200
( 4.0.0.0.0.1.0.0 )	0	10080	196560
( 3.3.0.0.0.0.0.0 )	-920640	66964800	1570200660
( 3.1.0.1.0.0.0.0 )	-15120	1562400	21180440
( 3.0.2.0.0.0.0.0 )	-35852	2386272	29256696
( 2.2.1.0.0.0.0.0 )	-31920	15620640	212633820
( 2.1.0.0.0.0.0.0 )	0	20160	126000
( 2.0.1.1.0.0.0.0 )	4368	175392	1099728
( 1.4.0.0.0.0.0.0 )	42000	6232800	83404440
( 1.2.0.1.0.0.0.0 )	5880	290640	2656080
( 1.1.2.0.0.0.0.0 )	26320	570080	5844468
( 1.0.1.0.1.0.0.0 )	224	1344	3864

P	LC	PSQ	T
( 1.0.0.2.0.0.0 )	312	1968	6480
( 0.3.1.0.0.0.0 )	10640	411040	3912720
( 0.2.0.0.1.0.0 )	280	1680	5040
( 0.0.1.1.1.0.0 )	1680	10080	70224
( 0.0.0.3.0.0.0 )	0	0	25452
( 0.0.0.0.1.1.0 )	8	16	24
-8-			
( 10.0.0.0.0.0.0 )	3946320	-35927327520	-1883525328720
( 8.1.0.0.0.0.0 )	-18390960	-35414779680	-1369390412880
( 7.0.1.0.0.0.0 )	372960	-939496320	-21592055520
( 6.2.0.0.0.0.0 )	25416720	-13188677040	-244468037520
( 6.0.0.1.0.0.0 )	37800	-9082080	232916040
( 5.1.1.1.0.0.0 )	1832880	-286685280	18258009840
( 5.0.0.0.1.0.0 )	0	75600	9903600
( 4.3.0.0.0.0.0 )	-12535320	750990240	70550814600
( 4.1.0.1.0.0.0 )	-89880	31947720	1171794960
( 4.0.2.0.0.0.0 )	-867720	59086944	1623677832
( 4.0.0.0.0.0.1 )	0	2520	37800
( 3.2.1.0.0.0.0 )	-4401600	644790720	16963349760
( 3.1.0.1.0.0.0 )	-3360	893760	15185520
( 3.0.1.0.1.0.0 )	-75264	8371104	106621200
( 2.4.0.0.0.0.0 )	-939540	466147080	11086897500
( 2.2.2.0.1.0.0 )	-89040	22496880	364006440
( 2.1.2.0.0.0.0 )	216048	47314176	807293424
( 2.1.0.0.0.1.0 )	0	5040	25200
( 2.0.0.1.0.1.0 )	1456	129920	874272
( 2.0.0.2.0.0.0 )	6594	189108	1177542
( 1.3.1.0.0.0.0 )	307440	65923200	1123802400
( 1.2.0.0.1.0.0 )	1820	274120	2223060
( 1.1.1.1.1.0.0 )	77504	2018912	22659168
( 1.0.3.0.0.0.0 )	11536	266336	7302288
( 1.0.1.0.0.0.1 )	56	336	840
( 1.0.0.1.0.1.0 )	624	3840	12336
( 1.0.0.0.1.1.0 )	59220	4933320	107326380
( 0.5.0.0.1.0.0 )	8890	405580	7980630
( 0.2.2.0.0.0.0 )	51716	1978312	20563620
( 0.2.0.0.0.1.0 )	70	420	1050
( 0.1.1.0.1.0.0 )	2520	15120	64344
( 0.1.0.2.0.0.0 )	986	5924	71598
( 0.0.2.1.0.0.0 )	924	5544	162204
( 0.0.0.1.0.1.0 )	2	4	6
( 0.0.0.0.2.0.0 )	6	12	18
-9-			
( 11.0.0.0.0.0.0 )	48988800	-893971572480	-77609988751680
( 9.1.0.0.0.0.0 )	-107049600	-1073067730560	-71346176002080
( 8.0.0.1.0.0.0 )	-28304840	-31366984320	-1598301240480
( 7.0.0.0.0.0.0 )	-362880	-561081427200	-22656556863360
( 7.0.0.1.0.0.0 )	0	-416949120	-7259868000
( 6.1.1.0.0.0.0 )	76325760	-37012066560	-198652487040
( 6.0.0.0.1.0.0 )	0	-5080320	251929440
( 5.3.0.0.0.0.0 )	124830720	-53762849280	1470780128160
( 5.1.0.1.0.0.0 )	2268000	36469440	45183186720
( 5.0.2.0.0.0.0 )	-725760	424932480	65337632640
( 5.0.0.0.0.1.0 )	0	0	3810240
( 4.2.1.0.0.0.0 )	-48323520	15781409280	1020552734880
( 4.1.0.0.1.0.0 )	0	22135680	1093992480
( 4.0.1.1.0.0.0 )	-1711584	256785984	7474457088
( 3.4.0.0.0.0.0 )	-78563520	20264912640	1028659746240
( 3.2.0.1.0.0.0 )	-3114720	1026920160	33877977840
( 3.1.2.0.0.0.0 )	-11573856	2586499776	78643649952
( 3.1.0.0.0.1.0 )	0	302400	6168960
( 3.0.1.0.1.0.0 )	-40320	8015616	112819392
( 3.0.0.2.0.0.0 )	-85104	10866528	140479920
( 2.3.1.0.0.0.0 )	-9646560	5841964800	175257583200
( 2.2.0.0.1.0.0 )	-50400	21420000	401027760
( 2.1.1.1.0.0.0 )	221760	194866560	3760313760
( 2.0.3.0.0.0.0 )	433440	41356224	1168540128
( 2.0.0.1.0.0.1 )	0	60480	357072
( 2.0.0.1.1.0.0 )	13392	445824	2919888
( 1.5.0.0.0.0.0 )	2721600	1364751360	37622869200
( 1.3.0.1.0.0.0 )	110880	11340000	2567224800
( 1.2.2.0.0.0.0 )	2336544	329277312	7071140160
( 1.2.0.0.0.1.0 )	0	151200	997920
( 1.1.1.0.1.0.0 )	58464	2632896	28171584
( 1.1.0.2.0.0.0 )	105912	2218032	28151928
( 1.0.2.1.0.0.0 )	93744	1977696	57050784

P	LC	PSQ	T
( 1.0.0.0.1.0.1.0 )	360	2160	6264
( 1.0.0.0.0.2.0.0 )	480	2976	10080
( 0.4.1.0.0.0.0.0 )	534240	82656000	2134082160
( 0.3.0.0.1.0.0.0 )	0	554400	10876320
( 0.2.1.1.0.0.0.0 )	192528	6094368	106242192
( 0.1.3.0.0.0.0.0 )	73920	4228224	55242432
( 0.1.1.0.0.1.0.0 )	1680	10080	31248
( 0.0.1.0.0.0.1.0 )	3960	23760	191592
( 0.0.0.2.0.1.0.0 )	3696	22176	207648
( 0.0.0.1.0.0.0.0 )	0	0	441936
( 0.0.0.0.0.1.1.0 )	8	16	24
( -10- )			
( 12.0.0.0.0.0.0.0 )	-853221600	-23787918907200	-3418910164908000
( 10.1.0.0.0.0.0.0 )	4030236000	-33680465884800	-3800952130399200
( 9.0.0.1.0.0.0.0 )	-92988000	-1033291728000	-100949278298400
( 8.2.0.0.0.0.0.0 )	-6718723200	-22201365362400	-1685156781218400
( 8.0.0.0.1.0.0.0 )	-6350400	-11515543200	-986175842400
( 7.1.1.0.0.0.0.0 )	-327499200	-1920152304000	-73843754846400
( 7.0.0.0.0.1.0.0 )	0	-118389600	-1118577600
( 6.3.0.0.0.0.0.0 )	4705495200	-5099819054400	-129065956437600
( 6.1.0.0.0.0.0.0 )	19769400	-31943041200	775840048200
( 6.0.2.0.0.0.0.0 )	149052960	-44608324320	1260189070560
( 6.0.0.0.0.0.1.0 )	0	-1814400	134038800
( 5.2.1.0.0.0.0.0 )	973198800	-33055646400	42956996166000
( 5.1.0.0.0.1.0.0 )	567000	-33944400	51218357400
( 5.0.1.1.0.0.0.0 )	5087880	3805900560	383183839080
( 5.0.0.0.0.0.0.1 )	0	0	680400
( 4.4.0.0.0.0.0.0 )	-1125684000	431775640800	69554844941400
( 4.2.0.1.0.0.0.0 )	1701000	28449489600	2338364019600
( 4.1.2.0.0.0.0.0 )	-233689680	91939921920	5840674333200
( 4.1.0.0.0.0.1.0 )	0	7030800	6275600
( 4.0.1.0.0.1.0.0 )	-405720	275672880	9805040280
( 4.0.0.1.0.0.0.0 )	-3205980	442096920	12077260380
( 3.3.1.0.0.0.0.0 )	-599785200	328469702400	1917707512000
( 3.2.0.0.0.0.0.0 )	-680400	1019088000	43712713800
( 3.1.1.1.0.0.0.0 )	-37391760	1207531040	425198077920
( 3.1.0.0.0.0.0.1 )	0	75600	1134000
( 3.0.0.3.0.0.0.0 )	-4324320	2950758720	133917265440
( 3.0.0.1.0.0.1.0 )	-10080	4168800	72969120
( 3.0.0.0.1.1.0.0 )	-167400	32402160	432808920
( 2.5.0.0.0.0.0.0 )	-69930000	136569384000	7006499400600
( 2.3.0.1.0.0.0.0 )	-14502600	10977157800	439427551500
( 2.2.2.0.0.0.0.0 )	-17884440	34603616880	1295238674520
( 2.2.0.0.0.0.1.0 )	-12600	12864600	274295700
( 2.1.1.0.0.1.0.0 )	-493920	287920080	572667680
( 2.1.0.2.0.0.0.0 )	1139580	255318120	5654025180
( 2.0.0.2.1.0.0.0 )	2063880	280027440	10551749040
( 2.0.0.1.0.0.0.1 )	0	15120	75600
( 2.0.0.0.1.0.1.0 )	4230	312300	2170530
( 2.0.0.0.0.2.0.0 )	16668	428136	2768004
( 1.4.1.0.0.0.0.0 )	15838200	22137242400	841533121800
( 1.3.0.0.1.0.0.0 )	-37800	141472800	4105306800
( 1.2.1.1.0.0.0.0 )	6897240	1424712240	41115082680
( 1.2.0.0.0.0.0.1 )	0	37800	189000
( 1.1.3.0.0.0.0.0 )	6004320	848793120	22264396560
( 1.1.1.0.0.0.1.0 )	18060	2421720	21461580
( 1.1.0.0.1.1.0.0 )	285210	7076700	93396510
( 1.0.2.0.0.1.0.0 )	207648	5424048	87385400
( 1.0.0.1.2.0.0.0 )	127350	2866140	180954810
( 1.0.0.0.1.0.0.1 )	90	540	1350
( 1.0.0.0.0.1.1.0 )	926	5652	18498
( 0.6.0.0.0.0.0.0 )	2016000	1620712800	50364946800
( 0.4.0.1.0.0.0.0 )	0	244314000	6220443600
( 0.3.2.0.0.0.0.0 )	4815720	532365120	20033652240
( 0.3.0.0.0.0.1.0 )	0	831600	8946000
( 0.2.1.0.0.1.0.0 )	113820	5811120	195938820
( 0.2.0.2.0.0.0.0 )	357030	10984860	155366370
( 0.1.2.1.0.0.0.0 )	520380	23438520	532881720
( 0.1.1.0.0.0.0.1 )	420	2520	6300
( 0.1.0.1.0.0.1.0 )	5940	35640	161820
( 0.1.0.0.0.2.0.0 )	1998	111996	173994
( 0.0.4.0.0.0.0.0 )	36288	5733504	56940408
( 0.0.2.0.0.0.1.0 )	5544	33264	162540
( 0.0.0.3.0.0.0.0 )	6006	36036	1511010
( 0.0.0.0.1.0.1.0 )	0	0	544320
( 0.0.0.0.0.1.0.1 )	2	4	6
( 0.0.0.0.0.0.2.0 )	6	12	18



P	SC	BCC	FCC
( 0 )			
( 2.0.0.0.0.0.0 )	-3	-3	-3
( 0.1.0.0.0.0.0 )	1	1	1
( 3.0.0.0.0.0.0 )	-72	-96	-144
( 1.1.0.0.0.0.0 )	24	32	48
( 4.0.0.0.0.0.0 )	-1818	-3384	-7956
( 2.1.0.0.0.0.0 )	522	1016	2484
( 1.0.1.0.0.0.0 )	6	8	12
( 0.2.0.0.0.0.0 )	18	24	36
( 5.0.0.0.0.0.0 )	-51408	-136512	-500256
( 3.1.0.0.0.0.0 )	10872	33888	136224
( 2.0.1.0.0.0.0 )	360	672	1728
( 1.2.0.0.0.0.0 )	1368	2592	7056
( 0.1.1.0.0.0.0 )	24	32	48
( 6.0.0.0.0.0.0 )	-1619028	-6179760	-35435880
( 4.1.0.0.0.0.0 )	184788	1108464	7733448
( 3.0.1.0.0.0.0 )	14112	40416	179856
( 2.0.2.0.0.0.0 )	74484	212064	949288
( 1.0.0.1.0.0.0 )	90	168	396
( 1.1.1.0.0.0.0 )	3108	5840	16152
( 0.3.0.0.0.0.0 )	1014	1896	7932
( 0.1.0.1.0.0.0 )	6	8	12
( 0.0.2.0.0.0.0 )	18	24	36
( 7.0.0.0.0.0.0 )	-56816640	-312353280	-2801148480
( 5.1.0.0.0.0.0 )	367200	31306560	432302400
( 4.0.1.0.0.0.0 )	485280	2258880	16888320
( 3.2.0.0.0.0.0 )	3331440	14990400	111293280
( 3.0.0.1.0.0.0 )	7200	20160	93600
( 2.1.1.0.0.0.0 )	236160	657280	3244800
( 1.3.0.0.0.0.0 )	194040	538400	3025680
( 1.1.0.1.0.0.0 )	1800	3360	8880
( 1.0.2.0.0.0.0 )	2928	5504	15936
( 0.2.1.0.0.0.0 )	4200	7840	39120
( 0.0.1.1.0.0.0 )	24	32	48
( 8.0.0.0.0.0.0 )	-2201868360	-17454843360	-244974397680
( 6.1.0.0.0.0.0 )	-237244680	248497920	20557251360
( 5.0.1.0.0.0.0 )	14794920	119969280	1536049440
( 4.2.0.0.0.0.0 )	132505740	994528800	12320573040
( 4.0.0.1.0.0.0 )	362880	1681200	14328360
( 3.1.1.0.0.0.0 )	14349240	62225760	521416080
( 3.0.0.0.1.0.0 )	1800	5040	19800
( 2.3.0.0.0.0.0 )	18929700	79714800	717719400
( 2.1.0.1.0.0.0 )	201690	564120	2885220
( 2.0.2.0.0.0.0 )	298692	819936	4217184
( 1.2.1.0.0.0.0 )	997020	2772960	19941120
( 1.1.0.0.1.0.0 )	450	840	1980
( 1.0.1.1.0.0.0 )	5958	11160	32148
( 0.4.0.0.0.0.0 )	198090	610200	3721140
( 0.2.0.1.0.0.0 )	6300	11760	41400
( 0.1.2.0.0.0.0 )	6264	11696	95256
( 0.0.1.0.1.0.0 )	6	8	12
( 0.0.0.2.0.0.0 )	18	24	36
( 9.0.0.0.0.0.0 )	-93655154880	-1071180633600	-23518678095360
( 7.1.0.0.0.0.0 )	-21078701280	-81006871680	218608891200
( 6.0.1.0.0.0.0 )	374401440	6193333600	138650218560
( 5.2.0.0.0.0.0 )	4425820560	62751769920	1329171439680
( 5.0.0.1.0.0.0 )	15331680	123802560	1850385600
( 4.1.1.0.0.0.0 )	755455680	5297066880	75076787520
( 4.0.0.0.1.0.0 )	151200	705600	6350400
( 3.3.0.0.0.0.0 )	1447044480	9485105280	138200958000
( 3.1.0.1.0.0.0 )	16102800	70338240	651188160
( 3.0.2.0.0.0.0 )	22507632	94721088	862493184
( 2.2.1.0.0.0.0 )	128807280	545442240	6036775920
( 2.1.0.0.1.0.0 )	100800	282240	1360800
( 2.0.1.1.0.0.0 )	795312	2186688	11696832
( 1.4.0.0.0.0.0 )	47643120	208017600	2302957440
( 1.2.0.1.0.0.0 )	1338120	3712800	27956880
( 1.1.2.0.0.0.0 )	2303280	6341440	61066992
( 1.0.1.0.1.0.0 )	3360	6272	16800

P	SC	BCC	FCC
( 1, 0, 0, 2, 0, 0, 0 )	4968	9312	28080
( 0, 3, 1, 0, 0, 0, 0 )	1537200	4773440	42756000
( 0, 2, 0, 0, 1, 0, 0 )	4200	7840	21840
( 0, 0, 1, 1, 0, 0, 0 )	25200	47040	290976
( 0, 0, 0, 3, 0, 0, 0 )	0	0	101808
( 0, 0, 0, 1, 1, 0, 0 )	24	32	48
-8-			
( 10, 0, 0, 0, 0, 0, 0 )	-4341352211280	-71656265580480	-2461342220598240
( 8, 1, 0, 0, 0, 0, 0 )	-1494315481680	-12042896886720	-167582225795040
( 7, 0, 1, 0, 0, 0, 0 )	2692418400	293847321600	12401644510080
( 6, 2, 0, 0, 0, 0, 0 )	83061961920	3705141575520	140703063485040
( 6, 0, 0, 1, 0, 0, 0 )	571936680	8445608640	222148815840
( 5, 1, 1, 0, 0, 0, 0 )	36242312400	428148719040	10239508228320
( 5, 0, 0, 0, 1, 0, 0 )	8210160	71255520	1247384880
( 4, 3, 0, 0, 0, 0, 0 )	94826972520	998254824000	23893649186400
( 4, 1, 0, 1, 0, 0, 0 )	1039086720	7454380080	121290051960
( 4, 0, 2, 0, 0, 0, 0 )	1468591992	98111112640	152669633760
( 4, 0, 0, 0, 0, 1, 0 )	37800	176400	1247400
( 3, 2, 1, 0, 0, 0, 0 )	12158455680	79899415680	1430280532800
( 3, 1, 0, 0, 1, 0, 0 )	10735200	48612480	476904960
( 3, 0, 1, 0, 0, 0, 0 )	76912416	323585472	3113024544
( 2, 4, 0, 0, 0, 0, 0 )	7243839540	46927582800	839128260600
( 2, 2, 0, 1, 0, 0, 0 )	196751520	843047520	10600959600
( 2, 1, 2, 0, 0, 0, 0 )	369441072	1553298432	22576237824
( 2, 1, 0, 0, 0, 1, 0 )	25200	70560	277200
( 2, 0, 1, 0, 1, 0, 0 )	621936	1730176	9331392
( 2, 0, 0, 2, 0, 0, 0 )	827766	2251176	12391452
( 1, 3, 1, 0, 0, 0, 0 )	490598640	2245770240	31651636800
( 1, 2, 0, 0, 1, 0, 0 )	1334340	3726800	23576280
( 1, 1, 1, 1, 0, 0, 0 )	8521632	23498048	236673696
( 1, 0, 3, 0, 0, 0, 0 )	1045296	2968000	77022624
( 1, 0, 1, 0, 0, 1, 0 )	840	1568	3696
( 1, 0, 0, 0, 0, 1, 0 )	9648	18048	53376
( 0, 5, 0, 0, 0, 0, 0 )	35125020	159178320	3092842200
( 0, 3, 0, 1, 0, 0, 0 )	1694070	4976440	85146180
( 0, 2, 2, 0, 0, 0, 0 )	7220556	22838480	234802680
( 0, 2, 0, 0, 0, 1, 0 )	1050	1960	4620
( 0, 1, 1, 0, 1, 0, 0 )	37800	70560	272496
( 0, 1, 0, 2, 0, 0, 0 )	14814	27656	292332
( 0, 0, 2, 1, 0, 0, 0 )	13860	25872	654360
( 0, 0, 0, 1, 0, 1, 0 )	6	8	12
( 0, 0, 0, 0, 2, 0, 0 )	18	24	36
-9-			
( 11, 0, 0, 0, 0, 0, 0 )	-218056931487360	-5194080120660480	-279054504944248320
( 9, 1, 0, 0, 0, 0, 0 )	-101205199872000	-1361344519584000	-41118364918229760
( 8, 0, 1, 0, 0, 0, 0 )	-675815736960	10618635928320	1066203123068160
( 7, 2, 0, 0, 0, 0, 0 )	-5387044682880	184762446543360	14379837775914240
( 7, 0, 0, 1, 0, 0, 0 )	18419244480	557501253120	25907585356800
( 6, 1, 1, 0, 0, 0, 0 )	1549948296960	33394899041280	1362124056948480
( 6, 0, 0, 0, 1, 0, 0 )	349997760	6092755200	198837555840
( 5, 3, 0, 0, 0, 0, 0 )	5561466583680	98253468633600	3898356222055680
( 5, 1, 0, 1, 0, 0, 0 )	59414977440	721622805120	20316716239680
( 5, 0, 2, 0, 0, 0, 0 )	85652743680	937633294080	24901023369600
( 5, 0, 0, 0, 0, 1, 0 )	2721600	25401600	489888000
( 4, 2, 1, 0, 0, 0, 0 )	969276248640	10122819678720	295824017341440
( 4, 1, 0, 0, 1, 0, 0 )	858392640	6552161280	120089329920
( 4, 0, 1, 1, 0, 0, 0 )	5991965280	40132471680	684804030272
( 3, 4, 0, 0, 0, 0, 0 )	815620155840	8135597594880	237527939013120
( 3, 2, 0, 1, 0, 0, 0 )	21148646400	143537244480	3026562265440
( 3, 1, 2, 0, 0, 0, 0 )	43056165600	280996813440	6377060587968
( 3, 1, 0, 0, 0, 1, 0 )	4536000	21168000	198676800
( 3, 0, 1, 0, 1, 0, 0 )	77874048	334849536	3374203392
( 3, 0, 0, 2, 0, 0, 0 )	95664240	396660672	3991941792
( 2, 3, 1, 0, 0, 0, 0 )	88089755040	594596298240	13590319881600
( 2, 2, 0, 0, 1, 0, 0 )	212647680	928468800	12049158240
( 2, 1, 1, 1, 0, 0, 0 )	1557299520	6542887680	106563461760
( 2, 0, 3, 0, 0, 0, 0 )	299974752	1279845504	33478861248
( 2, 0, 1, 0, 0, 1, 0 )	302400	846720	4173120
( 2, 0, 0, 1, 1, 0, 0 )	1991952	5443200	30720384
( 1, 5, 0, 0, 0, 0, 0 )	17648487360	117278219520	2787874528320
( 1, 3, 0, 1, 0, 0, 0 )	853947360	3906483840	74214826560
( 1, 2, 2, 0, 0, 0, 0 )	2368789920	11146883328	205226396928
( 1, 2, 0, 0, 0, 1, 0 )	756000	2116800	10735200
( 1, 1, 1, 0, 1, 0, 0 )	12029472	33328512	294694848
( 1, 1, 0, 2, 0, 0, 0 )	8945640	24543072	293521104
( 1, 0, 2, 1, 0, 0, 0 )	7901712	21857472	598818528

P	SC	BCC	FCC
(1,0,0,1,0,1,0)	5400	10080	27216
1,0,0,0,2,0,0,0	7488	14016	43488
0,4,1,0,0,0,0,0	580819680	2953681920	64156518720
0,3,0,0,1,0,0,0	2772000	7761600	114196320
0,2,1,1,0,0,0,0	22543920	69427008	1191861216
0,0,1,3,0,0,0,0	14503104	49437696	691649280
0,0,1,1,0,0,1,0	25200	47040	135072
0,0,1,0,1,1,0,0	59400	110880	790128
0,0,0,2,0,1,0,0	55440	103488	852768
0,0,0,1,2,0,0,0	0	0	1767744
(0,0,0,0,1,1,0)	24	32	48
(1,2,0,0,0,0,0,0)	-11800645178404000	-405643859331580800	-34085119865134161600
10,1,0,0,0,0,0,0	-6898946190746400	-144929516769676800	-7769742865912944000
9,0,0,1,0,0,0,0	-83372867071200	-123230375654400	79531682691484800
8,2,0,0,0,0,0,0	-992118250519200	4024146771086400	1336441291403148000
8,0,0,0,1,0,0,0	324767167200	34956615960000	2988569354954400
7,1,1,0,0,0,0,0	51184627704000	2520409149216000	17918174348224000
7,0,0,0,1,0,0,0	13312706400	479748225600	28719198194400
6,3,0,0,0,0,0,0	283563976197600	9219597948489600	615938439001032000
6,1,0,1,0,0,0,0	3077171256600	66131617860000	3213027072284400
6,0,0,2,0,0,0,0	4649991857280	86415932393280	388572128739440
6,0,0,1,0,0,1,0	129956400	2842257600	113528822400
6,0,0,1,0,0,0,1	69075700570800	1174959461289600	56584712143108800
5,1,0,0,1,0,0,0	55146306600	749275984800	25097685958800
5,0,0,1,1,0,0,0	411241312440	4523633987040	133790791523760
5,0,0,0,0,0,1,0	680400	6350400	89812800
4,4,0,0,0,0,0,0	77654951942400	1222549060118400	58358604989966400
4,2,0,1,0,0,0,0	1896560001000	20807885750400	732156760188000
4,1,2,0,0,0,0,0	4078118091600	42018925939200	1539856590975360
4,1,0,0,0,0,1,0	446569200	3748399200	75153582000
4,0,0,1,0,0,0,0	7269098760	50788694880	943986551760
4,0,0,0,2,0,0,0	8998430940	58760633520	1049795137800
3,3,1,0,0,0,0,0	11715152072400	120720550406400	4458405482395200
3,2,0,0,1,0,0,0	25708041200	18344738000	4266347652000
3,1,1,1,0,0,0,0	204572571840	134360338860	35558602022160
3,1,0,0,0,0,1,0	1134000	5292000	37422000
3,0,0,3,0,0,0,0	45399221280	300287191680	11006793846720
3,0,0,1,0,0,1,0	48641040	218383200	2267077680
3,0,0,0,1,1,0,0	285525000	1187796960	12373307280
2,5,0,0,0,0,0,0	3849007150800	38259819460800	1427113498154400
2,3,0,0,1,0,0,0	177339456000	1242274143600	36684218579400
2,2,2,0,0,0,0,0	495179055000	3472642041120	12263903496720
2,2,0,0,0,0,1,0	157550400	715050000	8528700600
2,1,1,0,1,0,0,0	2461248720	10447486560	166311880560
2,1,0,0,2,0,0,0	1984158180	8307749520	159262326360
2,0,2,1,0,0,0,0	2102156280	8957239200	304677661680
2,0,0,1,0,0,0,1	75600	211680	831600
2,0,0,0,1,0,1,0	1485810	4120920	23046660
2,0,0,0,0,0,0,1	1852164	5010192	28883448
1,4,1,0,0,0,0,0	288557753400	2067985987200	66014254908000
1,3,0,0,1,0,0,0	1196407800	5301172800	121595947200
1,2,1,1,0,0,0,0	10317472200	48540713760	1215866106000
1,2,0,0,0,0,0,1	189000	529200	2079000
1,1,3,0,0,0,0,0	5846904000	29732740800	696460978080
1,1,1,0,0,0,1,0	11757060	32812080	226474920
1,1,0,0,1,1,0,0	29748870	81719640	972952020
1,0,2,0,1,0,0,0	22916880	63219744	1015359408
1,0,0,1,2,0,0,0	11279250	31851000	1907519220
1,0,0,0,1,0,0,1	1350	2520	5940
1,0,0,0,0,1,1,0	14178	26504	79836
0,6,0,0,0,0,0,0	19745208000	151007270400	3998078028000
0,4,0,1,0,0,0,0	1709845200	9435938400	192168471600
0,3,0,0,0,0,0,0	3651759720	19616526720	638074009440
0,3,0,0,0,0,1,0	4158000	11642400	94222800
0,2,1,0,1,0,0,0	24919020	72542400	2109920400
0,2,0,2,0,0,0,0	40769730	124889400	1796162580
0,1,2,1,0,0,0,0	81636660	271116720	6617955960
0,1,1,0,0,0,0,1	6300	11760	27720
0,1,0,0,1,0,1,0	89100	166320	682920
0,1,0,0,0,2,0,0	29994	55992	707988
0,0,0,4,0,0,0,0	18271008	68281920	894444768
0,0,0,2,0,0,1,0	83160	155232	683424
0,0,0,1,1,0,0,0	90090	168168	6080076
0,0,0,0,3,0,0,0	0	0	2177280
0,0,0,0,0,0,1,1	6	8	12
0,0,0,0,0,0,0,2	18	24	36

P	HSC	HBCC
( 2.0.0.0.0.0.0.0 )	-3	-3
( 0.1.0.0.0.0.0.0 )	1	1
( 3.0.0.0.0.0.0.0 )	-96	-192
( 1.1.0.0.0.0.0.0 )	32	64
( 4.0.0.0.0.0.0.0 )	-3384	-14448
( 2.1.0.0.0.0.0.0 )	1016	4592
( 1.0.1.0.0.0.0.0 )	8	16
( 0.2.0.0.0.0.0.0 )	24	48
( 5.0.0.0.0.0.0.0 )	-136512	-1277568
( 3.1.0.0.0.0.0.0 )	33888	376512
( 2.0.1.0.0.0.0.0 )	672	2880
( 1.2.0.0.0.0.0.0 )	2592	11328
( 0.1.1.0.0.0.0.0 )	32	64
( 6.0.0.0.0.0.0.0 )	-6243696	-129648096
( 4.1.0.0.0.0.0.0 )	1148208	34378080
( 3.0.1.0.0.0.0.0 )	39840	408384
( 2.2.0.0.0.0.0.0 )	206880	2104512
( 2.0.0.1.0.0.0.0 )	168	720
( 1.1.1.0.0.0.0.0 )	5840	25248
( 0.3.0.0.0.0.0.0 )	1896	8144
( 0.1.0.1.0.0.0.0 )	8	16
( 0.0.2.0.0.0.0.0 )	24	48
( 7.0.0.0.0.0.0.0 )	-321442560	-14891604480
( 5.1.0.0.0.0.0.0 )	36421440	3448410240
( 4.0.1.0.0.0.0.0 )	2201280	56496000
( 3.2.0.0.0.0.0.0 )	14552640	360082560
( 3.0.0.1.0.0.0.0 )	20160	201600
( 2.1.1.0.0.0.0.0 )	645760	6406400
( 1.3.0.0.0.0.0.0 )	503840	4970560
( 1.1.0.1.0.0.0.0 )	3360	14400
( 1.0.2.0.0.0.0.0 )	5504	23808
( 0.2.1.0.0.0.0.0 )	7840	33600
( 0.0.1.1.0.0.0.0 )	32	64
( 8.0.0.0.0.0.0.0 )	-18425028960	-1910216882880
( 6.1.0.0.0.0.0.0 )	714954240	372500064000
( 5.0.1.0.0.0.0.0 )	118692800	7977611520
( 4.2.0.0.0.0.0.0 )	983918880	61133538240
( 4.0.0.1.0.0.0.0 )	1629360	42040800
( 3.1.1.0.0.0.0.0 )	59587680	1430604480
( 3.0.0.0.1.0.0.0 )	5040	50400
( 2.3.0.0.0.0.0.0 )	73488240	1718074080
( 2.1.0.1.0.0.0.0 )	558360	5574960
( 2.0.2.0.0.0.0.0 )	802656	7831872
( 1.2.1.0.0.0.0.0 )	2611680	25865280
( 1.1.0.0.1.0.0.0 )	840	3600
( 1.0.1.1.0.0.0.0 )	11160	48048
( 0.4.0.0.0.0.0.0 )	489240	5498160
( 0.2.0.1.0.0.0.0 )	11760	50400
( 0.1.2.0.0.0.0.0 )	11696	50144
( 0.0.1.0.0.1.0.0 )	8	16
( 0.0.0.2.0.0.0.0 )	24	48
( 9.0.0.0.0.0.0.0 )	-1165677488640	-270906981166080
( 7.1.0.0.0.0.0.0 )	-44212291200	42382346146560
( 6.0.1.0.0.0.0.0 )	6551879040	1178996878080
( 5.2.0.0.0.0.0.0 )	65407204800	10585093518720
( 5.0.0.1.0.0.0.0 )	117996480	8065008000
( 4.1.1.0.0.0.0.0 )	5049340800	302018384640
( 4.0.0.0.1.0.0.0 )	705600	18345600
( 3.3.0.0.0.0.0.0 )	8697655680	492997128960
( 3.1.0.1.0.0.0.0 )	67556160	1641628800
( 3.0.2.0.0.0.0.0 )	90729408	2108572032
( 2.2.1.0.0.0.0.0 )	494276160	11621904000
( 2.1.0.0.1.0.0.0 )	282240	2822400
( 2.0.1.1.0.0.0.0 )	2146368	20990592
( 1.4.0.0.0.0.0.0 )	175922880	4315785600
( 1.2.0.1.0.0.0.0 )	3632160	35918400
( 1.1.2.0.0.0.0.0 )	5897920	57653120
( 1.0.1.0.1.0.0.0 )	6272	26880

P	HSC	HBCC
( 1.0,0.2,0.0,0.0 )	9312	40128
0.3,1.0,0.0,0.0 )	3725120	42394240
0.2,0.0,1.0,0.0 )	7840	33600
0.1,1.1,0.0,0.0 )	47040	201600
0.0,3.0,0.0,0.0 )	0	0
0.0,0.1,1.0,0.0 )	32	64
-8-		
( 10.0,0.0,0.0,0.0 )	-80721591854400	-42097758294049920
8,1.0,0.0,0.0,0.0 )	-9378440688960	4900569696570240
7,0.1,0.0,0.0,0.0 )	351567014400	183168888053760
6,2.0,0.0,0.0,0.0 )	4266188166240	1895268783360960
6,0.0,1.0,0.0,0.0 )	8252254080	1517111366400
5,1,1.0,0.0,0.0,0.0 )	416198475840	63215025874560
5,0.0,0.0,1.0,0.0,0.0 )	67626720	4986475200
4,3,0,0,0.0,0.0,0.0 )	930601472640	130272939820800
4,1,0,1,0.0,0.0,0.0 )	6999147120	432594526560
4,0,2,0,0.0,0.0,0.0 )	9210897024	527981577984
4,0,0,0,0.0,1.0,0.0,0.0 )	176400	4586400
3,2,1,0,0.0,1.0,0.0,0.0 )	71206748240	4075977319680
3,1,0,1,0.0,0.0,0.0,0.0 )	47402880	1198176000
3,0,1,0,1.0,0.0,0.0,0.0 )	309054144	7195074432
2,4,0,0,0.0,0.0,0.0,0.0 )	39690304080	2265553936800
2,2,0,1,0.0,0.0,0.0,0.0 )	776821920	18506107200
2,1,2,0,0.0,0.0,0.0,0.0 )	1388870784	32471862528
2,1,0,0,0.0,1.0,0.0,0.0 )	70560	705600
2,0,1,0,1.0,0.0,0.0,0.0 )	1714048	17007872
2,0,0,2,0.0,0.0,0.0,0.0 )	2202792	21251664
1,3,1,0,0.0,0.0,0.0,0.0 )	1781404800	46279645440
1,2,0,0,1.0,0.0,0.0,0.0 )	3699920	36887200
1,1,1,1,0.0,0.0,0.0,0.0 )	22283072	218443904
1,0,1,3,0,0.0,0.0,0.0 )	2629312	26698112
1,0,0,1,0.0,0.0,1.0,0.0,0.0 )	1568	6720
1,0,0,1,1.0,0.0,0.0,0.0 )	18048	77568
0,5,0,0,0.0,0.0,0.0,0.0 )	126082320	3229957920
0,3,0,1,0.0,0.0,0.0,0.0 )	4378360	46330480
0,2,2,0,0.0,0.0,0.0,0.0 )	17219216	201024544
0,2,0,0,0.0,1.0,0.0,0.0 )	1960	8400
0,0,1,1,0.0,1.0,0.0,0.0 )	70560	302400
0,0,1,0,2,0.0,0.0,0.0 )	27656	118544
0,0,0,2,1,0.0,0.0,0.0 )	25872	110880
0,0,0,0,1,0.0,1.0,0.0 )	8	16
0,0,0,0,2,0.0,0.0,0.0 )	24	48
-9-		
( 11,0,0,0,0,0,0,0,0,0 )	-6076426019489280	-7116061627543034880
9,1,0,0,0,0,0,0,0,0 )	-1187463790437120	535919212294986240
8,0,1,0,0,0,0,0,0,0 )	17191683129600	29981943429419520
7,2,0,0,0,0,0,0,0,0 )	262658235409920	352709420609387520
7,0,0,1,0,0,0,0,0,0 )	577919784960	289910013926400
6,1,1,0,0,0,0,0,0,0 )	34092055388160	13392240549488640
6,0,0,0,1,0,0,0,0,0 )	5700844800	1206626803200
5,3,0,0,0,0,0,0,0,0 )	95130526256640	33403048525808640
5,1,0,1,0,0,0,0,0,0 )	677086542720	1 8276077064960
5,0,2,0,0,0,0,0,0,0 )	884192682240	127632198597120
5,0,0,0,0,0,1.0,0.0,0.0 )	25401600	1981324800
4,2,1,0,0,0,0,0,0,0 )	9009529966080	1276660592686080
4,1,0,0,1,0,0,0,0,0 )	6151541760	406120780800
4,0,0,1,1,0,0,0,0,0 )	37449336960	2160817489152
3,4,0,0,0,0,0,0,0,0 )	6928463485440	949977372395520
3,2,0,1,0,0,0,0,0,0 )	127972595520	7566099408000
3,1,2,0,0,0,0,0,0,0 )	243188346240	13877730494208
3,1,0,0,0,0,1.0,0.0,0.0 )	21168000	550368000
3,0,1,0,0,1,0,0,0,0 )	321302016	7683701760
3,0,0,2,0,0,0,0,0,0 )	378081216	8650523520
2,3,1,0,0,0,0,0,0,0 )	476983261440	28657537251840
2,2,0,0,1,0,0,0,0,0 )	885407040	21564547200
2,1,1,1,0,0,0,0,0,0 )	5919217920	138018746880
2,0,0,3,0,0,0,0,0,0 )	1091873664	26031317760
2,0,0,1,0,0,1.0,0.0,0.0 )	846720	8467200
1,0,0,0,1,1,0,0,0,0 )	5346432	51902208
1,5,0,0,0,0,0,0,0,0 )	89395246080	5341526184960
1,3,0,1,0,0,0,0,0,0 )	3128711040	80939416320
1,2,2,0,0,0,0,0,0,0 )	8441685504	227434798080
1,2,0,0,0,0,1.0,0.0,0.0 )	2116800	21168000
1,1,1,0,0,1.0,0.0,0.0 )	32554368	321350400
1,1,0,2,0,0,0,0,0,0 )	22898016	222881472
1,0,2,1,0,0,0,0,0,0 )	20115648	197769600

P	HSC	HBC
(1.0.0.1.0.1.0)	10080	43200
(1.0.0.0.2.0.0.0)	14016	60288
(0.4.1.0.0.0.0.0)	2040433920	60190824960
(0.3.0.0.1.0.0.0)	7761600	77616000
(0.2.1.1.0.0.0.0)	54379584	612920448
(0.1.3.0.0.0.0.0)	32936752	427080192
(0.1.0.1.0.0.1.0)	47040	201600
(0.0.2.0.0.0.0.0)	110880	475200
(0.0.1.2.0.0.0.0)	103488	443520
(0.0.0.0.0.1.1.0)	0	0
(0.0.0.0.0.1.1.0)	32	64
-10-		
(12.0.0.0.0.0.0.0)	-494149407736924800	-1300088046600125395200
(10.1.0.0.0.0.0.0)	-136073758812364800	43417405533546777600
(9.0.1.0.0.0.0.0)	544923491212800	5151435458512896000
(8.2.0.0.0.0.0.0)	13372643707819200	68296932748947772800
(8.0.0.0.1.0.0.0.0)	40308353870400	56974591221609600
(7.1.1.0.0.0.0.0)	2795226069484800	2909447193528691200
(7.0.0.0.0.1.0.0.0)	464741323200	280634193302400
(6.3.0.0.0.0.0.0)	9508468913596800	8529355232422214400
(6.1.0.1.0.0.0.0)	63833684796000	26718880113374400
(6.0.2.0.0.0.0.0)	83658869945280	30778593240608640
(6.0.0.0.0.0.1.0)	2624529600	656644060800
(5.2.1.0.0.0.0.0)	1067155876483200	378415158584198400
(5.1.0.0.1.0.0.0)	691410232800	123467186001600
(5.0.0.1.1.0.0.0)	4174402811040	611868850689600
(5.0.0.0.0.0.0.1)	6350400	495331200
(4.4.0.0.0.0.0.0)	1060161723432000	355120112249481600
(4.2.0.1.0.0.0.0)	18243489902400	2727739255248000
(4.1.2.0.0.0.0.0)	35940379184640	5090680482048000
(4.1.0.0.0.0.1.0)	3585103200	258937560000
(4.0.0.1.0.1.0.0)	47348411040	2861841648960
(4.0.0.0.2.0.0.0)	5439422800	305984487600
(3.3.1.0.0.0.0.0)	97087236220800	13997495767852800
(3.2.0.0.1.0.0.0)	165922646400	10307300371200
(3.1.1.1.0.0.0.0)	1167080654880	67011590318400
(3.1.0.0.0.0.0.1)	5292000	137592000
(3.0.3.0.0.0.0.0)	249720831360	14637587086080
(3.0.1.0.0.1.0.0)	213302880	5346532800
(3.0.0.1.1.0.0.0)	1133157600	26059078080
(2.5.0.0.0.0.0.0)	29569677782400	4155591579148800
(2.3.0.1.0.0.0.0)	985325468400	61686990741600
(2.2.2.0.0.0.0.0)	2617271042400	165554438777280
(2.2.0.0.0.1.0.0)	700534800	17756676000
(2.1.1.0.1.0.0.0)	9652416480	227638998720
(2.1.0.2.0.0.0.0)	7458385680	173440853280
(2.0.2.1.0.0.0.1)	776779040	184705456320
(2.0.1.0.0.0.0.1)	211680	2116800
(2.0.0.1.0.1.0.0)	4086360	40405680
(2.0.0.0.2.0.0.0)	4906512	47026464
(1.4.1.0.0.0.0.0)	1461533068800	95931140256000
(1.3.0.0.0.1.0.0)	4664016000	115726867200
(1.2.1.1.0.0.0.0)	36931517280	993210240960
(1.2.0.0.0.0.0.1)	529200	5292000
(1.1.3.0.0.0.0.0)	20170207680	600843949440
(1.1.1.0.0.1.0.0)	32570160	324424800
(1.1.0.1.1.0.0.0)	77676120	757946160
(1.0.2.0.1.0.0.0)	59953824	588087360
(1.0.1.2.0.0.0.0)	28429560	286717680
(1.0.0.1.0.0.1.0)	2520	10800
(1.0.0.0.1.1.0.0)	26504	113808
(0.6.0.0.0.0.0.0)	91511582400	6833222121600
(0.4.0.1.0.0.0.0)	5905720800	193130078400
(0.3.2.0.0.0.0.0)	12681385920	399077723520
(0.3.0.0.0.0.1.0)	11642400	116424000
(0.2.1.0.1.0.0.0)	65264640	682899840
(0.2.0.2.0.0.0.0)	98597880	1103566320
(0.1.2.1.0.0.0.0)	187997040	2350141920
(0.1.1.0.0.0.0.1)	11760	50400
(0.1.0.1.0.1.0.0)	166320	712800
(0.1.0.0.2.0.0.0)	55992	239984
(0.0.4.0.0.0.0.0)	38828160	578285568
(0.0.2.0.0.0.1.0)	155232	665280
(0.0.0.1.1.0.0.0)	168168	720720
(0.0.0.0.3.0.0.0)	0	0
(0.0.0.0.1.0.1.0)	8	16
(0.0.0.0.0.2.0.0)	24	48

Table AIII. The Second Moment  $\mu_2$

P	LC	PSQ	P	LC	PSQ
-0-			-9-		
( 0,0,0,0,0,0 )	0	0	( 10,0,0,0,0,0 )	-816480	27569263680
( -1-			( 8,1,0,0,0,0 )	5443200	35322557760
( 2,0,0,0,0,0 )	2	4	( 7,0,1,0,0,0 )	0	1079386560
( -2-			( 6,2,0,0,0,0 )	-6342840	23882780880
( 3,0,0,0,0,0 )	16	64	( 6,0,0,1,0,0 )	0	10523520
( -3-			( 5,1,1,0,0,0 )	-861840	2521683360
( 4,0,0,0,0,0 )	90	900	( 5,0,0,0,1,0 )	0	5821653600
( 2,1,0,0,0,0 )	12	72	( 4,3,0,0,0,0 )	710640	42910560
( 0,2,0,0,0,0 )	2	4	( 4,1,0,1,0,0 )	0	114402960
( -4-			( 4,0,2,0,0,0 )	410760	114402960
( 5,0,0,0,0,0 )	384	13056	( 3,2,1,0,0,0 )	1985760	649837440
( 3,1,0,0,0,0 )	192	3072	( 3,1,0,0,1,0 )	0	151200
( 1,2,0,0,0,0 )	64	256	( 3,0,1,1,0,0 )	52416	5711328
( -5-			( 2,4,0,0,0,0 )	3351600	442612800
( 6,0,0,0,0,0 )	1200	202560	( 2,4,0,1,0,0 )	65520	12605040
( 4,1,0,0,0,0 )	1440	88560	( 2,2,0,1,0,0 )	355824	21141792
( 3,0,1,0,0,0 )	0	720	( 2,0,1,0,1,0 )	0	30240
( 2,2,0,0,0,0 )	1170	13140	( 2,0,0,2,0,0 )	6138	83556
( 1,1,1,0,0,0 )	60	360	( 1,3,1,0,0,0 )	569520	34191360
( 0,3,0,0,0,0 )	0	0	( 1,2,0,0,1,0 )	0	75600
( 0,0,2,0,0,0 )	2	4	( 1,1,1,1,0,0 )	53928	712656
( -6-			( 1,0,3,0,0,0 )	0	0
( 7,0,0,0,0,0 )	4320	3412800	( 1,0,0,1,1,0 )	180	1080
( 5,1,0,0,0,0 )	1440	2243520	( 0,5,0,0,0,0 )	0	0
( 4,0,1,0,0,0 )	0	40320	( 0,3,0,1,0,0 )	0	0
( 3,2,0,0,0,0 )	14880	575040	( 0,2,2,0,0,0 )	53424	852768
( 2,1,1,0,0,0 )	1440	26880	( 0,1,1,0,1,0 )	840	5040
( 1,3,0,0,0,0 )	960	14400	( 0,1,0,2,0,0 )	0	0
( 1,0,2,0,0,0 )	96	384	( 0,0,2,1,0,0 )	0	0
( 0,2,1,0,0,0 )	160	640	( 0,0,0,0,2,0 )	2	4
( -7-			( -10-		
( 8,0,0,0,0,0 )	44100	62881560	( 11,0,0,0,0,0 )	-18144000	648321408000
( 6,1,0,0,0,0 )	-80640	54855360	( 9,1,0,0,0,0 )	29030400	962952883200
( 5,0,1,0,0,0 )	0	1391040	( 8,0,1,0,0,0 )	0	29393280000
( 4,2,0,0,0,0 )	116340	21602280	( 7,2,0,0,0,0 )	53222400	774464544000
( 4,0,0,1,0,0 )	0	5040	( 7,0,0,1,0,0 )	0	250387200
( 3,1,1,0,0,0 )	15960	1459920	( 6,1,1,0,0,0 )	-6652800	89360409600
( 2,3,0,0,0,0 )	31920	1559040	( 6,0,0,0,1,0 )	0	0
( 2,1,0,1,0,0 )	0	10080	( 5,3,0,0,0,0 )	-109468800	268696915200
( 2,0,2,0,0,0 )	2940	36680	( 5,1,0,1,0,0 )	0	1854316800
( 1,2,1,0,0,0 )	6720	82880	( 5,0,2,0,0,0 )	2298240	4975488000
( 1,0,1,1,0,0 )	112	672	( 4,2,1,0,0,0 )	-4233600	38957990400
( 0,4,0,0,0,0 )	2310	30380	( 4,1,0,0,1,0 )	0	12096000
( 0,2,0,1,0,0 )	140	840	( 4,0,1,1,0,0 )	282240	336510720
( 0,1,2,0,0,0 )	0	0	( 3,4,0,0,0,0 )	51559200	36058276800
( 0,0,0,2,0,0 )	2	4	( 3,2,0,1,0,0 )	352800	931089600
( -8-			( 3,1,2,0,0,0 )	4515840	1923909120
( 9,0,0,0,0,0 )	322560	1264112640	( 3,0,1,0,1,0 )	0	3064320
( 7,1,0,0,0,0 )	-483840	1363944960	( 3,0,0,2,0,0 )	106560	7009920
( 6,0,1,0,0,0 )	0	40158720	( 2,3,1,0,0,0 )	17640000	4257590400
( 5,2,0,0,0,0 )	120960	733420800	( 2,2,0,0,1,0 )	0	8668800
( 5,0,0,1,0,0 )	0	322560	( 2,1,1,1,0,0 )	1431360	95840640
( 4,1,1,0,0,0 )	53760	64942080	( 2,0,3,0,0,0 )	201600	10725120
( 3,3,0,0,0,0 )	470400	108998400	( 2,0,0,1,1,0 )	7200	138240
( 3,1,0,1,0,0 )	0	806400	( 1,5,0,0,0,0 )	3427200	692294400
( 3,0,2,0,0,0 )	43904	2245376	( 1,3,0,1,0,0 )	201600	34675200
( 2,2,1,0,0,0 )	170240	8798720	( 1,2,2,0,0,0 )	3087840	154096320
( 2,0,1,1,0,0 )	3584	68096	( 1,1,1,0,1,0 )	33600	994560
( 1,4,0,0,0,0 )	116480	4067840	( 1,1,0,2,0,0 )	46080	633600
( 1,2,0,1,0,0 )	4480	125440	( 1,0,2,1,0,0 )	40320	584640
( 1,1,2,0,0,0 )	11648	166656	( 1,0,0,0,2,0 )	160	640
( 1,0,0,2,0,0 )	128	512	( 0,4,1,0,0,0 )	1142400	42470400
( 0,3,1,0,0,0 )	4480	107520	( 0,3,0,0,1,0 )	0	268800
( 0,1,1,1,0,0 )	896	3584	( 0,2,1,1,0,0 )	80640	1612800
( 0,0,3,0,0,0 )	0	0	( 0,1,3,0,0,0 )	20160	1048320
			( 0,1,0,1,1,0 )	1920	7680
			( 0,0,2,0,1,0 )	2016	8064
			( 0,0,1,2,0,0 )	0	0

P	T	SC	P	T	SC
-0-			-9-		
( 0.0,0,0,0,0 )	0	0	( 10.0,0,0,0,0 )	2091166126560	4495820565600
-1-			( 8.1,0,0,0,0 )	2225242756800	3230986086720
( 2.0,0,0,0,0 )	6	6	( 7.0,1,0,0,0 )	67914806400	73869122880
-2-			( 6.2,0,0,0,0 )	1081454771880	1027201989240
( 3.0,0,0,0,0 )	144	144	( 6.0,0,1,0,0 )	715508640	663798240
-3-			( 5.1,1,0,0,0 )	78764782320	61070662800
( 4.0,0,0,0,0 )	3294	3294	( 5.0,0,0,1,0 )	1360800	1360800
( 2.1,0,0,0,0 )	180	180	( 4.3,0,0,0,0 )	190133107920	120618726480
( 0.2,0,0,0,0 )	6	6	( 4.1,0,1,0,0 )	983676960	726939360
-4-			( 4.0,2,0,0,0 )	2049523560	1352022840
( 5.0,0,0,0,0 )	79056	82944	( 3.2,1,0,0,0 )	16202592000	7657040160
( 3.1,0,0,0,0 )	12960	12096	( 3.1,0,0,1,0 )	2268000	2268000
( 1.2,0,0,0,0 )	720	576	( 3.0,1,1,0,0 )	60383232	40515552
-5-			( 2.4,0,0,0,0 )	9579283560	4551377040
( 6.0,0,0,0,0 )	2040120	2347920	( 2.2,0,1,0,0 )	185499720	89903520
( 4.1,0,0,0,0 )	646920	594000	( 2.1,2,0,0,0 )	449175888	136615248
( 3.0,1,0,0,0 )	3600	3600	( 2.0,1,0,1,0 )	151200	151200
( 2.2,0,0,0,0 )	64350	48870	( 2.0,0,2,0,0 )	459918	323838
( 1.1,1,0,0,0 )	900	900	( 1.3,1,0,0,0 )	563855040	207612720
( 0.3,0,0,0,0 )	360	0	( 1.2,0,0,1,0 )	378000	378000
( 0.0,2,0,0,0 )	6	6	( 1.1,1,1,0,0 )	8269128	2689848
-6-			( 1.0,3,0,0,0 )	2721600	0
( 7.0,0,0,0,0 )	57166560	74766240	( 1.0,0,1,1,0 )	2700	2700
( 5.1,0,0,0,0 )	28434240	27384480	( 0.5,0,0,0,0 )	54416880	0
( 4.0,1,0,0,0 )	371520	336960	( 0.3,0,1,0,0 )	2721600	0
( 3.2,0,0,0,0 )	4807080	3659040	( 0.2,2,0,0,0 )	7570584	2936304
( 2.1,1,0,0,0 )	140400	108000	( 0.1,1,0,1,0 )	12600	12600
( 1.3,0,0,0,0 )	120960	51840	( 0.1,0,2,0,0 )	15120	0
( 1.0,2,0,0,0 )	1224	864	( 0.0,2,1,0,0 )	37800	0
( 0.2,1,0,0,0 )	2880	1440	( 0,0,0,0,2,0 )	6	6
-7-			-10-		
( 8.0,0,0,0,0 )	1745418780	2655431100	( 11.0,0,0,0,0 )	8028692784000	211145941036800
( 6.1,0,0,0,0 )	1200633840	1280059200	( 9.1,0,0,0,0 )	103342551278400	176930203564800
( 5.0,1,0,0,0 )	24433920	21833280	( 8.0,1,0,0,0 )	3264180897600	4373643859200
( 4.2,0,0,0,0 )	314976060	246996540	( 7.2,0,0,0,0 )	59730344200800	67476683232000
( 4.0,0,1,0,0 )	75600	75600	( 7.0,0,1,0,0 )	45464328000	45031593600
( 3.1,1,0,0,0 )	13958280	10117800	( 6.1,1,0,0,0 )	5244792638400	4398829545600
( 2.3,0,0,0,0 )	18632880	9802800	( 6.0,0,0,1,0 )	179625600	179625600
( 2.1,0,1,0,0 )	50400	50400	( 5.3,0,0,0,0 )	1568262124800	10926042825600
( 2.0,2,0,0,0 )	194964	139524	( 5.1,0,1,0,0 )	81496951200	64207987200
( 1.2,1,0,0,0 )	803040	309120	( 5.0,2,0,0,0 )	157331250720	112057706880
( 1.0,1,1,0,0 )	1680	1680	( 4.2,1,0,0,0 )	1607942145600	871058966400
( 0.4,0,0,0,0 )	149730	104370	( 4.1,0,0,1,0 )	430012800	348364800
( 0.2,0,1,0,0 )	2100	2100	( 4.0,1,1,0,0 )	6931643040	4414435200
( 0.1,2,0,0,0 )	5040	0	( 3.4,0,0,0,0 )	1357936876800	684945525600
( 0.0,0,2,0,0 )	6	6	( 3.2,0,1,0,0 )	26174080800	12381012000
-8-			( 3.1,2,0,0,0 )	65498963040	22269461760
( 9.0,0,0,0,0 )	58015258560	104309130240	( 3.0,1,0,1,0 )	38344320	26853120
( 7.1,0,0,0,0 )	50917507200	62575027200	( 3.0,0,2,0,0 )	78003000	47329920
( 6.0,1,0,0,0 )	1338906240	1278789120	( 2.3,1,0,0,0 )	126014767200	46007438400
( 5.2,0,0,0,0 )	18916269120	15951600000	( 2.2,0,0,1,0 )	132148800	80740800
( 5.0,0,1,0,0 )	9434880	8709120	( 2.1,1,1,0,0 )	1868438880	628568640
( 4.1,1,0,0,0 )	1118355840	818657280	( 2.0,3,0,0,0 )	558220320	69552200
( 3.3,0,0,0,0 )	2069907840	1208511360	( 2.0,0,1,1,0 )	892080	557280
( 3.1,0,1,0,0 )	9112320	7015680	( 1.5,0,0,0,0 )	25250097600	6619536000
( 3.0,2,0,0,0 )	22416576	14765184	( 1.3,0,1,0,0 )	1158040800	228009600
( 2.2,1,0,0,0 )	132216000	56448000	( 1.2,2,0,0,0 )	3297026880	910012320
( 2.0,1,1,0,0 )	397824	274176	( 1.1,1,0,1,0 )	8356320	4173120
( 1.4,0,0,0,0 )	49791840	23788800	( 1.1,0,2,0,0 )	9447840	2315520
( 1.2,0,1,0,0 )	920640	524160	( 1.0,2,1,0,0 )	22367520	2116800
( 1.1,2,0,0,0 )	2222976	604800	( 1.0,0,0,2,0 )	2520	1440
( 1.0,0,2,0,0 )	1824	1152	( 0.4,1,0,0,0 )	1032292800	242524800
( 0.3,1,0,0,0 )	1357440	362880	( 0.3,0,0,1,0 )	3225600	1209600
( 0.1,1,1,0,0 )	18816	8064	( 0.2,1,1,0,0 )	36298080	5564160
( 0.0,3,0,0,0 )	6720	0	( 0.1,3,0,0,0 )	18355680	3326400
			( 0.1,0,1,1,0 )	46080	17280
			( 0.0,2,0,1,0 )	48384	18144
			( 0.0,1,2,0,0 )	110880	0



P	BCC	FCC	P	BCC	FCC
-0-			-9-		
( 0,0,0,0,0,0 )	0	0	(10,0,0,0,0,0 )	97203332016000	4987066700064960
-1-			( 8,1,0,0,0,0 )	52628686346880	2170696355432640
( 2,0,0,0,0,0 )	8	12	( 7,0,1,0,0,0 )	954788446080	31402121808960
-2-			( 6,2,0,0,0,0 )	11863433564640	380181901987440
( 3,0,0,0,0,0 )	256	576	( 6,0,0,1,0,0 )	6885648000	170464694400
-3-			( 5,1,1,0,0,0 )	503671089600	11836307075040
( 4,0,0,0,0,0 )	8136	28620	( 5,0,0,0,1,0 )	12700800	179625600
( 2,1,0,0,0,0 )	336	792	( 4,3,0,0,0,0 )	973073183040	25087493158560
( 0,2,0,0,0,0 )	8	12	( 4,1,0,1,0,0 )	4386312000	68369767200
-4-			( 4,0,2,0,0,0 )	7433002080	114651981360
( 5,0,0,0,0,0 )	291840	1601856	( 3,2,1,0,0,0 )	43856789760	914319342720
( 3,1,0,0,0,0 )	30720	120960	( 3,1,0,0,1,0 )	10584000	74844000
( 1,2,0,0,0,0 )	1024	2880	( 3,0,1,1,0,0 )	154808640	1412818848
-5-			( 2,4,0,0,0,0 )	26173183680	503109986400
( 6,0,0,0,0,0 )	11847360	101688480	( 2,2,0,1,0,0 )	349322400	4512458160
( 4,1,0,0,0,0 )	2155680	13878000	( 2,1,2,0,0,0 )	533937600	10226194272
( 3,0,1,0,0,0 )	10080	39600	( 2,0,1,0,1,0 )	423360	1663200
( 2,2,0,0,0,0 )	124200	573660	( 2,0,0,2,0,0 )	842760	4280364
( 1,1,1,0,0,0 )	1680	3960	( 1,3,1,0,0,0 )	871799040	13154218560
( 0,3,0,0,0,0 )	0	1440	( 1,2,0,0,1,0 )	1058400	4158000
( 0,0,2,0,0,0 )	8	12	( 1,1,1,1,0,0 )	7086240	77387184
-6-			( 1,0,3,0,0,0 )	0	26006400
( 7,0,0,0,0,0 )	542056320	7274422080	( 1,0,0,1,1,0 )	5040	11880
( 5,1,0,0,0,0 )	144708480	1494987840	( 0,5,0,0,0,0 )	0	1208208960
( 4,0,1,0,0,0 )	1313280	9417600	( 0,3,0,1,0,0 )	0	26006400
( 3,2,0,0,0,0 )	13307520	100694880	( 0,2,2,0,0,0 )	8668800	76289472
( 2,1,1,0,0,0 )	276480	1339200	( 0,1,1,0,1,0 )	23520	55440
( 1,3,0,0,0,0 )	136320	1097280	( 0,1,0,2,0,0 )	0	60480
( 1,0,2,0,0,0 )	1536	4896	( 0,0,2,1,0,0 )	0	151200
( 0,2,1,0,0,0 )	2560	11520	( 0,0,0,0,2,0 )	8	12
-7-			-10-		
( 8,0,0,0,0,0 )	27689553360	581135060520	(11,0,0,0,0,0 )	6576908186419200	527505045793689600
( 6,1,0,0,0,0 )	9861546240	162388074240	( 9,1,0,0,0,0 )	4183098750028800	271946632765248000
( 5,0,1,0,0,0 )	126080640	1543268160	( 8,0,1,0,0,0 )	83731439232000	4431158495769600
( 4,2,0,0,0,0 )	1311379440	16187252760	( 7,2,0,0,0,0 )	1145876738227200	58638977446089600
( 4,0,0,1,0,0 )	352800	2494800	( 7,0,0,1,0,0 )	731195942400	30807586656000
( 3,1,1,0,0,0 )	38004960	317162160	( 6,1,1,0,0,0 )	54405867801600	2099704961491200
( 2,3,0,0,0,0 )	37242240	398603520	( 6,0,0,0,1,0 )	2467584000	72503424000
( 2,1,0,1,0,0 )	141120	554400	( 5,3,0,0,0,0 )	130711362163200	5369689921478400
( 2,0,2,0,0,0 )	359856	1779960	( 5,1,0,1,0,0 )	588569587200	16018956576000
( 1,2,1,0,0,0 )	806400	7371840	( 5,0,2,0,0,0 )	920602851840	24091235602560
( 1,0,1,1,0,0 )	3136	7392	( 4,2,1,0,0,0 )	7408964505600	242584746566400
( 0,4,0,0,0,0 )	294840	1378020	( 4,1,0,0,1,0 )	2370816000	39354336000
( 0,2,0,1,0,0 )	3920	9240	( 4,0,1,1,0,0 )	24952757760	415164476160
( 0,1,2,0,0,0 )	0	20160	( 3,4,0,0,0,0 )	5712234998400	180774607809600
( 0,0,0,2,0,0 )	8	12	( 3,2,0,1,0,0 )	72602812800	1654278292800
-8-			( 3,1,2,0,0,0 )	129615897600	3672740171520
( 9,0,0,0,0,0 )	1565864294400	51382077062400	( 3,0,1,0,1,0 )	106444800	1029369600
( 7,1,0,0,0,0 )	701510906880	18310805775360	( 3,0,0,2,0,0 )	176302080	1772292960
( 6,0,1,0,0,0 )	11075097600	22389121600	( 2,3,1,0,0,0 )	278141472000	7156095811200
( 5,2,0,0,0,0 )	124944422400	249302698320	( 2,2,0,0,1,0 )	326592000	3662064000
( 5,0,0,1,0,0 )	58060800	805593600	( 2,1,1,1,0,0 )	2434440960	44988652800
( 4,1,1,0,0,0 )	4525086720	63975098880	( 2,0,3,0,0,0 )	276917760	14543827200
( 3,3,0,0,0,0 )	6627264000	107935188480	( 2,0,0,1,1,0 )	1428480	8596800
( 3,1,0,1,0,0 )	27740160	241113600	( 1,5,0,0,0,0 )	41012697600	1373651395200
( 3,0,2,0,0,0 )	54602240	492608256	( 1,3,0,1,0,0 )	972518400	28544140800
( 2,2,1,0,0,0 )	216903680	2953870080	( 1,2,2,0,0,0 )	3945244800	82117224000
( 2,0,1,1,0,0 )	702464	3816960	( 1,1,1,0,1,0 )	10859520	82051200
( 1,4,0,0,0,0 )	95083520	1075885440	( 1,1,0,2,0,0 )	5967360	89320320
( 1,2,0,1,0,0 )	1361920	9004800	( 1,0,2,1,0,0 )	5523840	196459200
( 1,1,2,0,0,0 )	1573376	20697600	( 1,0,0,2,0,0 )	2560	10080
( 1,0,0,2,0,0 )	2048	7296	( 0,4,1,0,0,0 )	1116595200	24792163200
( 0,3,1,0,0,0 )	1039360	13171200	( 0,3,0,1,0,0 )	3225600	32256000
( 0,1,1,1,0,0 )	14336	75264	( 0,2,1,1,0,0 )	15482880	364976640
( 0,0,1,3,0,0 )	0	26880	( 0,1,3,0,0,0 )	10321920	208051200
			( 0,1,0,1,1,0 )	30720	184320
			( 0,0,2,0,1,0 )	32256	193536
			( 0,0,1,2,0,0 )	0	443520

P	HSC	HBCC	P	HSC	HBCC
-0-			-9-		
( 0,0,0,0,0,0 )	0	0	( 10,0,0,0,0,0 )	108737731912320	111452928594981120
-1-			( 8,1,0,0,0,0 )	53292210249600	26940300054071040
( 2,0,0,0,0,0 )	8	16	( 7,0,1,0,0,0 )	918704384640	214048944057600
-2-			( 6,2,0,0,0,0 )	11110002331680	2581453465899840
( 3,0,0,0,0,0 )	256	1024	( 6,0,0,1,0,0 )	6689692800	917419426560
-3-			( 5,1,1,0,0,0 )	464611775040	50146107177600
( 4,0,0,0,0,0 )	8136	69264	( 5,0,0,0,1,0 )	12700800	990662400
( 2,1,0,0,0,0 )	336	1440	( 4,3,0,0,0,0 )	862386436800	90867064982400
( 0,2,0,0,0,0 )	8	16	( 4,1,0,1,0,0 )	4186002240	214463168640
-4-			( 4,0,2,0,0,0 )	6867211680	316281268800
( 5,0,0,0,0,0 )	291840	5443584	( 3,2,1,0,0,0 )	38510357760	1868211878400
( 3,1,0,0,0,0 )	30720	270336	( 3,1,0,0,1,0 )	10584000	275184000
( 1,2,0,0,0,0 )	1024	4096	( 3,0,1,1,0,0 )	148034880	3070505088
-5-			( 2,4,0,0,0,0 )	21526081920	1051809937920
( 6,0,0,0,0,0 )	11959680	493785600	( 2,2,0,1,0,0 )	327791520	6932681280
( 4,1,0,0,0,0 )	2126880	41290560	( 2,1,2,0,0,0 )	476481600	10168083072
( 3,0,1,0,0,0 )	10080	100800	( 2,0,1,0,1,0 )	423360	4233600
( 2,2,0,0,0,0 )	121320	1072080	( 2,0,0,2,0,0 )	818568	7463952
( 1,1,1,0,0,0 )	1680	7200	( 1,3,1,0,0,0 )	694350720	1625420160
( 0,3,0,0,0,0 )	0	0	( 1,2,0,0,1,0 )	1058400	10584000
( 0,0,2,0,0,0 )	8	16	( 1,1,1,1,0,0 )	6699168	61975872
-6-			( 1,0,3,0,0,0 )	0	0
( 7,0,0,0,0,0 )	556882560	51154018560	( 1,0,1,1,1,0 )	5040	21600
( 5,1,0,0,0,0 )	141356160	6175238400	( 0,5,0,0,0,0 )	0	0
( 4,0,1,0,0,0 )	1313280	27740160	( 0,3,0,1,0,0 )	0	0
( 3,2,0,0,0,0 )	12812160	248620800	( 0,2,2,0,0,0 )	6842304	73374336
( 2,1,1,0,0,0 )	276480	2457600	( 0,1,1,0,1,0 )	23520	100800
( 1,3,0,0,0,0 )	124800	1140480	( 0,1,0,2,0,0 )	0	0
( 1,0,2,0,0,0 )	1536	6144	( 0,0,2,1,0,0 )	0	0
( 0,2,1,0,0,0 )	2560	10240	( 0,0,0,0,2,0 )	8	16
-7-			-10-		
( 8,0,0,0,0,0 )	29135176560	5970478116960	( 11,0,0,0,0,0 )	7624481289062400	17504638127243366400
( 6,1,0,0,0,0 )	9659180160	954131270400	( 9,1,0,0,0,0 )	4348369804262400	4969285253494732800
( 5,0,1,0,0,0 )	123177600	5990826240	( 8,0,1,0,0,0 )	81568674432000	49436286633216000
( 4,2,0,0,0,0 )	1241474640	54682551840	( 7,2,0,0,0,0 )	1084176709506000	578349978875827200
( 4,0,0,1,0,0 )	352800	9172800	( 7,0,0,1,0,0 )	697738406400	230941578470400
( 3,1,1,0,0,0 )	36613920	742728000	( 6,1,1,0,0,0 )	49643212953600	12564439411507200
( 2,3,0,0,0,0 )	33855360	696433920	( 6,0,0,0,1,0 )	2467584000	433249689600
( 2,1,0,1,0,0 )	141120	1411200	( 5,3,0,0,0,0 )	114807405888000	27990850082227200
( 2,0,2,0,0,0 )	349776	3151904	( 5,1,0,1,0,0 )	546838387200	66205206144000
( 1,2,1,0,0,0 )	766080	6997760	( 5,0,2,0,0,0 )	830215249920	89300665681920
( 1,0,1,1,0,0 )	3136	15440	( 4,2,1,0,0,0 )	6373895270400	716468459212800
( 0,4,0,0,0,0 )	244440	2473520	( 4,1,0,0,1,0 )	2370816000	137371852800
( 0,2,0,1,0,0 )	3920	16800	( 4,0,1,1,0,0 )	23322216960	1106883671040
( 0,1,2,0,0,0 )	0	0	( 3,4,0,0,0,0 )	4691614435200	517073339462400
( 0,0,0,2,0,0 )	8	16	( 3,2,0,1,0,0 )	65167401600	3236910163200
-8-			( 3,1,2,0,0,0 )	110759362560	5466210140160
( 9,0,0,0,0,0 )	1695560509440	776603874816000	( 3,0,1,0,1,0 )	106444800	2294046720
( 7,1,0,0,0,0 )	695923522560	155539733207040	( 3,0,0,2,0,0 )	169528320	3384990720
( 6,0,1,0,0,0 )	10651253760	1203691345920	( 2,3,1,0,0,0 )	220921747200	11490110553600
( 5,2,0,0,0,0 )	116975577600	11820578595840	( 2,2,0,0,1,0 )	326592000	7202764800
( 5,0,0,1,0,0 )	58060800	3287531520	( 2,1,1,1,0,0 )	2205262080	46130434560
( 4,1,1,0,0,0 )	4260587520	196914278400	( 2,0,3,0,0,0 )	239823360	5165798400
( 3,3,0,0,0,0 )	5953436160	273002419200	( 2,0,0,1,1,0 )	1428480	12718080
( 3,1,0,1,0,0 )	27740160	596090880	( 1,5,0,0,0,0 )	29595686400	1604202163200
( 3,0,2,0,0,0 )	52344320	1036442624	( 1,3,0,1,0,0 )	782208000	18350438400
( 2,2,1,0,0,0 )	196259840	4066979840	( 1,2,2,0,0,0 )	2987483520	71995365120
( 2,0,1,1,0,0 )	702464	6250496	( 1,1,1,0,1,0 )	10859520	98488320
( 1,4,0,0,0,0 )	78955520	1721108480	( 1,1,0,2,0,0 )	5644800	50365440
( 1,2,0,1,0,0 )	1361920	12328960	( 1,0,2,1,0,0 )	5120640	46368000
( 1,1,2,0,0,0 )	1465856	13224960	( 1,0,0,0,2,0 )	2560	10240
( 1,0,0,2,0,0 )	2048	8192	( 0,4,1,0,0,0 )	790809600	20423424000
( 0,3,1,0,0,0 )	824320	8386560	( 0,3,0,0,1,0 )	3225600	30105600
( 0,1,1,1,0,0 )	14336	57344	( 0,2,1,1,0,0 )	1290240	126443520
( 0,0,3,0,0,0 )	D	D	( 0,1,3,0,0,0 )	7096320	80640000
			( 0,1,0,1,1,0 )	30720	122880
			( 0,0,2,0,1,0 )	32256	129024
			( 0,0,1,2,0,0 )	0	0

## ACKNOWLEDGMENTS

We are grateful to J. D. Bessis, E. Brézin, M. E. Fisher, J. L. Gammel, J. Glimm, A. Jaffe, L. Kadanoff, N. Khuri, B. McCoy, B. G. Nickel, and J. Stevenson for helpful conversations, and to L. W. Fullerton for assistance with the many ALTRAN-related problems we encountered. One of us (JMK) is pleased to acknowledge the hospitality that the Statistical Physics and Materials Theory Group at LASL extended to him while much of this work was in progress.

## REFERENCES

1. B. Widom, *J. Chem. Phys.* **43**:3892, 3898 (1965); L. P. Kadanoff, *Physics* **2**:263 (1966).
2. M. E. Fisher, *Rep. Prog. Phys.* **30**:615 (1967).
3. G. Stell, in *Proceedings of the International School of Physics "Enrico Fermi," Critical Phenomena, Course LI*, M. S. Green, ed. (Academic, New York, 1971), p. 188, and references therein. See also G. Stell, *Phys. Rev. B* **5**:981 (1972).
4. M. E. Fisher, in *Proceedings of the Twenty-Fourth Nobel Symposium on Collective Properties of Physical Systems, Aspenasgården, Sweden, 1973*, B. Lundquist and S. Lundquist, eds. (Academic, New York, 1973), p. 16.
5. L. P. Kadanoff, in *Proceedings of the International School of Physics "Enrico Fermi," Critical Phenomena, Course LI*, M. S. Green, ed. (Academic, New York, 1971), p. 100; L. P. Kadanoff, in *Phase Transitions and Critical Phenomena*, C. Domb and M. S. Green, eds. (Academic, New York, 1976), Vol. 5A, p. 1.
6. C. Domb, in *Phase Transitions and Critical Phenomena*, C. Domb and M. S. Green, eds. (Academic, New York, 1974), Vol. 3, p. 357.
7. L. P. Kadanoff, *Phys. Rev.* **188**:859 (1969).
8. J. Stephenson, *J. Math. Phys.* **5**:1009 (1964).
9. B. M. McCoy and T. T. Wu, *The Two-dimensional Ising Model* (Harvard University Press, Cambridge, Massachusetts, 1973), pp. 186–199.
10. B. M. McCoy, C. A. Tracy, and T. T. Wu, *Phys. Rev. Lett.* **38**:793 (1977); B. M. McCoy and T. T. Wu, *Phys. Rev. D* **18**:1243, 1253, 1259 (1978); *Scientia Sinica XXII*:1021 (1979).
11. G. A. Baker, Jr., *Phys. Rev. B* **15**:1552 (1977).
12. D. S. Gaunt and M. F. Sykes, *J. Phys. A* **12**:L25 (1979); D. S. Gaunt, M. F. Sykes, and S. McKenzie, *J. Phys. A* **12**:A871 (1979).
13. B. G. Nickel and B. Sharpe, *J. Phys. A* **12**:1819 (1979).
14. J. J. Rehr, *J. Phys. A* **12**:L179 (1979); J. Zinn-Justin, *J. Phys. (Paris)* **40**:969 (1979); S. McKenzie, *J. Phys. A* **12**:L185 (1979); J. W. Essam and M. E. Fisher, *J. Chem. Phys.* **38**:802 (1963).
15. P. C. Hohenberg, in *Microscopic Structure and Dynamics of Liquids*, J. Dupuy and A. J. Dianoux, eds. (Plenum, New York, 1979).
16. J. V. Sengers and J. M. H. Levelt Sengers, in *Progress in Liquid Physics*, C. A. Croxton, ed. (Wiley, Chichester, U.K., 1978), p. 103.
17. R. B. Griffiths, *Phys. Rev. Lett.* **24**:715 (1970); J. M. Kincaid and E. G. D. Cohen, *Phys. Rep.* **22C**:57 (1975).
18. K. G. Wilson and J. Kogut, *Phys. Rep.* **12C**:75 (1974).
19. E. Brezin, J. C. LeGuillou, and J. Zinn-Justin, in *Phase Transitions and Critical Phenomena*, C. Domb and M. S. Green, eds. (Academic, New York, 1976), Vol. 6, p. 127.
20. K. Symanzik, *J. Math. Phys.* **7**:510 (1966).
21. G. A. Baker, Jr., *J. Math. Phys.* **16**:1324 (1975).
22. M. A. Moore, *Lett. Nuovo Cimento* **3**:275 (1972); C. DiCastro, *Rev. Nuovo Cimento* **1**:199 (1971).
23. K. Symanzik, in *Local Quantum Field Theory*, R. Jost, ed. (Academic, New York, 1969), p. 152.
24. J. D. Bjorken and S. D. Drell, *Relativistic Quantum Fields* (McGraw-Hill, New York, 1965).
25. N. N. Bogolubov and D. V. Shirkov, *Introduction to the Theory of Quantized Fields* (Interscience, New York, 1959).
26. T. H. Berlin and M. Kac, *Phys. Rev.* **86**:821 (1952).
27. G. Caginalp, The  $\phi^4$  Lattice Field Theory as an Asymptotic Expansion about the Ising Limit, The Rockefeller University, preprint (1979); F. Constantinescu, *Phys. Rev. Lett.* **43**:1632 (1979); C. M. Bender, F. Cooper, G. S. Garalnik, and D. Sharp, *Phys. Rev. D* **19**:865 (1979).

28. J. Glimm and A. Jaffe, The Coupling Constant in a  $\phi^4$  Field Theory, The Rockefeller University, preprint (1979).
29. W. Ford and G. E. Uhlenbeck, in *Studies in Statistical Mechanics*, J. de Boer, ed. (North-Holland, Amsterdam, 1962), Vol. 1, p. 119.
30. R. Schrader, *Phys. Rev. B* **14**:172 (1976); G. A. Baker, Jr., and S. Krinsky, *J. Math. Phys.* **18**:590 (1977).
31. R. Schrader, *Commun. Math. Phys.* **49**:131 (1976); **50**:97 (1976); *Ann. Inst. Henri Poincaré* **26**:295 (1977); R. Schrader and E. Tränkle, A Possible Constructive Approach to  $\phi^4$  IV, Free University of Berlin, preprint (1980).
32. G. A. Baker, Jr., B. G. Nickel, M. S. Green, and D. Meiron, *Phys. Rev. Lett.* **36**:1351 (1976); G. A. Baker, Jr., B. G. Nickel, and D. Meiron, *Phys. Rev. B* **17**:1365 (1978).
33. J. C. LeGuillou and J. Zinn-Justin, *Phys. Rev. Lett.* **39**:95 (1977).
34. M. Wortis, in *Phase Transitions and Critical Phenomena*, C. Domb and M. S. Green, eds. (Academic, New York, 1974), Vol. 3, p. 114.
35. J. P. Van Dyke and W. J. Camp, *Phys. Rev. Lett.* **35**:323 (1975); J. P. Van Dyke and W. J. Camp, in *Magnetism and Magnetic Materials—1973* G. D. Graham, Jr., and J. J. Rhyne, eds., AIP Conference Proceedings No. 18 (American Institute of Physics, New York, 1974), p. 878.
36. A. D. Hall, *Commun. ACM* **14**:517 (1971).
37. G. A. Baker, Jr., H. E. Gilbert, J. Eve, and G. S. Rushbrooke, Brookhaven National Laboratory Report No. BNL 50053 (1967).
38. M. F. Sykes, private communication.
39. C. Domb and B. R. Hcap, *Proc. Phys. Soc.* **90**:985 (1967).
40. J. M. Kincaid, G. A. Baker, Jr., and L. W. Fullerton, Los Alamos Scientific Laboratory Report No. LA-UR-79-1575 (1979).
41. C. Domb, *Adv. Phys.* **9**:149, 245 (1960).
42. M. A. Moore, *Phys. Rev. Lett.* **23**:861 (1969).
43. J. W. Essam and D. L. Hunter, *J. Phys. C* **1**:392 (1968), and private communication.
44. R. K. Wehner and D. Baeriswyl, *Physica* **81A**:129 (1975).
45. D. L. Hunter and G. A. Baker, Jr., *Phys. Rev. B* **7**:3346 (1973).
46. G. A. Baker, Jr. and D. L. Hunter, *Phys. Rev. B* **7**:3377 (1973).
47. D. L. Hunter and G. A. Baker, Jr., *Phys. Rev. B* **19**:3808 (1979).
48. A. J. Guttman and G. S. Joyce, *J. Phys. A* **5**:281 (1974); J. L. Gammel, in *Padé Approximants and Their Applications*, P. R. Graves-Morris, ed. (Academic, London, 1973); M. E. Fisher and H. Au-Yang, *J. Phys. A* **12**:1677 (1979).
49. J. Glimm and A. Jaffe, *Acta Phys. Austriaca Suppl.* **16**:147 (1976).
50. D. Isaacson, *Commun. Pure Appl. Math.* **29**:531 (1976).
51. D. Marchesin, Ph.D. thesis, New York University (1975).
52. C. M. Bender, F. Cooper, G. S. Guralnik, R. Roskies, and D. Sharp, in *Proceedings of Orbis Scientiae 80*, A. Perlmutter, ed. (1980), to be published.
53. J. P. Eckman, J. Magnen, and R. Sénéor, *Commun. Math. Phys.* **39**:251 (1975); J. Dimock, *Commun. Math. Phys.* **35**:347 (1974); J. Glimm, A. Jaffe, and T. Spencer, in *Constructive Field Theory*, G. Velo and A. Wightman, eds. (Springer, Berlin, 1973), p. 1.
54. J. M. H. Levelt Sengers, in *Proceedings of the Seventh Symposium on Thermophysical Properties*, A. Cezairliyan, ed. (American Society of Mechanical Engineers, New York, 1977), p. 766.
55. J. Feldman and K. Osterwalder, *Ann. Phys. (N.Y.)* **97**:80 (1976); J. Magnen and R. Sénéor, *Ann. Inst. Henri Poincaré*, **24**:95 (1976); J. Glimm and A. Jaffe, *Fortschr. Phys.* **21**:327 (1973).
56. G. A. Baker, Jr., *Phys. Rev. Lett.* **34**:268 (1975); O. McBryan and J. Rosen, *Commun. Math. Phys.* **51**:97 (1976).